

**ENHANCING WATER RESOURCE MANAGEMENT:  
A COMPARATIVE ANALYSIS OF EXPENSIVE AND  
AFFORDABLE LORAWAN SENSORS FOR USING SOIL AS A  
WATER RESERVOIR.**

**Master Thesis**

**at Hof University**

**Department of Sustainable water management and Engineering**

**Submitted to  
Prof. Günter Müller Czygan  
Alfons-Goppel-Platz 1  
95028 Hof  
Germany**

**Submitted by  
Thanipparambu Narayanan  
Kutty Harikrishnan  
Vorstadt 9  
95028 Hof  
Germany**

**Hof, 14.12.2023**

## ACKNOWLEDGEMENT

I am profoundly grateful for the support and assistance of everyone who has helped me in completing this thesis. First and foremost, I would like to express my thanks to God Almighty for granting me good health, strength, and the opportunity to undertake this journey. Without his blessings and guidance, this achievement would not have been possible.

I am deeply indebted to my thesis supervisor, Professor Günter Müller-Czygan, whose unwavering guidance, mentorship, encouragement, and support have been the cornerstones of this entire process. Professor Müller-Czygan's feedback and invaluable insights have been instrumental in shaping this thesis. I would also like to express my appreciation to Professor Tobias Schnabel, my second supervisor, for his valuable words of support and assistance.

I extend my sincere appreciation to Mr. Pavel Timofeev, the research assistant at inwa, Hof University of Applied Sciences, whose technical guidance and support were indispensable throughout the project. Additionally, my gratitude goes to Mr. Michael Schmidt, another research assistant at inwa, Hof University of Applied Sciences, for his consistent support in setting up the LoRaWAN test station. I am equally grateful to Ms. Viktoria Tarasyuk for her valuable comments and insights.

I would like to acknowledge Dr. Christoph Hader for his insightful perspectives on the evolving challenges of water stress experienced by farmers in agricultural fields.

Finally, I want to express my heartfelt appreciation to my father, Narayanan Kutty C S, my mother, Kaladevi P R, and my brother, T N Harivinayak, for their unwavering support and unwavering belief in me. Their encouragement has been a vital source of motivation and focus, sustaining me through the highs and lows of this thesis journey.

## EXECUTIVE SUMMARY

Approximately 71% of Earth's surface is covered by water, with only 3% being fresh water suitable for human use, a majority of which is trapped in glaciers and permafrost. Freshwater ecosystems, vital for sustaining life and biodiversity, face heavy utilization by humans, mainly for agriculture, industry, and municipal needs, leading to an annual freshwater consumption of 32,928 km<sup>3</sup>. Agriculture is responsible for approximately 70% of this consumption, highlighting the critical need to enhance water-use efficiency in the face of escalating scarcity and the projected requirement for a 15% increase in freshwater withdrawals, necessary to support a 50% growth in agricultural production by 2050. Soil health plays a pivotal role in sustainable agriculture, influencing plant production, water quality, and nutrient recycling. In this context, precision agriculture, particularly sensor-based approaches like LoRaWAN, emerges as a key solution with its low power usage, long-range capabilities, and cost-effectiveness. However, their adoption is limited in small to medium-scale farms, primarily in regions lacking mechanized farming, due to high initial investments and extended return periods. Challenges include the cost of new technology adoption, training, and the high expense of purchasing and maintaining advanced hardware.

This thesis focuses on making precision agriculture more accessible to smaller farms by exploring affordable hardware alternatives based on LoRaWAN technologies. This involves establishing a LoRaWAN test station at Hochschule Hof to test both affordable and expensive sensors variants in agricultural-like conditions for generating valuable data. The objective is to assess the practicality of using more economical sensor variants against their expensive counterparts and to develop a method for a data-driven comparative analysis of these sensors' performance in agricultural applications.

The conclusion of the thesis reveals that the LoRaWAN test station at Hochschule Hof successfully tested both affordable and expensive sensor variants. The affordable sensors effectively measured parameters like air temperature, humidity, and light intensity, but were less precise for scientific research in aspects like wind direction. Notable deviations in some weather and soil profile measurements indicate the necessity of additional studies. The research also evaluated the independent system set up at the university, noting its effectiveness and economic benefits compared to the Decentlab platform, albeit lacking in data visualization. Ultimately, the feasibility of replacing expensive sensors with affordable variants in precision agriculture was explored, with detailed findings and recommendations presented.

# Table of Contents

Executive Summary.....	iii
List of Figures.....	vi
List of Tables.....	ix
List of Abbreviations.....	x
1. Introduction.....	1
1.1. General.....	1
1.2. Problem statement and motivation.....	4
1.3. Objectives.....	4
1.4. Structure of thesis.....	5
2. LoRaWAN (Long Range Wide Area Network) Test Station.....	6
2.1. Selection of equipment's for test station.....	7
2.1.1. Weather Station.....	7
2.1.2. Sensors to measure soil conductivity and soil moisture.....	7
2.1.3. Profile sensors to measure soil moisture and soil temperature at various levels..	7
2.1.4. Sensors to measure the pH of the soil.....	8
2.1.5. Growing tank and other accessories.....	8
2.2. 3D Rendered Plan of the Test Station.....	14
2.3. Setting up of the test station.....	15
3. Data analysis.....	20
3.1. Overview.....	20
3.2. Data interpolation.....	20
3.3. Method Description.....	21
3.4. Correlation heatmap generation and analysis.....	21
3.4.1. Sensecap weather station (1) Vs Decentlab weather station (1).....	24
3.4.2. Sensecap weather station (2) Vs Decentlab Weather station (2).....	26
3.4.3. Sensecap weather station (1) Vs Sensecap weather station (2).....	28
3.4.4. Decentlab weather station (1) Vs Decentlab weather station (2).....	30
3.4.5. Dragino conductivity sensor Vs Decentlab Conductivity sensor.....	32
3.4.6. Conductivity sensor (17678) from Decentlab Vs Conductivity sensor (17679) from Decentlab.....	34

3.4.7.	Soil profile sensor (17674) from Decentlab Vs Soil profile sensor (17675) from Decentlab.....	36
3.4.8.	Decentlab weather station in Decentlab Platform vs Decentlab weather station in Google Sheets.....	39
3.4.9.	Decentlab Conductivity sensor in Decentlab Platform vs Decentlab Conductivity sensor in Google Sheets.....	41
3.4.10.	Decentlab soil profile sensor in Decentlab Platform vs Decentlab soil profile sensor in Google Sheets.....	42
3.4.11.	Dragino pH sensor in Decentlab Platform vs Dragino pH sensor in Google Sheets.....	44
3.4.12.	Anomalies in gathering data from Sensoterra soil profile sensor.....	45
4.	Conclusion, limits, recommendations, and future scope.....	46
4.1.	Conclusion.....	46
4.2.	Limits.....	49
4.3.	Recommendation.....	49
4.4.	Future scope of the study in authors perspective.....	50
4.4.1.	Development of an internet connected applications for real-time measurement visualization.....	50
4.4.2.	Optimization of Sensor Utilization Through Correlation-Based Machine Learning Models.....	52
4.4.3.	Integrating NDVI Cameras for Enhanced Monitoring of Growing Areas.....	53
4.4.4.	Integration of Drone Imaging and Sensor Data in Machine Learning Models for Precision Agriculture.....	54
4.4.5.	Concept of a severity scale developed by the author for assessing the extend of water stress.....	55
4.4.6.	Remediation measures based on this severity scale to combat water stress.....	56
4.4.7.	Field Implementation and virtual twin of Dr. Hader’s agricultural field.....	57
	Appendix.....	58
	Affidavit.....	63
	References.....	64

## List of Figures

<b>Figure 1.</b> <i>World Freshwater Resources.</i> .....	1
<b>Figure 2.</b> <i>Percentage of global freshwater consumption.</i> .....	2
<b>Figure 3.</b> <i>Basic Block Diagram of a LoRaWAN system.</i> .....	6
<b>Figure 4.</b> <i>3D Visualisation of the growing containers.</i> .....	14
<b>Figure 5.</b> <i>3D Visualisation of the growing containers next to the 20 ft container laboratory.</i> 14	
<b>Figure 6.</b> <i>3D image showing growing area with sensor placement.</i> .....	15
<b>Figure 7.</b> <i>3D image showing sensor placement.</i> .....	15
<b>Figure 8.</b> <i>System architecture diagram.</i> .....	16
<b>Figure 9.</b> <i>Photo of the soil profile sensor deployed in the test station.</i> .....	17
<b>Figure 10.</b> <i>Photo of the soil conductivity sensors deployed in the test station.</i> .....	18
<b>Figure 11.</b> <i>Photo of the soil pH sensors deployed in the test station.</i> .....	18
<b>Figure 12.</b> <i>Photo of the weather stations deployed in the test station.</i> .....	19
<b>Figure 13.</b> <i>Photo showing the growing containers.</i> .....	19
<b>Figure 14.</b> <i>Screenshot of the datapoints.</i> .....	21
<b>Figure 15.</b> <i>Overall correlation heatmap of Sensecap weather station (1) Vs Decentlab weather station (1).</i> .....	24
<b>Figure 16.</b> <i>Simplified correlation heatmap of Sensecap weather station (1) Vs Decentlab weather station (1).</i> .....	25
<b>Figure 17.</b> <i>Simplified coefficient of determination (<math>R^2</math>) heatmap of Sensecap weather station (1) Vs Decentlab weather station (1).</i> .....	25
<b>Figure 18.</b> <i>Overall correlation heatmap of Sensecap weather station (2) Vs Decentlab weather station (2).</i> .....	26
<b>Figure 19.</b> <i>Simplified correlation heatmap of Sensecap weather station (2) Vs Decentlab weather station (2).</i> .....	27
<b>Figure 20.</b> <i>Simplified coefficient of determination (<math>R^2</math>) heatmap of Sensecap weather station (2) Vs Decentlab weather station (2).</i> .....	27
<b>Figure 21.</b> <i>Overall correlation heatmap of Sensecap weather station (1) Vs Sensecap weather station (2).</i> .....	28
<b>Figure 22.</b> <i>Simplified correlation heatmap of Sensecap weather station (1) Vs Sensecap weather station (2).</i> .....	29
<b>Figure 23.</b> <i>Simplified coefficient of determination (<math>R^2</math>) heatmap of Sensecap weather station (1) Vs Sensecap weather station (2).</i> .....	29

<b>Figure 24.</b> Overall correlation heatmap of Decentlab weather station (1) Vs Decentlab weather station (2). .....	30
<b>Figure 25.</b> Simplified correlation heatmap of Decentlab weather station (1) Vs Decentlab weather station (2). .....	31
<b>Figure 26.</b> Simplified coefficient of determination ( $R^2$ ) heatmap of Decentlab weather station (1) Vs Decentlab weather station (2). .....	31
<b>Figure 27.</b> Overall correlation heatmap of Dragino conductivity sensor Vs Decentlab Conductivity sensor. ....	32
<b>Figure 28.</b> Simplified correlation heatmap of Dragino conductivity sensor Vs Decentlab Conductivity sensor. ....	33
<b>Figure 29.</b> Simplified coefficient of determination ( $R^2$ ) heatmap of Dragino conductivity sensor Vs Decentlab Conductivity sensor. ....	33
<b>Figure 30.</b> Overall correlation heatmap of Conductivity sensor (17678) from Decentlab Vs Conductivity sensor (17679) from Decentlab. ....	34
<b>Figure 31.</b> Simplified correlation heatmap of Conductivity sensor (17678) from Decentlab Vs Conductivity sensor (17679) from Decentlab. ....	35
<b>Figure 32.</b> Simplified coefficient of determination ( $R^2$ ) heatmap of Conductivity sensor (17678) from Decentlab Vs Conductivity sensor (17679) from Decentlab. ....	35
<b>Figure 33.</b> Overall correlation heatmap of Soil profile sensor (17674) from Decentlab Vs Soil profile sensor (17675) from Decentlab. ....	36
<b>Figure 34.</b> Simplified correlation heatmap of Soil profile sensor (17674) from Decentlab Vs Soil profile sensor (17675) from Decentlab. ....	37
<b>Figure 35.</b> Simplified coefficient of determination ( $R^2$ ) heatmap of Soil profile sensor (17674) from Decentlab Vs Soil profile sensor (17675) from Decentlab. ....	38
<b>Figure 36.</b> Overall correlation heatmap of Decentlab weather station in Decentlab Platform vs Decentlab weather station in Google Sheets. ....	39
<b>Figure 37.</b> Simplified coefficient of determination ( $R^2$ ) heatmap of Decentlab weather station in Decentlab Platform vs Decentlab weather station in Google Sheets. ....	40
<b>Figure 38.</b> Overall correlation heatmap of Decentlab Conductivity sensor in Decentlab Platform vs Decentlab Conductivity sensor in Google Sheets. ....	41
<b>Figure 39.</b> Simplified coefficient of determination ( $R^2$ ) heatmap of Decentlab Conductivity sensor in Decentlab Platform vs Decentlab Conductivity sensor in Google Sheets. ....	41
<b>Figure 40.</b> Overall correlation heatmap of Decentlab soil profile sensor in Decentlab Platform vs Decentlab soil profile sensor in Google Sheets. ....	42

<b>Figure 41.</b> <i>Simplified coefficient of determination (<math>R^2</math>) heatmap of Decentlab soil profile sensor in Decentlab Platform vs Decentlab soil profile sensor in Google Sheets. ....</i>	43
<b>Figure 42.</b> <i>Overall correlation heatmap of Dragino pH sensor in Decentlab Platform vs Dragino pH sensor in Google Sheets. ....</i>	44
<b>Figure 43.</b> <i>Simplified coefficient of determination (<math>R^2</math>) heatmap of Dragino pH sensor in Decentlab Platform vs Dragino pH sensor in Google Sheets. ....</i>	44
<b>Figure 44.</b> <i>Figure showing instruction to download data for Sensoterra sensor. ....</i>	45
<b>Figure 45.</b> <i>Figure showing the non-responsive page from Sensoterra website. ....</i>	45
<b>Figure 46.</b> <i>Screenshot (1) of Preliminary work done in unity game engine. ....</i>	51
<b>Figure 47.</b> <i>Screenshot (2) of Preliminary work done in unity game engine. ....</i>	51
<b>Figure 48.</b> <i>Screenshot (3) of Preliminary work done in unity game engine. ....</i>	52
<b>Figure 49.</b> <i>Agrocam NDVI Camera. ....</i>	53
<b>Figure 50.</b> <i>DJI Mavic 3 Multispectral drone. ....</i>	54
<b>Figure 51.</b> <i>Severity scale for assessing water stress. ....</i>	55



## List of Tables

<b>Table 1.</b> <i>Comparison expensive and affordable weather station variant chosen for LoRaWAN test station. ....</i>	9
<b>Table 2.</b> <i>Comparison expensive and affordable soil conductivity sensor variant chosen for LoRaWAN test station. ....</i>	10
<b>Table 3.</b> <i>Comparison expensive and affordable soil profile sensor variant chosen for LoRaWAN test station. ....</i>	11
<b>Table 4.</b> <i>Soil pH sensor variant chosen for LoRaWAN test station. ....</i>	12
<b>Table 5.</b> <i>Comparison expensive and affordable gateway and platform variant chosen for LoRaWAN test station. ....</i>	13
<b>Table 6.</b> <i>Table showing the interpretation of the values of Pearson correlation coefficient (R). ....</i>	22
<b>Table 7.</b> <i>Table showing the interpretation of the values of coefficient of determination (<math>R^2</math>). ....</i>	22
<b>Table 8.</b> <i>Table showing the recommended sensor variant for measuring each parameter. ....</i>	48

## List of Abbreviations

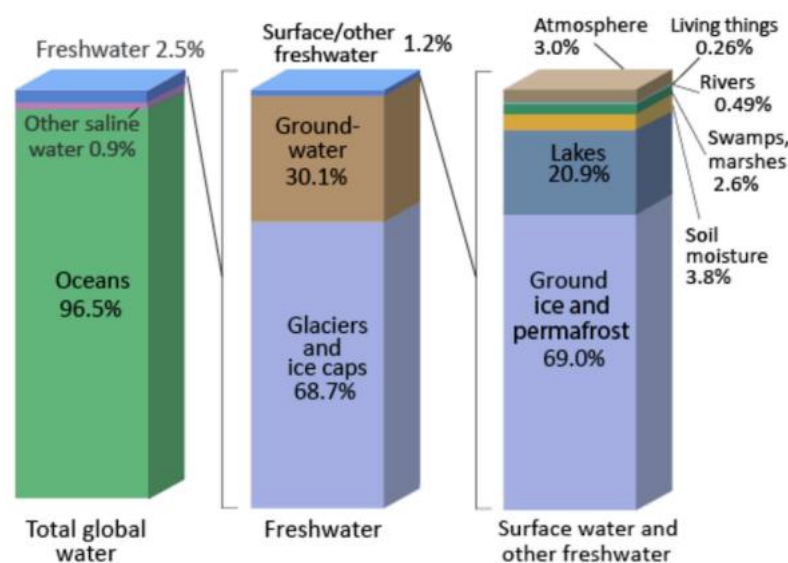
LoRaWAN	Long Range Wide Area Network
LPWANs	Low-Power Wide-Area Networks
ZigBee	Zonal Intercommunication Global standard
Wi-Fi	Wireless Fidelity
MHz	Megahertz
GHz	Gigahertz
3D	Three Dimensional
4G LTE	Fourth Generation Long Term Evolution
LAN	Local Area Network
pH	Potential of Hydrogen
IBC	Intermediate Bulk Containers
VWC	Volumetric Water Content
PoE	Power over Ethernet
csv	Comma Separated Value
ipybn	Interactive Python Notebook
VS Code	Visual Studio Code
UV	Ultraviolet
ML	Machine Learning
NDVI	Normalized Difference Vegetation Index
MP	Megapixels
RGB	Red Green Blue

# 1. Introduction

## 1.1. General

Enveloping a remarkable 71% of our planet's surface, water stands as the predominant element that shapes the physical character and natural landscape of Earth (Bernacchi, 2015). However, a minor 3% of this water qualifies as fresh water fit for human consumption and use (Ahuja, 2021). A significant portion of this freshwater is encased in glaciers, ground ice and permafrost (Shiklomanov, 1993). The breakup of the water distribution is shown in figure 1, given below.

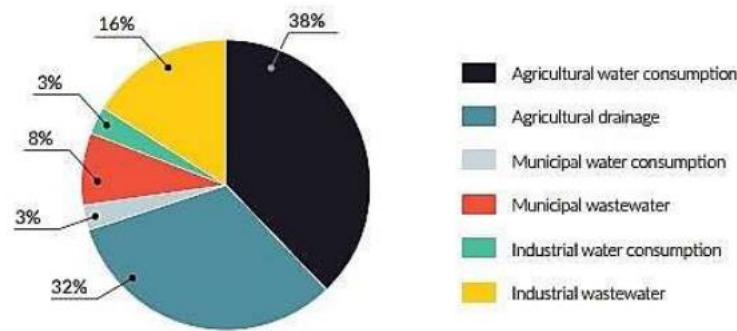
Figure 1. World Freshwater Resources.



Note. From "World Fresh Water Resources" in *Water in Crisis: A Guide to the World's Fresh Water Resources*, by I. A. Shiklomanov, 1993, Oxford University Press, New York.

Freshwater ecosystems, consisting of surface and groundwater resources, play a vital role in sustaining terrestrial life by supporting a diverse array of ecological processes (Apostolaki, 2019). Freshwater ecosystem is also essential in maintaining the terrestrial biodiversity (Apostolaki, 2019). According to (Shettima Lawan, 2021) annual global freshwater consumption by humans stands at 32,928 km<sup>3</sup> /year. The fresh water that is extracted by humans are being mainly used for agricultural use, industrial use, and municipal use. The breakdown of which is given in the figure below.

**Figure 2.** *Percentage of global freshwater consumption.*



Note. Adapted from "Development of a community system for water reclamation from grey water in Gujba: a conceptual method," by M. Shettima Lawan & S. Surendran, 2021, *International Journal of Environment and Waste Management*, 27, p. 211. (<https://doi.org/10.1504/IJEW.2021.112952>)

It is evident that about 70 percent of fresh water extracted by humans is being used for irrigation of agricultural lands. The efficiency of water use in agriculture is less due to various reasons including engineering, environmental, biological, managerial, social, and economic facets (Hsiao T, 2003). There is urgent need to improve the water-use efficiency in agriculture as even a small improvement of the efficiency of water use can translate into significant benefits (Sharma, 2015) (Hsiao T. a., 2007). According to (Rosegrant M, 2009), there must be a conscious effort to ensure that farmers' water access remains unimpaired to maintain crop yields and incomes for increasing the efficiency of water use. Limiting water availability could lead to reduced crop yields and, consequently, lower farmer incomes. Additionally, acknowledgement should be given for the role of water in various ecosystem services. This comprehensive consideration is vital for sustainable agricultural practices.

By the year 2050, the agricultural output is expected to increase by 50% as the global population would exceed 9 billion, an increase of 2 billion from the 2014 figures (Fukase, 2017). This surge in productivity is anticipated to demand a 15% rise in freshwater withdrawals for agriculture, adding additional strain to already strained water resources (McNabb, 2019). The shortage of water for irrigated agriculture will become more severe as compared to the present situation. Water scarcity for farming will become the standard rather than the exception, and the focus of irrigation management will change from maximizing yield per acre to yield per unit of water used, or water productivity (Fererres, 2006). Additionally, because of the uneven spatial and temporal distributions of the freshwater resources, various regions are also facing difficulties in meeting its domestic, economic development and environmental water

demands (Cosgrove, 2015). The above-mentioned reasons indicate to a strong need to develop sustainable agriculture solutions for judicious use of freshwater resources.

According to (M. Tahat, 2020), one of the main factors which is closely related with sustainable agriculture is the health of the soil. Imbalances in soil nutrients, overfertilization, soil pollution, and soil loss processes originating from conventional farming have a negative impact on soil health and quality (Laishram, 2012). A healthy soil is instrumental in providing several ecosystem services mainly, sustaining plant production and water quality. It can also regulate soil nutrient recycling, decomposition, and absorption of greenhouse gases from the environment (M. Tahat, 2020). According to (Lal, 2015), improving soil quality over an extended period of time (>10 years) can boost net biome productivity and enhance water and fertilizer usage efficiency. This enhanced efficiency of water use in soil, originating from improved soil health through optimised management practices, significantly reinforces the soil's function as a natural water reservoir, vital for sustaining agricultural productivity and ecological balance.

Precision agriculture can be used to achieve these targets sustainably. Precision agriculture is an advanced farming approach that enhances management decisions and crop yields through targeted, efficient use of resources. It aims to minimize agricultural impacts on the environment by employing technologies for precise input application and monitoring of crop health (Shannon, 2018). According to (Sanjeevi, 2020), wireless sensor-based precision agriculture can be employed to optimise the utilization of water resources. As stated in (Kumar, 2018), the wireless sensor technology can be used to collect, monitor, and analyse data from the field of agriculture. This is achieved by sensors in the agriculture field which collect and transmit the data to a base station. After the analysis of the data gathered in this base station, informed decisions can be taken for optimised resource allocation.

According to (Singh R. K., 2020), one of the most successful Low-Power Wide-Area Networks (LPWANs) is Long Range Wide Area Network (LoRaWAN). Even though LoRaWAN has the limitation of a low data rate, its success is aided by its low power consumption, ability to transmit over large distances, and low developmental and operational costs. A comparative study conducted by (Sadowski, 2020) between Zonal Intercommunication Global standard (ZigBee), LoRaWAN and Wireless Fidelity (Wi-Fi) 2.4 GHz technologies found that the optimal technology that can be used in agricultural monitoring is LoRaWAN when priority is given to the power consumption and network lifetime.

## **1.2. Problem statement and motivation**

According to a study conducted by (Lowenberg-DeBoer, 2019) that reviews worldwide available public data on farm level implementation of precision agriculture, it was found there is a big gap in the adoption of precision agriculture technologies in small to medium scale farms particularly in the parts of the world that do not use mechanised farming. Research conducted by (Masi, 2020) states that one of the main hinderance to the adoption of precision farming is the huge economic investment that must be done initially combined with very long return of investment. This makes it impossible for small-medium farms to implement precision agriculture. Additionally, the cost associated with adaptation of the new technologies along with training cost serves as further economic barriers (Rodríguez, 2020). One of the main challenges to overcome is the cost associated with purchase and maintenance of sophisticated hardware required for precision agriculture (Bhattacharya, 2023).

Motivation for this thesis is to investigate the ways to make precision agriculture more accessible to small and medium scale farms. This thesis adopts an approach that originates from the recognition that hardware costs significantly impede the implementation of precision agriculture. An exploration into the potential of utilizing LoRaWAN based affordable hardware alternatives as opposed to their expensive counterparts is carried out in this thesis. Inspirations were taken from studies conducted by (Liu H.-Y. a., 2019) and (Karagulian, 2019) on the performance of low-cost sensors for monitoring air quality.

## **1.3. Objectives**

The objective of this thesis are as follows,

1. To develop and set up a LoRaWAN test station at the Hochschule Hof for the purpose of testing the affordable and expensive sensors variant in close to agriculture field conditions as possible and to generate useful data.
2. To check the feasibility of using the affordable sensor variant instead of the expensive sensor variant.
3. To develop a method to do a data driven comparative study on the performance of affordable and expensive variant of LoRaWAN based sensors used in agriculture.

To avoid any bias in sensor quality, the sensor manufacturers were not informed of the testing.

## 1.4. Structure of thesis

The thesis including the introductory chapter is divided into four chapters. An overview of the chapters are given below:

**Chapter 2:** includes details on fundamentals of LoRaWAN test station, selection of equipment for the test station, 3D (Three Dimensional) rendered plan of the test station and finally setting up of the test station with expensive and affordable variant of the sensors.

**Chapter 3:** includes details on the data analysis of the data gathered from the test station, correlation heatmap generation and interpretation of the heatmaps.

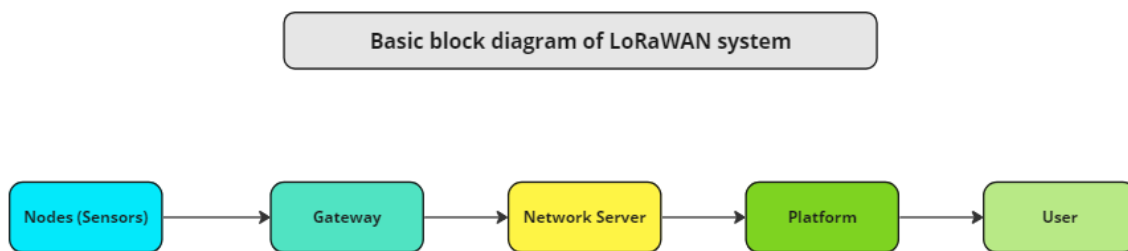
**Chapter 4:** includes the conclusion to be drawn from the interpretation of correlation heatmap on the efficacy of the affordable sensors variant as compared with the expensive sensor variant. It investigates the aspect of limits of this thesis, recommendations, and future scope.

## 2. LoRaWAN (Long Range Wide Area Network) Test Station

Before the field deployment of sensors, it was decided to set up a test station at Hochschule Hof. The aim for setting up this test station was to check the performance of affordable variant of the sensors as compared with the expensive variant of the sensors. This step is necessary to find the feasibility of using affordable sensor variant instead of expensive sensor variant and to find optimum number and types of sensors required for the field deployment. Although sensors with various communication protocols can be used, LoRaWAN based sensors were chosen as an ideal candidate for test station and later field deployment. This is because of the need for long-range and low-power communication capabilities offered by LoRaWAN (Sadowski, 2020).

The subsequent diagram illustrates the fundamental architectural framework of a LoRaWAN test station.

**Figure 3.** Basic Block Diagram of a LoRaWAN system.



Note. The figure shows basic components of a LoRaWAN system in a block diagram. Created by the author, [2023].

**Nodes (Sensors):** These constitute the foundational elements of the LoRaWAN system. responsible for the collection and transmission of data from various sources, including sensors places inside the soil, sensors placed on the surface of the soil as well as weather data through weather stations. The collected data is passed on to the LoRaWAN based gateway through the LoRaWAN Protocol.

**Gateway:** The gateway is responsible for receiving the data sent from the nodes through LoRaWAN communication protocol and forwarding it to the network server through internet. The data transmission from gateway to network server occurs through Wi-Fi, Fourth Generation Long Term Evolution (4G LTE) transmission or Local area network (LAN) cable. The gateway can handle the data coming simultaneously from multiple nodes at the same time.



Network Server: Network server is regarded as the nerve centre of the system. It manages the networking and ensuring efficient processing and routing of the data to the appropriate platform.

Platform: Platform receives the raw data from network server collected by the nodes and does further analysis of the data. Beyond mere data reception, the platform can also perform data analysis. It not only facilitates data storage but also transforms this data into actionable information for the user. These information are instrumental in guiding agricultural practices, optimizing irrigation strategies, and forecasting crop yields.

User: The end user receives this refined data, equipped with data analytics and insights. This empowers them to make well-informed decisions, furthering the optimization of their agricultural endeavours.

## **2.1. Selection of equipment's for test station**

Literature research was conducted to find sensors that are essential for the LoRaWAN test station. The following are the result of the literature research.

### **2.1.1. Weather Station**

The weather station records essential meteorological data, including solar radiation, precipitation, relative humidity, air temperature, and wind characteristics, offering vital insights into the conditions of the surrounding environment. This data is crucial for understanding soil moisture content, potential evapotranspiration rates, and soil temperature changes. The data from the weather stations can be further analysed to determine effects of the weather patterns on the soil (Singh D. K.-N., 2022).

### **2.1.2. Sensors to measure soil conductivity and soil moisture**

Another important part of evaluating the soil conditions is the use of sensors that detect soil conductivity. These sensors provide essential data on the soil's chemical and physical characteristics. This data helps in understanding the soil's ability to retain water, the availability of nutrients, and its general health (Ramson, 2021).

### **2.1.3. Profile sensors to measure soil moisture and soil temperature at various levels**

Profile sensors Profile sensors can measure soil moisture and soil temperature at various depths. This data is crucial in providing information about the subsurface soil conditions. Analysis of this data can give insights into the soil's moisture distribution and temperature gradients, essential for understanding root zone health, water uptake patterns, and potential

growth conditions. The insights derived from this data will help in optimizing water consumption and enhancing the understanding of subsurface soil dynamics (Sriphanthaboot, 2021).

#### **2.1.4. Sensors to measure the pH of the soil**

Potential of Hydrogen (pH) sensors record the acidity or alkalinity levels of the soil, which provides insights into the soil's health and ability of the soil to sustain life for different crops. Soil pH can significantly influence nutrient availability, microbial activity, and overall soil structure. The data obtained can help in understanding nutrient absorption rates and promote healthier plant (Goh, 2023).

#### **2.1.5. Growing tank and other accessories**

Prior to field implementation, it was decided to test the sensors in a controlled growing environment. To achieve this, a 1000 Liter Intermediate Bulk Container (IBC) water tank was repurposed as a growing tank. The choice of the 1000 Liter IBC water tank was influenced by several factors such as its large dimensions, structural reinforcement, use of inert materials, and economic feasibility.



The modification process involved cutting out the top portion of the water tank and filling it with soil in layered segments. Plants were then allowed to grow naturally within this setup. Sensors were strategically placed within the soil to continuously monitor and collect data corresponding to various soil conditions.

After considering the availability from multiple suppliers, sensors within the following classifications were chosen for incorporating into the LoRaWAN test station:

- i) Whether stations.
- ii) Sensors to measure soil conductivity and soil moisture.
- iii) Profile sensors to measure soil moisture and soil temperature at various levels.
- iv) Sensors to measure the pH of the soil.



After finalizing the sensor types, the specific models of the sensors were selected based the market availability and cost. For expensive sensor variant, the sensors and platform were chosen for an end-to-end supplier based in Switzerland named Decentlab GmbH. For the affordable sensor variant, the sensors were chosen based on affordability and was able to measure almost same parameters as expensive sensor variant. The final list of equipment's is listed in the below tables,

**Table 1.** Comparison expensive and affordable weather station variant chosen for LoRaWAN test station.

SI No	Type of sensor	Category	Expensive Variant	Affordable Variant
1	Weather Station	Name	Eleven Parameter Weather Station for LoRaWAN	8-in-1 LoRaWAN Weather Station
		Model Number	DL-ATM41-001	S2120
		Parameters measured	<b>Solar radiation</b> :- Range: 0 - 1,750 W/m <sup>2</sup> ; Resolution: 1 W/m <sup>2</sup> ; Accuracy: ±5%	<b>Light intensity</b> :- Range: 0 - 200000 lux ; Resolution: 1lux ; Accuracy: ± 5%
			<b>Precipitation</b> :- Range: 0 - 400 mm/h ; Resolution: 0.017 mm ; Accuracy: ±5%	<b>Precipitation</b> :- Range: 0 - 450 mm/h ; Accuracy: ± 7%
			<b>Relative humidity</b> :- Range: 0 - 100% RH ; Resolution: 0.1% RH ; Accuracy: ±3% RH	<b>Air humidity(Relative)</b> :- Range: 1 - 99 % RH ; Resolution: 1%RH ; Accuracy: ±4%
			<b>Air temperature</b> :- Range: -50 - +60 °C ; Resolution: 0.1 °C ; Accuracy: ±0.6 °C	<b>Air temperature</b> :- Range: - 40.0 - 80.0 °C ; Resolution 0.1°C ; Accuracy ±0.6°C (0~80°C)
			<b>Wind Speed</b> :- Range: 0 - 30 m/s ; Resolution: 0.01 m/s ; Accuracy: 3%	<b>Wind speed</b> :- Range: 0 - 50.0m/s ; Resolution: 0.1 m/s ; Accuracy: ±10%
			<b>Wind direction</b> :- Range: 0 - 359° ; Resolution: 1° ; Accuracy: ±5°	<b>Wind direction</b> :- Range: 0 - 360° ; Resolution: 1° ; Accuracy: ± 8°
			<b>Barometric pressure</b> :- Range: 50 - 110 kPa ; Resolution: 0.01 kPa ; Accuracy: ±0.5	<b>Barometric pressure</b> :- Range: 540 - 1100hPa ; Resolution: 1hPa ; Accuracy: ±8hPa
			<b>Vapor pressure</b> :- Range: 0 - 47 kPa ; Resolution: 0.01 kPa ; Accuracy: ±0.2 kPa	<b>UV index</b> :- Range: 0 - 16.0 ; Accuracy: ±10% ; Resolution: 0.1
			<b>Wind gust</b> :- Range: 0 - 30 m/s ; Resolution: 0.01 m/s ; Accuracy: 3%	
			<b>Tilt</b> :- Range: -90° - +90° ; Resolution: 0.1° ; Accuracy: ±1°	
		<b>Lightning strike count</b> :- Range: 0 - 65,535 strikes ; Resolution: 1 strike		
		<b>Lightning average distance</b> :- Range: 0 ... 40 km ; Resolution: 3 km		
Data gathering frequency	10 mins	5 mins		
Cost in Euro	3651.7	360		
Number of sensors purchased	2	2		
Photo				
Vendor name	Decentlab GmbH	Sensecap		
Country of origin	Switzerland	China		



Note. Created by the author, [2023].

**Table 2.** Comparison expensive and affordable soil conductivity sensor variant chosen for LoRaWAN test station.

SI No	Type of sensor	Category	Expensive Variant	Affordable Variant
2	Soil Conductivity Sensor	Name	Soil Moisture and Temperature Sensor for LoRaWAN	Soil Moisture, Temperature and Conductivity Sensor
		Model Number	DL-TRS12-001	DRA LSE01
		Parameters measured	<b>Volumetric water content (VWC)</b> :- Range : Mineral soil 0.00 - 0.70 m <sup>3</sup> /m <sup>3</sup> , Soilless media 0.0 - 1.0 m <sup>3</sup> /m <sup>3</sup> , Apparent dielectric permittivity $\epsilon_a$ : 1 (air) to 80 (water) ;Resolution : 0.001 m <sup>3</sup> /m <sup>3</sup> ; Accuracy : $\pm 0.03$ m <sup>3</sup> /m <sup>3</sup> <b>Temperature</b> :- Range : -40 - +60 °C ; Resolution : 0.1 °C ; Accuracy : $\pm 0.5$ °C <b>Bulk electrical conductivity</b> :- Range : 0 - 20 dS/m (bulk) ; Resolution : 0.001 dS/m ; Accuracy : $\pm 8\%$ dS/m	<b>Soil moisture</b> :- Range : 0-100.00% V/V % ; Resolution : 0.01% ; Accuracy : $\pm 5\%$ (>53%) <b>Soil temperature</b> :- Range : -40.00°C-85.00°C ; Resolution : 0.01°C ; Accuracy : $< 0.6$ °C <b>Soil conductivity</b> :- Range : 0-20000 uS/cm ; Resolution : 1 uS/cm ; Accuracy : 2%FS
		Data gathering frequency	10 mins	20 mins
		Cost in Euro	1045	119
		Number of sensors purchased	2	1
		Photo		
		Vendor name	Decentlab GmbH	Dragino
		Country of origin	Switzerland	China


Note. Created by the author, [2023].

**Table 3.** Comparison expensive and affordable soil profile sensor variant chosen for LoRaWAN test station.

SI No	Type of sensor	Category	Expensive Variant	Affordable Variant
3	Soil Profile Sensor	Name	Soil Moisture and Temperature Profile for LoRaWAN	Sensoterra Multi Depth Sensor for Soil Humidity
		Model Number	DL-SMTP-001	Sensoterra Multi Depth Sensor
		Specification	<b>Moisture</b> :- Range: 0 (air) - 100% (water) ; Resolution: 0.01 ; Accuracy: $\pm 1\%$ at calibration	<b>Moisture</b> :- Range: 0 (air) - 100% (water) ; Resolution: 0.1% ; Accuracy: $\pm 1.5\%$ at calibration
			<b>Temperature</b> :- Range: -20 - +50 °C ; Resolution: 0.1 °C ; Accuracy: $\pm 0.2$ °C, 0.1% per °C	<b>Temperature</b> :- Range: - 20 to + 60°C; Resolution: 0.5°C ; Accuracy: $\pm 0.2$ °C
		Data gathering frequency	10 mins	60 mins
		Cost in Euro	1857	1070
		Number of sensors purchased	2	1
		Photo		
		Vendor name	Decentlab GmbH	Sensoterra
		Country of origin	Switzerland	Netherlands



Note. Created by the author, [2023].

**Table 4.** Soil pH sensor variant chosen for LoRaWAN test station.

SI No	Type of sensor	Category	Expensive Variant	Affordable Variant
4	Soil pH Sensor	Name	Dragino Soil Temperature and pH Sensor	
		Model Number	DRA LSPH01	
		Specification	pH :- Range: 3 to 10 pH ; Resolution: 0.01 pH ; Accuracy: ±2%	
			Temperature :- Range: -40 and 85 °C ; Resolution: 0.1 °C; Accuracy: ±0.5°C	
		Data gathering frequency	20 mins	
		Cost in Euro	160 + 2346 integration cost = 2506	160
		Number of sensors purchased	3 ( 2 in use 1 spare )	
		Photo		
		Vendor name	Dragino	
		Country of origin	China	

Note. Created by the author, [2023].

**Table 5.** Comparison expensive and affordable gateway and platform variant chosen for LoRaWAN test station.

SI No	Type of sensor	Category	Expensive Variant	Affordable Variant
5	Gateway	Name	Kerlink Wirnet iStation 868 MHz	Dragino Outdoor LoRaWAN Gateway
		Model Number		DLOS8-868-EC25-E
		Specification	4G and Ethernet (PoE)	4G, WiFi and Ethernet (PoE)
		Cost in Euro	2015	1070
		Number of gateways purchased	1	1
		Photo		
		Vendor name	Decentlab GmbH	Dragino
Country of origin	Switzerland	China		
6	Network Server	Name	The Things Network	The Things Network
		Cost in Euro	Included with the platform cost	Free (for upto 10 devices)
		Vendor name	Decentlab GmbH	The Things Network
		Country of origin	Switzerland	Netherlands
7	Data Storage	Name	Decentlab Platform	Google Sheets
		Cost in Euro	300	Free
		Vendor name	Decentlab GmbH	Google
		Country of origin	Switzerland	USA
8	Visualisation	Name	Decentlab Platform	Nil
		Cost in Euro	955	Nil
		Vendor name	Decentlab GmbH	Nil
		Country of origin	Switzerland	Nil

Note. Created by the author, [2023]

## 2.2. 3D Rendered Plan of the Test Station

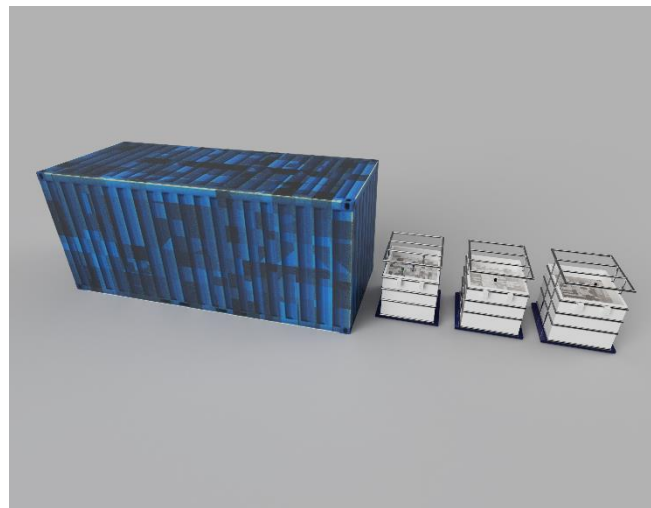
A 3D rendering was made to gain better understanding on how the test station would look like once build and to decide on the placement of the monitoring sensors. The 3D rendering was made in fusion 360. The following are the rendered images.

**Figure 4.** *3D Visualisation of the growing containers.*



Note. 3D model of the growing container made in Autodesk Fusion 360 software. Created by the author, [2023].

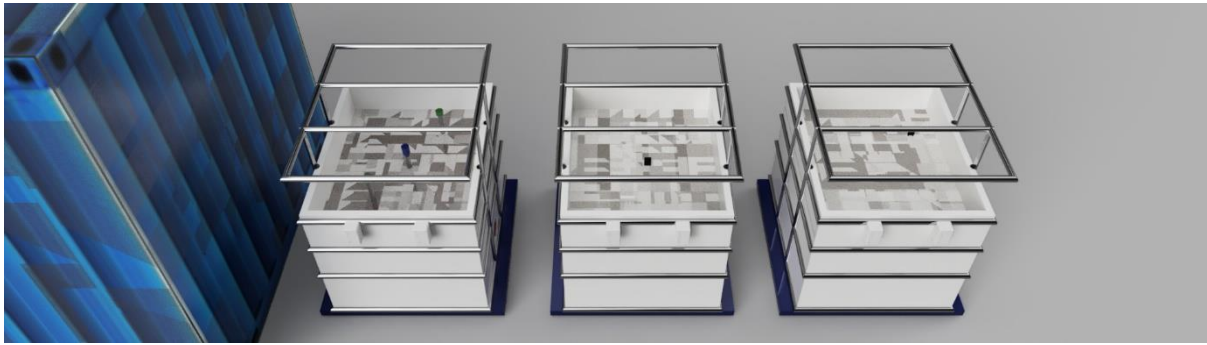
**Figure 5.** *3D Visualisation of the growing containers next to the 20 ft container laboratory.*



Note. 3D Visualisation of the growing containers placed next to the 20 ft container laboratory made in Autodesk Fusion 360 software. Created by the author, [2023].



**Figure 6.** 3D image showing growing area with sensor placement.



Note. Closeup 3D image showing growing area with sensor placement made in Autodesk Fusion 360 software. Created by the author, [2023].

**Figure 7.** 3D image showing sensor placement.

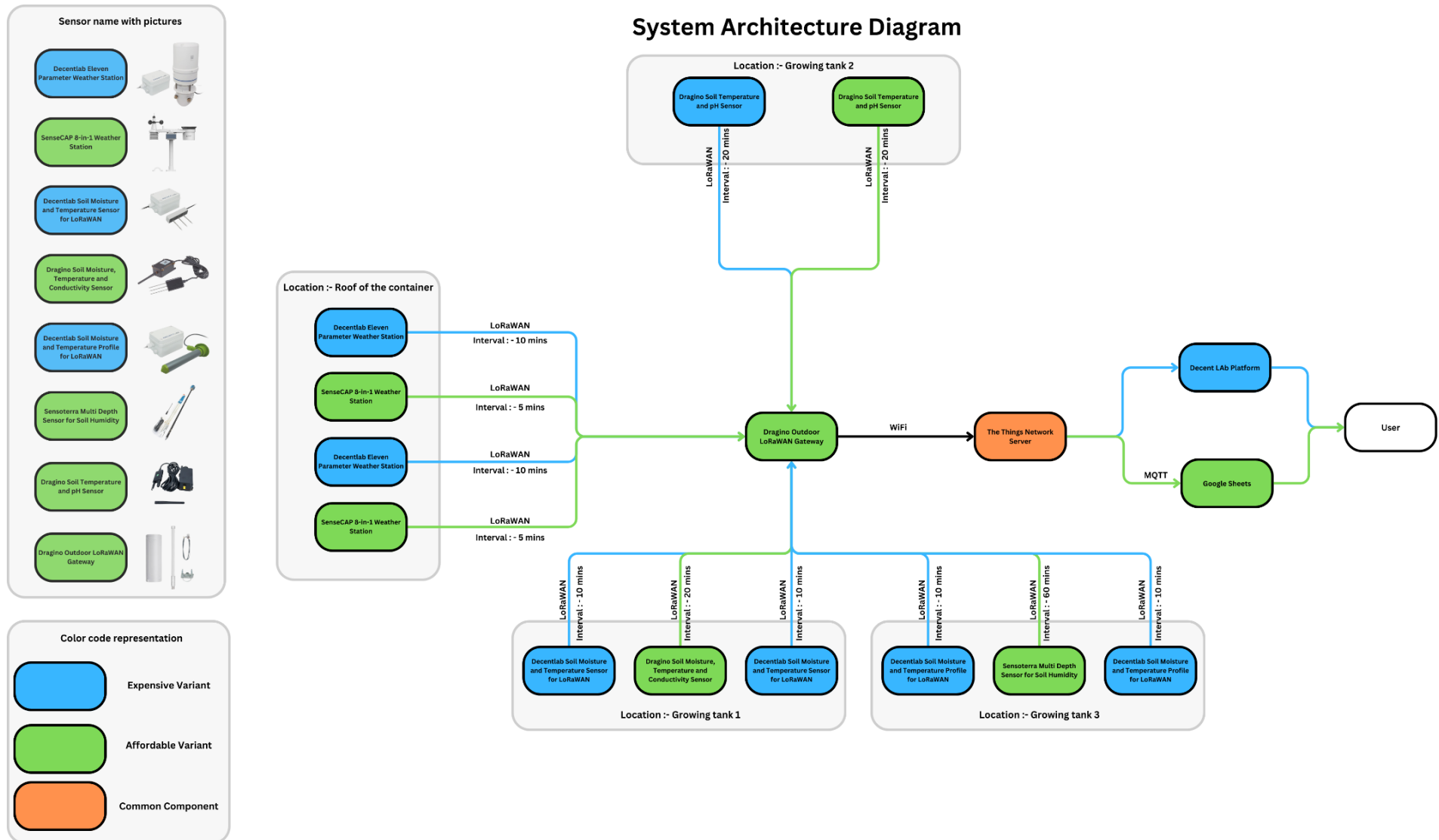


Note. 3D image Sensor placement from various angles made in Autodesk Fusion 360 software. Created by the author, [2023].

### **2.3. Setting up of the test station**

To check the performance of affordable variant of the sensors as compared with the expensive variant of the sensors, 2 parallel systems were set up. Each system has similar set of sensors that collects similar set of data. This data is then analysed to assess the performance of the affordable variant with that of expensive variant. The system architecture diagram is given on the next page.

Figure 8. System architecture diagram.



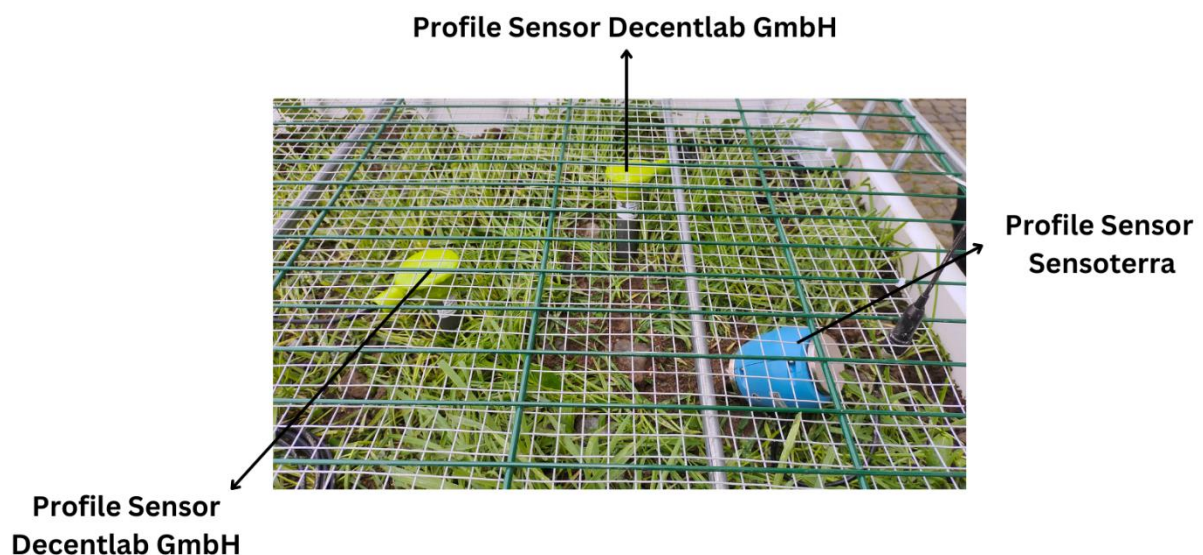
Note. System architecture diagram created in Canva showing the placement and connection between all the components. Created by the author, [2023].

In this system architecture diagram, the green colour represents the system consisting of affordable variants while the blue colour represents the system consisting of expensive variants as shown in the bottom left corner of the diagram. To gain better understanding of the sensors that are used, the sensor names and the respective images are shown in the left-hand side.

All the sensors are divided based on its type and are placed in 4 locations, with each type of sensor being placed collectively at a single location. The 4 weather stations are placed on the top of the existing laboratory container. The 3 soil conductivity sensors are placed together inside the first growing tank. The 2 pH sensors are placed inside the second growing tank. The 3 soil profile sensors are placed together inside the third growing tank.

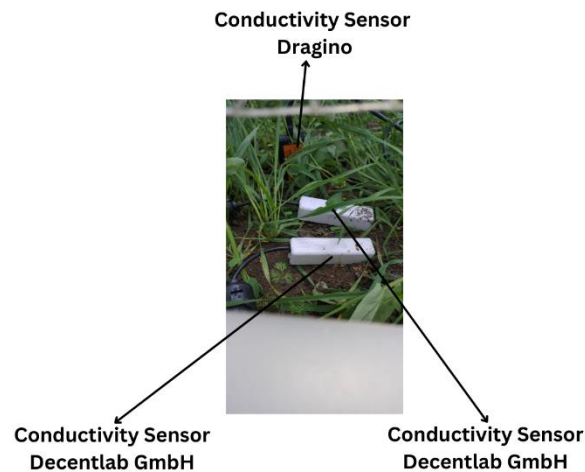
The type of protocol used for communication and the interval at which the data gets transferred is also mentioned. All the data collected by the sensors are sent to the Dragino outdoor LoRaWAN gateway (As only this gateway variant has ability to connect to the internet over Wi-Fi). The data is then transferred to the network server through Wi-Fi connected to internet. Once the data reaches the network server, it is then directed to various platform. The data from expensive sensor variant gets transferred to the Decentlab platform while the data from affordable sensor variant gets transferred to Google Sheets forming an independent system. The performance of this independent system with that of Decentlab Platform is also assessed in this thesis.

**Figure 9.** Photo of the soil profile sensor deployed in the test station.



Note. Photo of soil profile sensors deployed in growing tank 3 of the test station. Created by the author, [2023].

**Figure 10.** *Photo of the soil conductivity sensors deployed in the test station.*



Note. Photo of soil conductivity sensors deployed in growing tank 1 of the test station. Created by the author, [2023].

**Figure 11.** *Photo of the soil pH sensors deployed in the test station.*



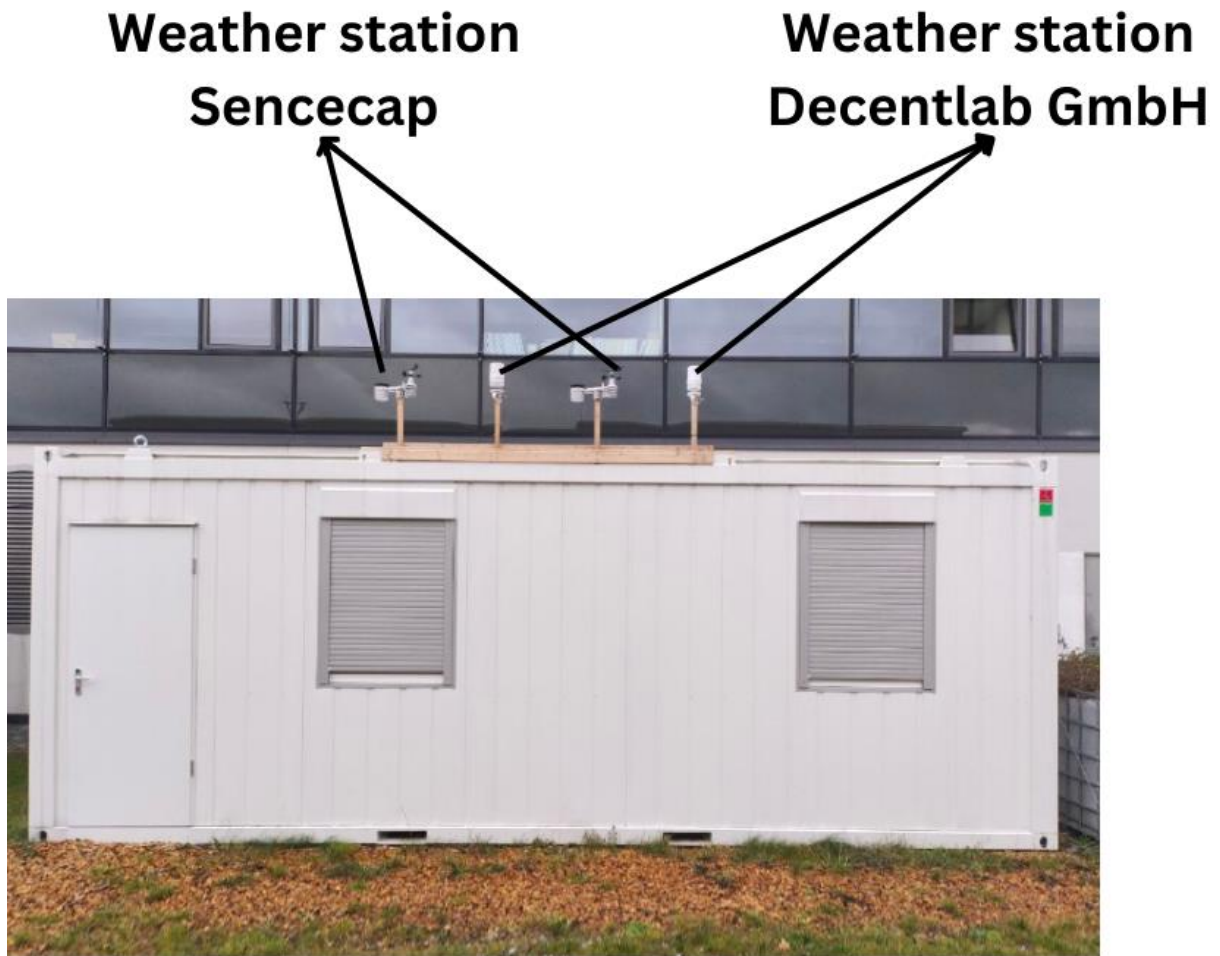
Note. Photo of soil pH sensors deployed in growing tank 2 of the test station. Of the 3 pH sensors, only 2 are included in the test station. Created by the author, [2023].

It was decided to place the 4 weather stations lengthwise on top of the container as this would guarantee even and homogeneous conditions across all the weather stations. An assembly was made from wood to house all the weather stations and later all the weather stations were placed within this assembly.

The setting up of the LoRaWAN test station at Hochschule Hof was done by the author, Mr Pavel Timofeev (Wissenschaftlicher Mitarbeiter at Hochschule Hof) and Mr Michael Schmidt (Wissenschaftlicher Mitarbeiter at Hochschule Hof) under the guidance of Professor Günter Müller-Czygan.



**Figure 12.** *Photo of the weather stations deployed in the test station.*



Note. Photo of weather stations deployed for the test station, located top of the laboratory container. Of the 3 pH sensors, only 2 are included in the test station. Created by the author, [2023].

**Figure 13.** *Photo showing the growing containers.*



Note. Photo showing the 3 1000 L IBC container with soil in which soil sensors are placed. Created by the author, [2023].

### **3. Data analysis**

#### **3.1. Overview**

The data captured from the sensors were stored in google sheets and in the Decentlab platform. The data collection was done for 2.5 months form Aug 1st, 2023, to Oct 15th, 2023. The data from both platforms can be extracted in the comma separated value (‘.csv’) format. The '.csv' format is used because of its ease of managing tabular data and its use in data analytics.

The data that is received in the ‘.csv’ format must be cleaned before analysing it. Although, data cleaning and data analysis can be done in any integrated development environment software, Visual Studio Code (VS Code) software was chosen for preliminary data analysis. The reason for choosing VS Code software was that for preliminary data analysis, the memory usage and the processing power needed is less and VS code can also be used offline unlike Google Colab. The programming file format used in coding is Interactive Python Notebook (‘.ipynb’) format. The reason for choosing this format is because ‘.ipynb’ facilitate interactive computing, enabling users to write and execute code in a flexible and interactive manner, while supporting the inclusion of text, images, and other media which is particularly useful for data analysis and scientific research.

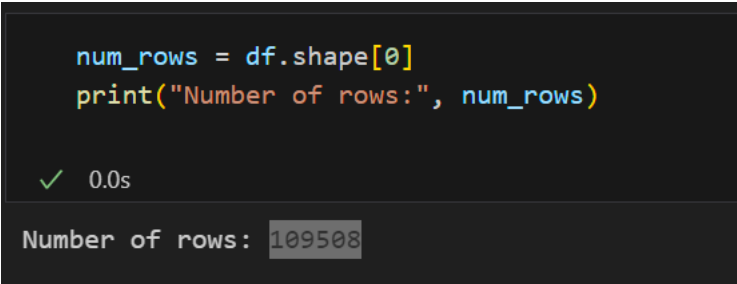
#### **3.2. Data interpolation**

The data from various sensors is being gathered at different intervals. Some of the sensors are generating data at an interval of 5 mins, some at 10 mins, and the rest at 20 mins. Due to this irregularity in data collection, for effective comparison of the data, the data needs to be cleaned and interpolated accordingly. In the data cleaning part, data from the original dataset is copied and pasted into a new dataset that has the timestamp in the format “Date-Month-Year Hour: Minute” omitting the “Seconds” form the new dataset. Once the original dataset is copied to the new dataset based on the timestamp, all the missing values are filled with ‘0’ or ‘Nan’. After this step linear data interpolation is carried out. Data interpolation on a linear basis involves estimating unknown values between two known data points by drawing a straight line between them. The assumption is that the change between the two data points is consistent and linear. Using this linear relationship, values within a given interval is filled in. Once data interpolation is done, a dataset of continuous data is available with 109,508 distinct rows of datapoints for each parameter (1 row of data every minute from 00:00 01.08.2023 to 00:00 16.10.2023). The correlation matrix is calculated from this dataset and correlation heatmaps are generated for the same.

### 3.3. Method Description

The heatmaps are generated through the analysis of the dataset by a programming code written in VS Code. Initially the code imports the libraries required for the functioning of the programme. Then dataset in '.csv' format is imported into the programme and the parameters are renamed into a standard form. Except for the 'A\_Timestamp' column (which has date and time data), the entire parameter list is converted into float to make it comparable with other. A new empty dataset is created on 'A\_Timestamp' from 00:00 01.08.2023 to 00:00 16.10.2023. Both the datasets are merged on 'A\_Timestamp' variable. The missing values are filled in using linear interpolation method to have 109,508 distinct rows of datapoints. In the subsequent section correlation matrix is calculated and correlation heatmaps are generated. It is to be noted that although in the core part, the programme uses the standardised method for generation of correlation heatmaps, other parts of the programme have been custom made by the author for this use case scenario. A sample code for the same is given in the appendix section.

Figure 14. Screenshot of the datapoints.



```
num_rows = df.shape[0]
print("Number of rows:", num_rows)

✓ 0.0s
Number of rows: 109508
```

Note. Screenshot taken from programme running on VS Code showing the number of datapoints. Created by the author, [2023].

### 3.4. Correlation heatmap generation and analysis

For the scope of this master's thesis, the data from the sensors are used to generate a correlation heatmap. A correlation heatmap is a graphical representation of the correlation matrix between various parameters in a dataset. It is in the opinion of the author that this graphical representation makes it easier to understand the relation between various parameters and hence is the primary reason for choosing correlation heatmap for data analysis. The correlation matrix is a matrix that consist of a collection of pairwise individual correlations (Pearson correlation coefficient) between measured parameters. Pearson correlation coefficient (R) measures the relationship between two individual parameters (Benesty, 2009). Pearson correlation coefficient closer to 1 implies a strong positive correlation. Pearson correlation coefficient closer to -1 implies a strong negative correlation and a value close to 0 indicates no correlation.

The below given table from an article published by (Schober, 2018) showing the interpretation of the values of Pearson correlation coefficient.

**Table 6.** Table showing the interpretation of the values of Pearson correlation coefficient (R).

<b>Absolute magnitude of the observed Pearson correlation coefficient (R)</b>	<b>Interpretation</b>
0.00 – 0.10	Negligible correlation
0.10 – 0.39	Weak correlation
0.40 – 0.69	Moderate correlation
0.70 – 0.89	Strong correlation
0.90 – 1.00	Very strong correlation

Note. Note. Adapted from "Correlation Coefficients: Appropriate Use and Interpretation," by P. Schober, C. Boer, & L. Schwarte, 2018, *Anesthesia & Analgesia*, 126, p. 1. <https://doi.org/10.1213/ANE.0000000000002864>

The square of Pearson correlation coefficient is termed as coefficient of determination ( $R^2$ ). The coefficient of determination measures the extent to which the changes in one factor can be explained by changes in other factors, in the form of a percentage (Liu H.-Y. a., 2019). In the scope of this master's thesis, a  $R^2$  value near 1 suggests that the output of the affordable sensor variant closely aligns with that of expensive sensor variant, showing strong linearity. Conversely, a low value closer to 0 indicates a weak linear connection. The below given table is showing the interpretation of the values of coefficient of determination ( $R^2$ ) inferred from a published article (Chang, 2001). The use of the coefficient of determination ( $R^2$ ) is advised as a standard for assessing regression analyses across various scientific fields (Chicco, 2021).

**Table 7.** Table showing the interpretation of the values of coefficient of determination ( $R^2$ ).

<b>Magnitude of the coefficient of determination (<math>R^2</math>)</b>	<b>Interpretation</b>
0.00 – 0.50	Negligible correlation
0.50 – 0.60	Weak to moderate correlation
0.60 – 0.80	Moderate to strong correlation
0.80 – 1.00	Very strong correlation

Note. Table created by the author based on analysis and interpretation of data presented in "Near-Infrared Reflectance Spectroscopy–Principal Components Regression Analyses of Soil Properties," by C.-W. Chang, D. Laird, M. Mausbach, & C. Hurburgh, 2001, *Soil Science Society of America Journal*, 65, pp. 480-490. <https://doi.org/10.2136/sssaj2001.652480x>



In the scope of this master's thesis, "coolwarm" correlation heatmap are being generated from the datasets of expensive and affordable sensor variants. This type of heatmap uses a colour gradient, where cooler colours (like blue) represent negative correlation values and warmer colours (like red) indicate positive correlation values.

Correlation heatmaps were generated for checking the correlation of the following conditions:

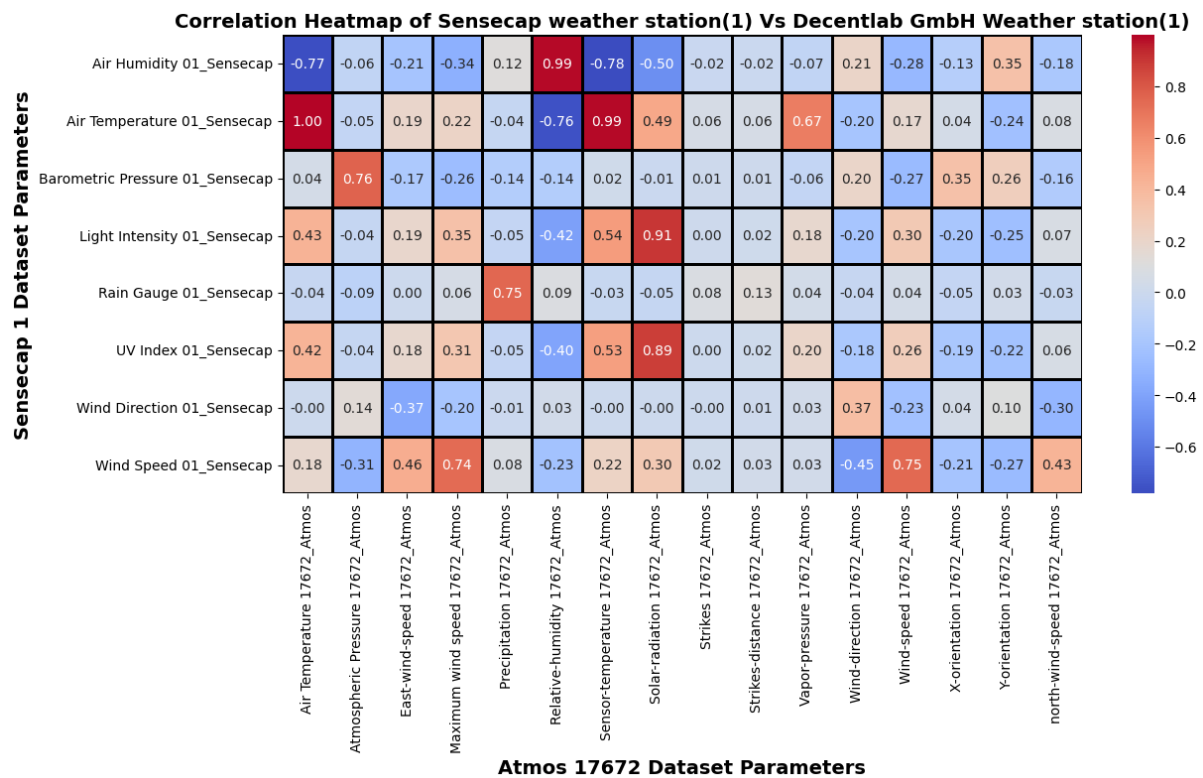
1. To check the correlation between data gathered from affordable and expensive sensors.
  - a. Sensecap weather station (1) Vs Decentlab weather station (1).
  - b. Sensecap weather station (2) Vs Decentlab weather station (2).
  - c. Sensecap weather station (1) Vs Sensecap weather station (2).
  - d. Decentlab weather station (1) Vs Decentlab weather station (2).
  - e. Conductivity sensor (17678) from Decentlab Vs Conductivity sensor from Dragino.
  - f. Conductivity sensor (17678) from Decentlab Vs Conductivity sensor (17679) from Decentlab.
  - g. Soil profile sensor (17674) from Decentlab Vs Soil profile sensor (17675) from Decentlab
2. To check the correlation between the data collected by Decentlab platform and the data collected in google sheets over MQTT (Message Queuing Telemetry Transport) protocol.
  - a. Decentlab Weather station in Decentlab Platform vs Decentlab Weather station in Google Sheets.
  - b. Decentlab Conductivity sensor in Decentlab Platform vs Decentlab Conductivity sensor in Google Sheets.
  - c. Decentlab soil profile sensor in Decentlab Platform vs Decentlab soil profile sensor in Google Sheets.
  - d. Dragino pH sensor in Decentlab Platform vs Dragino pH sensor in Google Sheets.
3. Anomalies in gathering data from Sensoterra soil profile sensor.

The pH sensor was not present in the inventory of the Decentlab GmbH and hence it was decided to purchase the pH sensor from an affordable sensor manufacturer and integrate the same in the Decentlab Platform at an additional cost. This was done to check whether there is any difference in the quality of data collected over the Decentlab Platform and the independent system that was set up at Hochschule Hof. This step was deemed necessary to check whether there is a need to use Decentlab Platform for integration of sensors (along with 3<sup>rd</sup> party sensors) in the planned field implementation.

The first correlation heatmap shows the overall Pearson correlation coefficient (R) between all parameters of expensive and affordable variant of the sensor. The second correlation heatmap highlights those parameters having Pearson correlation coefficient (R) between 0.74 and 1. The third correlation heatmap shows coefficient of determination ( $R^2$ ) value of the highlighted parameters between 0.55 and 1.

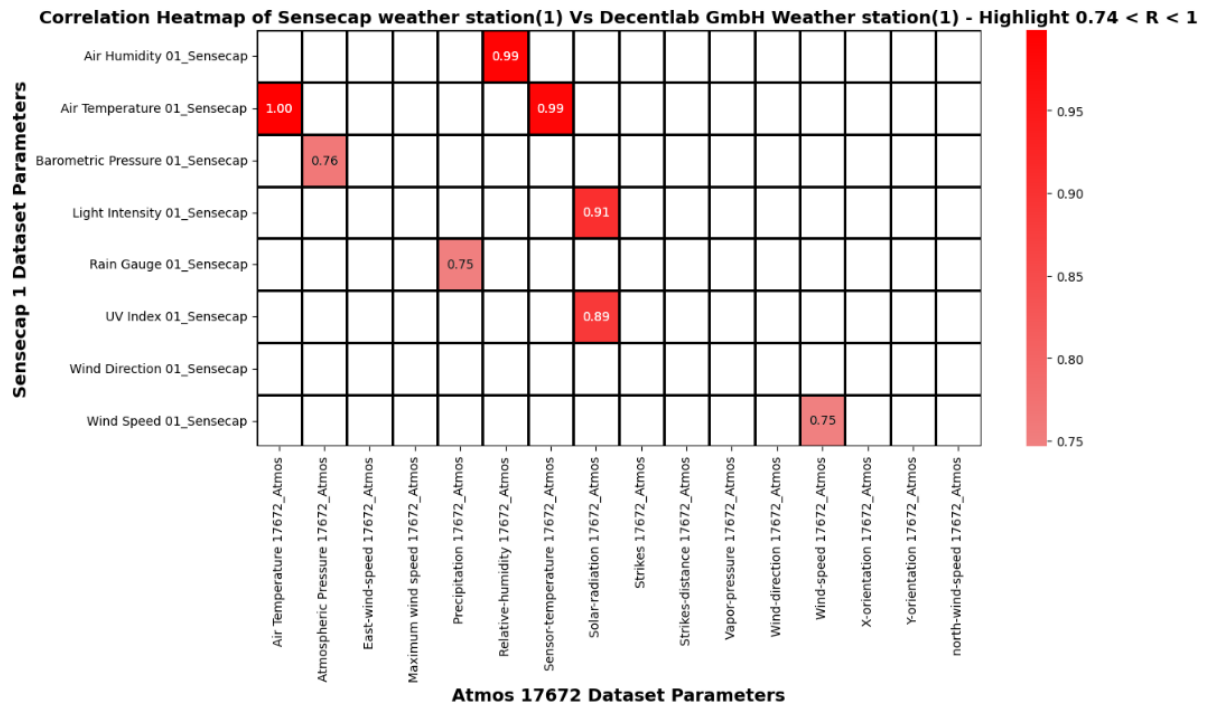
### 3.4.1. Sensecap weather station (1) Vs Decentlab weather station (1)

Figure 15. Overall correlation heatmap of Sensecap weather station (1) Vs Decentlab weather station (1).



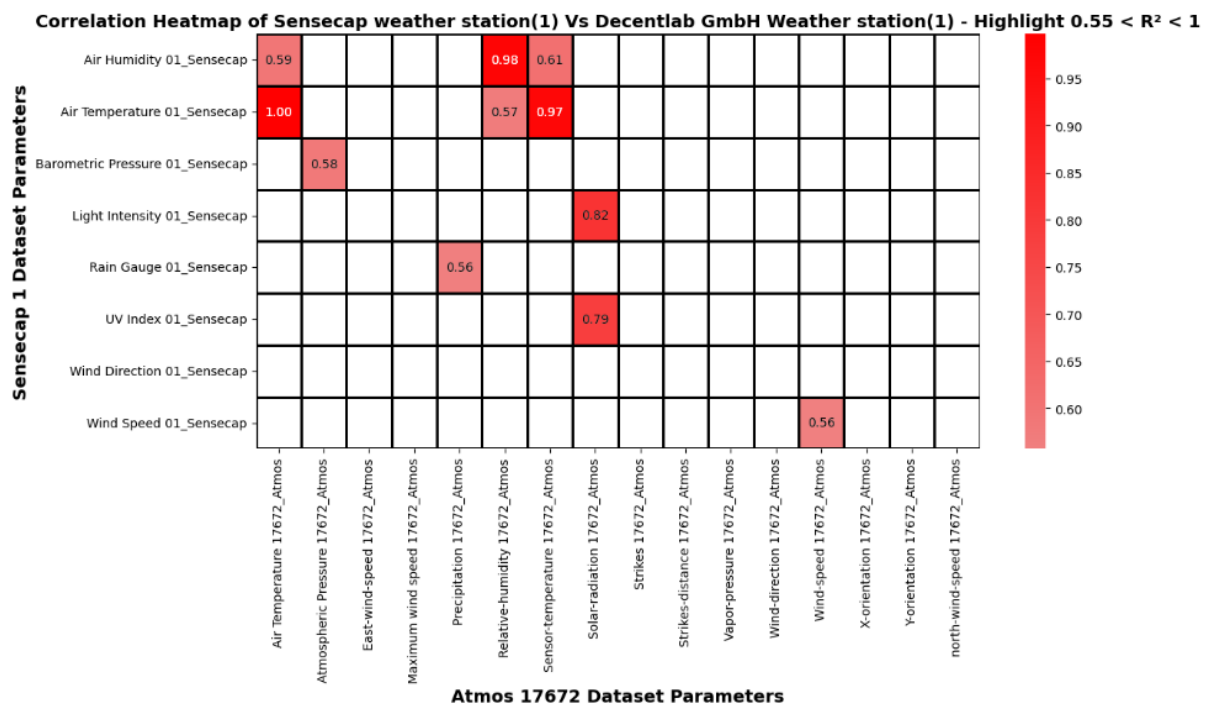
Note. Overall correlation heatmap depicting Pearson correlation coefficient (R) between all parameters measured by Sensecap weather station (1) Vs Decentlab weather station (1). Created by the author, [2023].

Figure 16. Simplified correlation heatmap of Sensecap weather station (1) Vs Decentlab weather station (1).



Note. Simplified Correlation heatmap depicting Pearson correlation coefficient (R) between 0.74 and 1.0 between the parameters measured by Sensecap weather station (1) Vs Decentlab weather station (1). Created by the author, [2023].

Figure 17. Simplified coefficient of determination ( $R^2$ ) heatmap of Sensecap weather station (1) Vs Decentlab weather station (1).



Note. Simplified correlation heatmap depicting coefficient of determination ( $R^2$ ) above 0.55 and 1 between the parameters measured by Sensecap weather station (1) Vs Decentlab weather station (1). Created by the author, [2023].

### Classification based on heatmaps:

From all three heat maps it can be interpreted that there exists a very strong correlation between air temperature, air humidity and light intensity measured by affordable sensor variant with that of air temperature, relative humidity and solar radiation measured by expensive sensor variant.

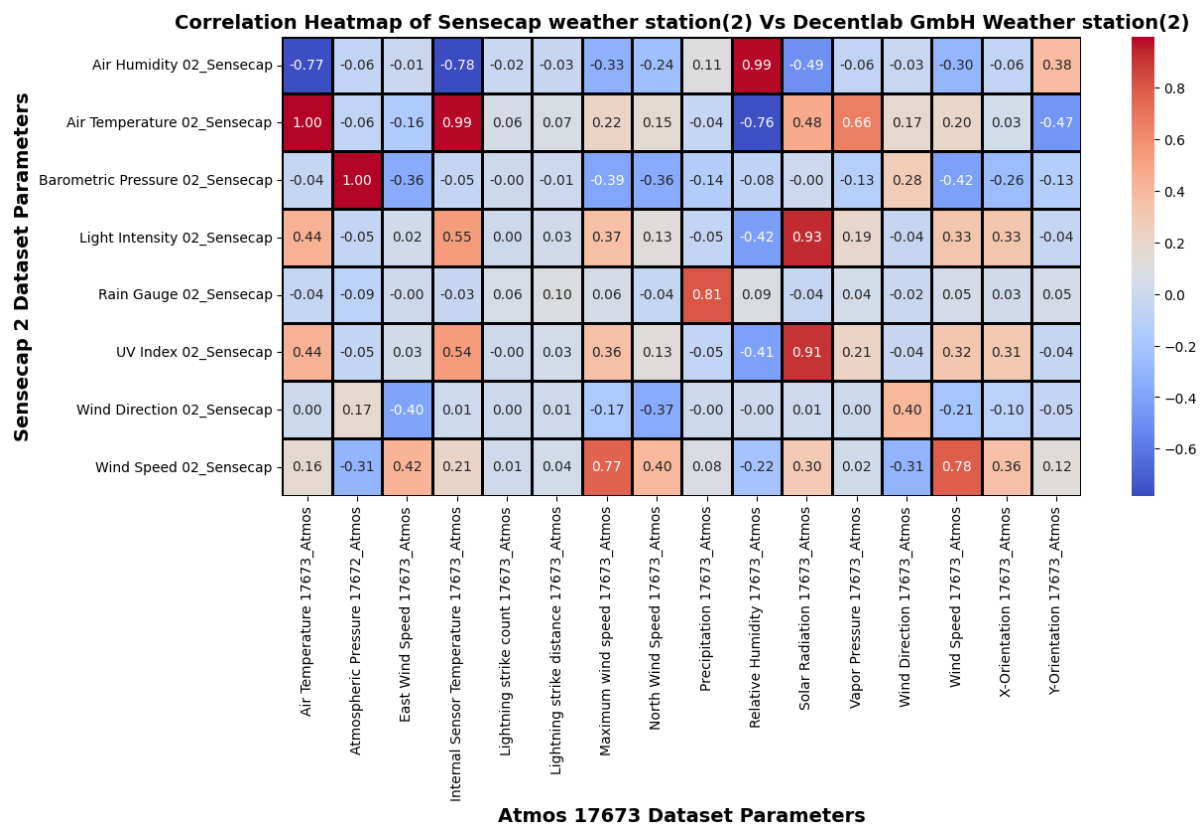
There exists a moderate to strong correlation between ultraviolet index (UV Index) measured by affordable sensor variant with that of solar radiation measured by expensive sensor variant.

There exists a weak to moderate correlation between barometric pressure, rain gauge and wind speed measured by affordable sensor variant with that atmospheric pressure, precipitation and wind speed measured by expensive sensor variant.

There exists negligible correlation between wind direction measured by affordable sensor variant with that of wind direction measured by expensive sensor variant.

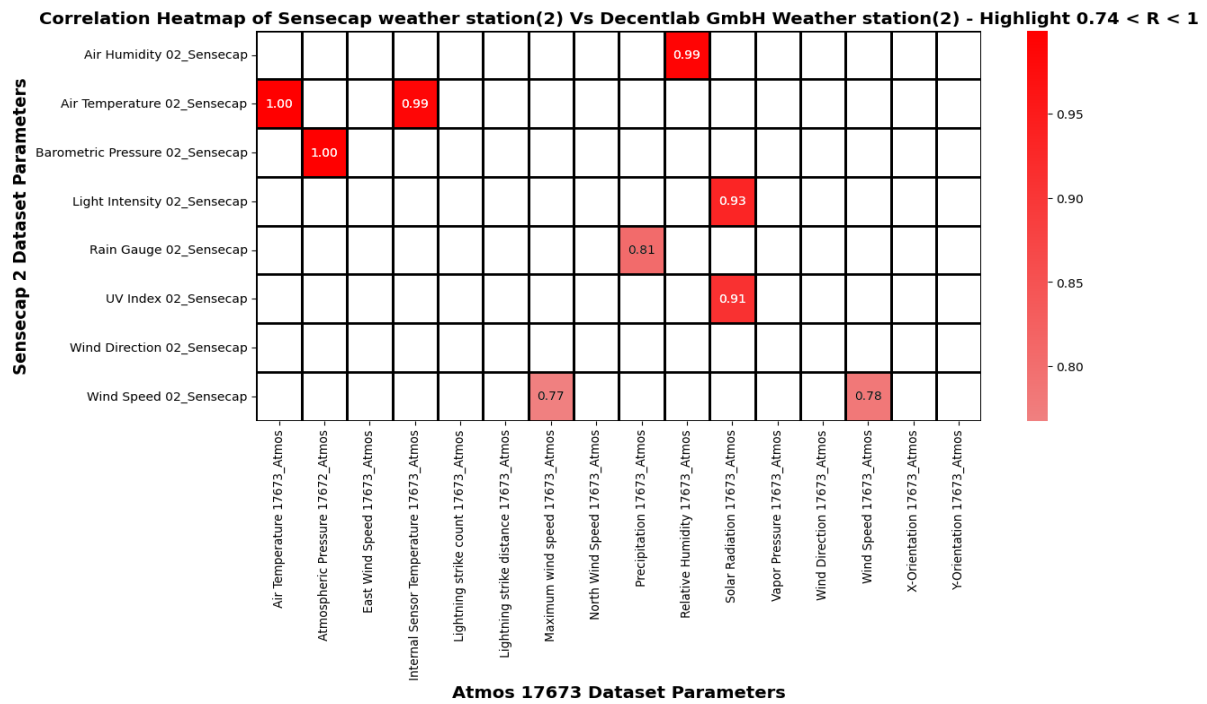
### 3.4.2. Sensecap weather station (2) Vs Decentlab Weather station (2)

Figure 18. Overall correlation heatmap of Sensecap weather station (2) Vs Decentlab weather station (2).



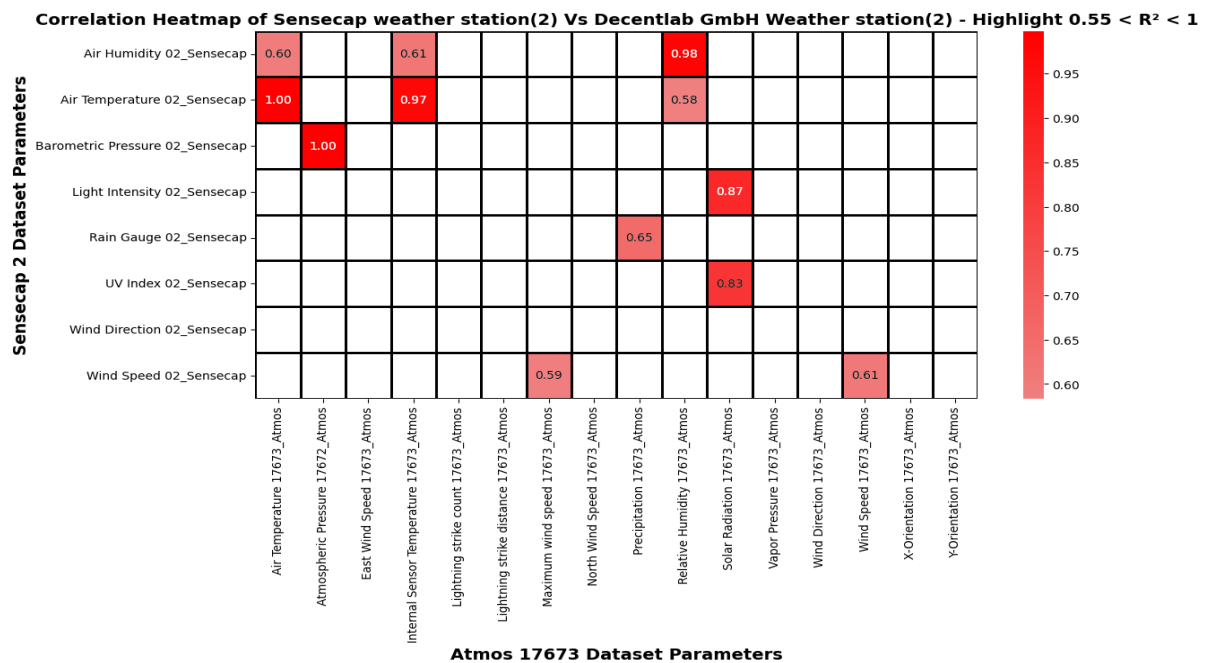
Note. Overall correlation heatmap depicting Pearson correlation coefficient (R) between all parameters measured by Sensecap weather station (2) Vs Decentlab weather station (2). Created by the author, [2023].

Figure 19. Simplified correlation heatmap of Sensecap weather station (2) Vs Decentlab weather station (2).



Note. Simplified Correlation heatmap depicting Pearson correlation coefficient (R) between 0.74 and 1.0 between the parameters measured by Sensecap weather station (2) Vs Decentlab weather station (2). Created by the author, [2023].

Figure 20. Simplified coefficient of determination ( $R^2$ ) heatmap of Sensecap weather station (2) Vs Decentlab weather station (2).



Note. Simplified correlation heatmap depicting coefficient of determination ( $R^2$ ) above 0.55 and 1 between the parameters measured by Sensecap weather station (2) Vs Decentlab weather station (2). Created by the author, [2023].

### Classification based on heatmaps:

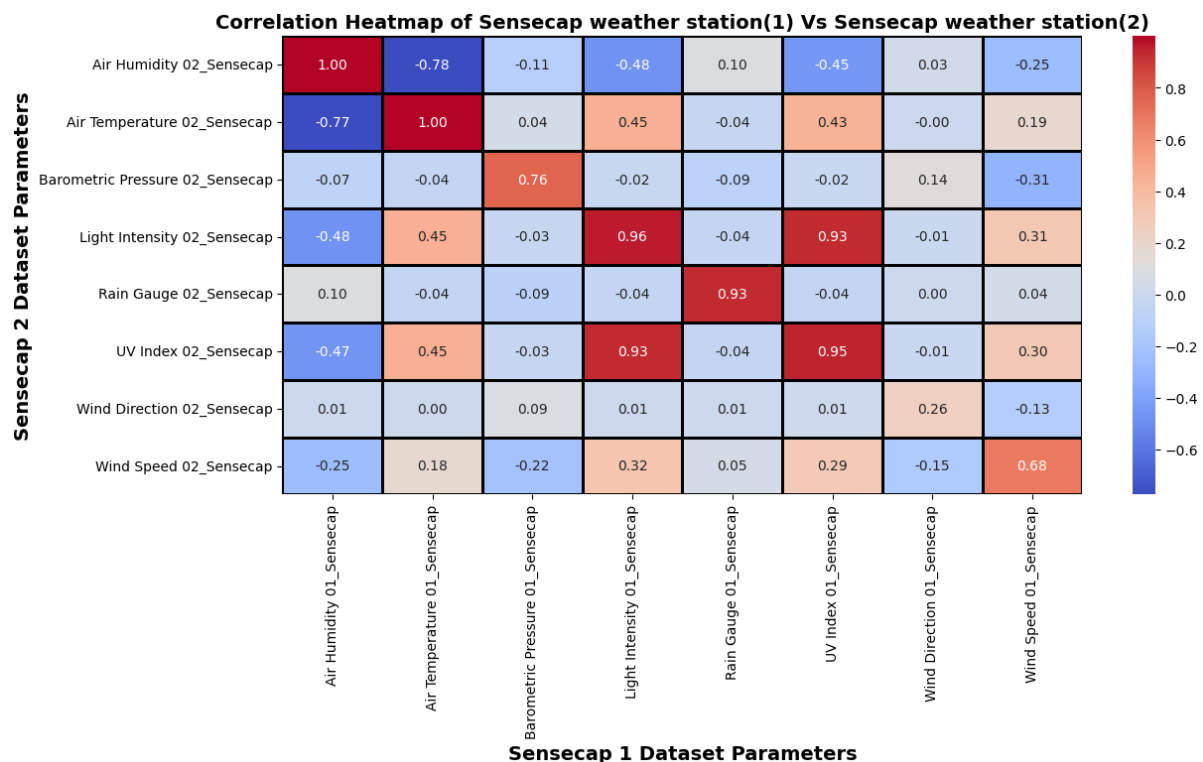
From all three heat maps it can be interpreted that there exists a very strong correlation between air temperature, air humidity, barometric pressure, UV Index, and light intensity measured by affordable sensor variant with that of air temperature, relative humidity, atmospheric pressure, solar radiation, and solar radiation measured by expensive sensor variant.

There exists a moderate to strong correlation between rain gauge and wind speed measured by affordable sensor variant with that of precipitation and wind speed measured by expensive sensor variant.

There exists negligible correlation between wind direction measured by affordable sensor variant with that of wind direction measured by expensive sensor variant.

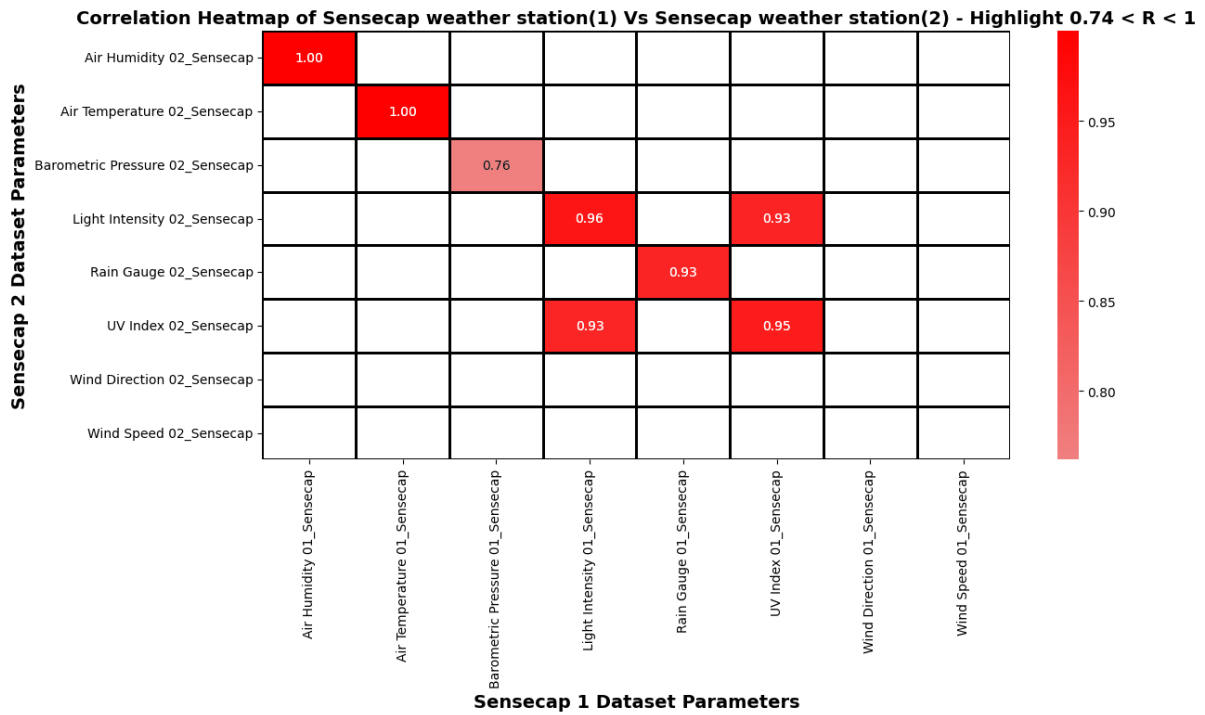
### 3.4.3. Sensecap weather station (1) Vs Sensecap weather station (2)

Figure 21. Overall correlation heatmap of Sensecap weather station (1) Vs Sensecap weather station (2).



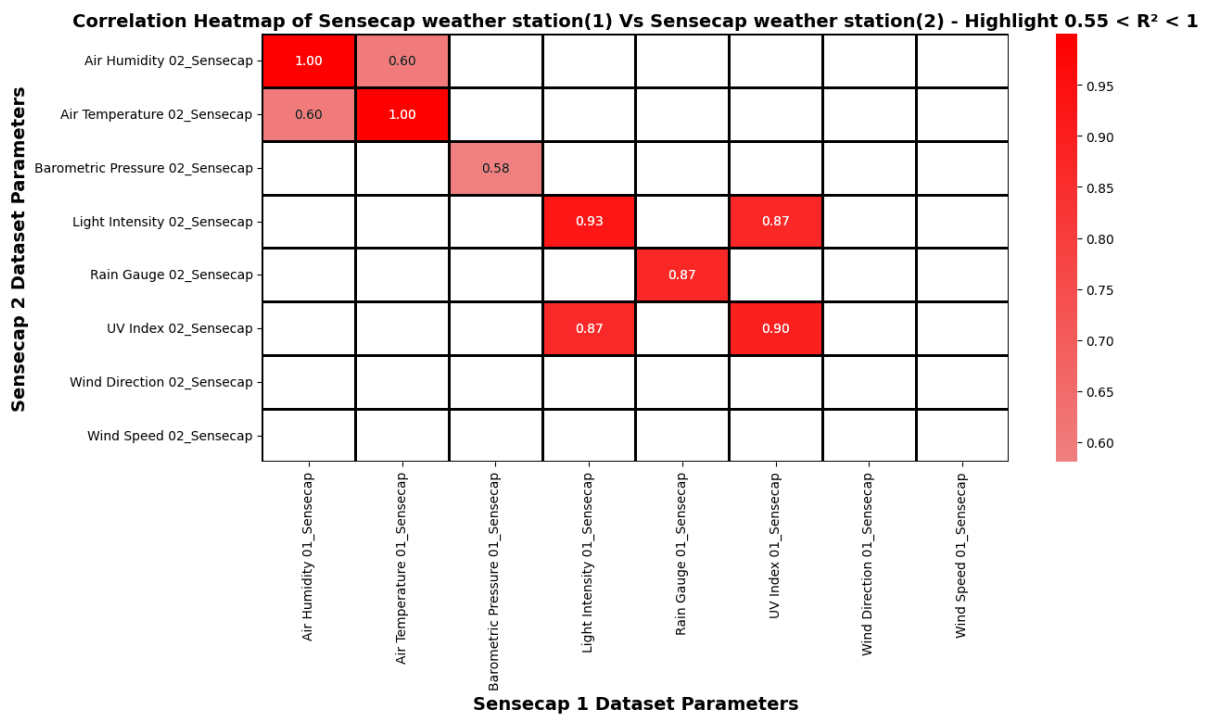
Note. Overall correlation heatmap depicting Pearson correlation coefficient (R) between all parameters measured by Sensecap weather station (1) Vs Sensecap weather station (2). Created by the author, [2023].

**Figure 22.** Simplified correlation heatmap of Sensecap weather station (1) Vs Sensecap weather station (2).



Note. Simplified Correlation heatmap depicting Pearson correlation coefficient (R) between 0.74 and 1.0 between the parameters measured by Sensecap weather station (1) Vs Sensecap weather station (2). Created by the author, [2023].

**Figure 23.** Simplified coefficient of determination ( $R^2$ ) heatmap of Sensecap weather station (1) Vs Sensecap weather station (2).



Note. Simplified correlation heatmap depicting coefficient of determination ( $R^2$ ) above 0.55 and 1 between the parameters measured by Sensecap weather station (1) Vs Sensecap weather station (2). Created by the author, [2023].

### Classification based on heatmaps:

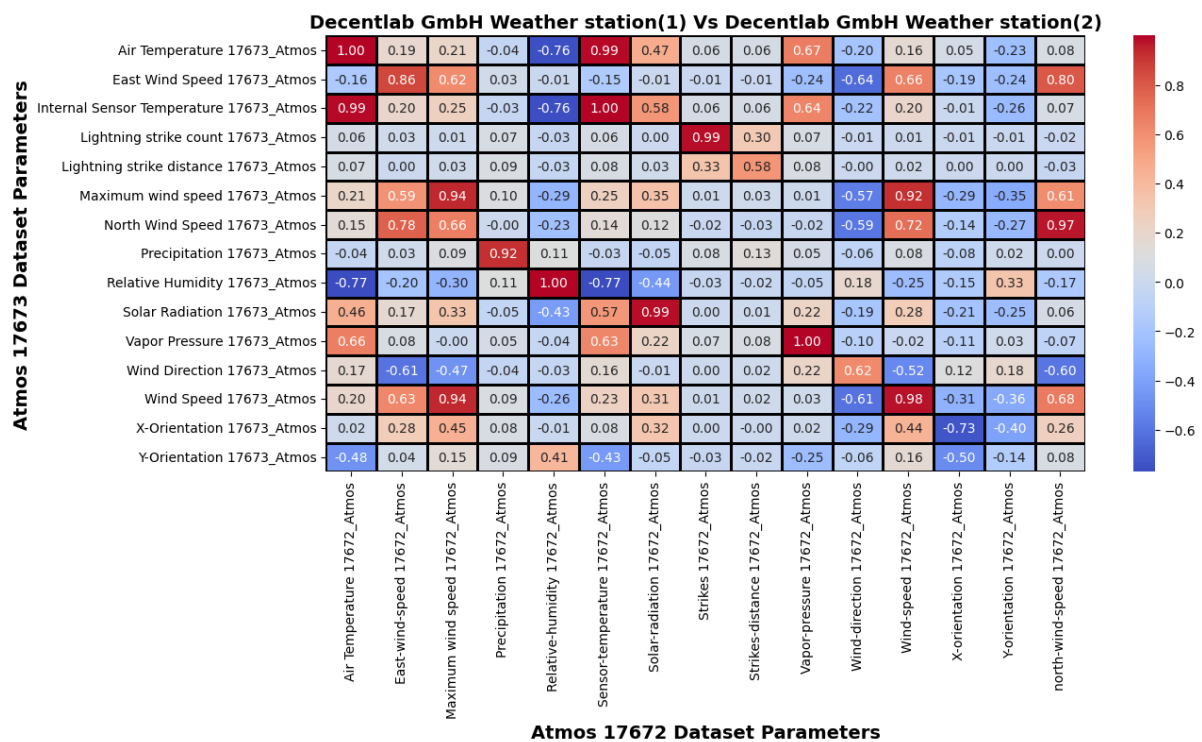
From all three heat maps it can be interpreted that there exists a very strong correlation between air temperature, air humidity, rain gauge, UV Index and light intensity measured by Sensecap 1 with that of air temperature, air humidity, rain gauge, UV Index and light intensity measured by Sensecap 2.

There exists a weak to moderate correlation between barometric pressure measured by Sensecap 1 with that of barometric pressure measured by Sensecap 2.

There exists negligible correlation between wind speed and wind direction measured by Sensecap 1 with that of wind speed and wind direction measured by Sensecap 2.

### 3.4.4. Decentlab weather station (1) Vs Decentlab weather station (2)

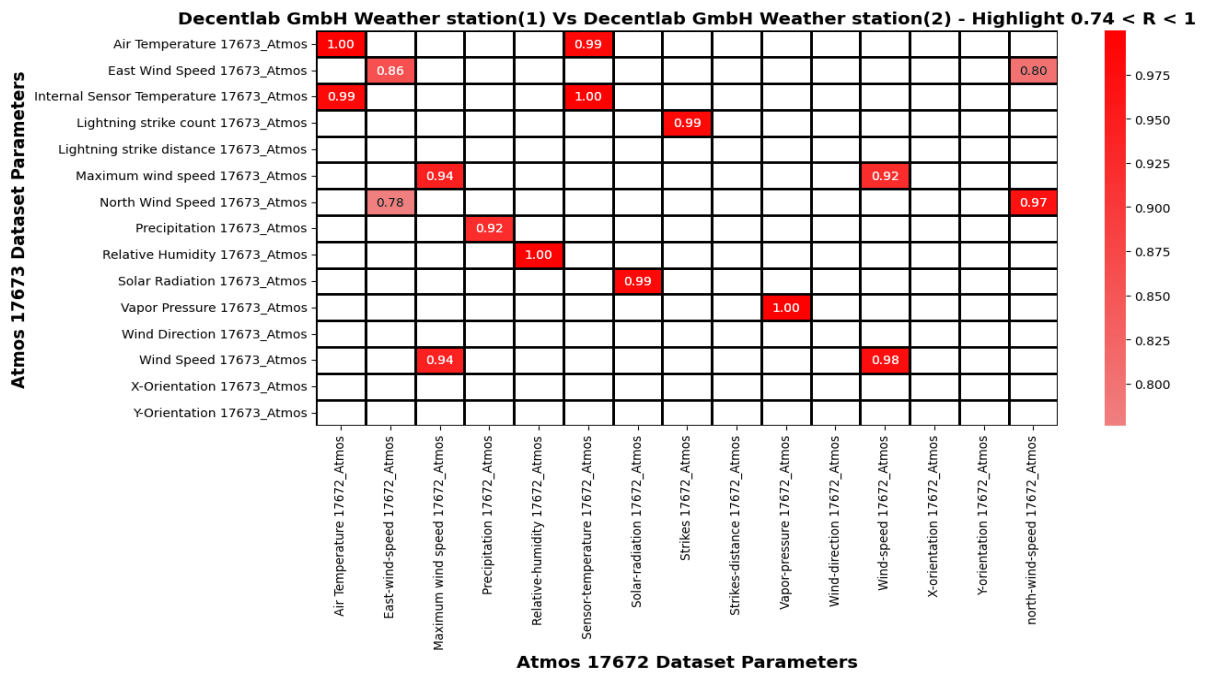
Figure 24. Overall correlation heatmap of Decentlab weather station (1) Vs Decentlab weather station (2).



Note. Overall correlation heatmap depicting Pearson correlation coefficient (R) between all parameters measured by Decentlab weather station (1) Vs Decentlab weather station (2). Created by the author, [2023].

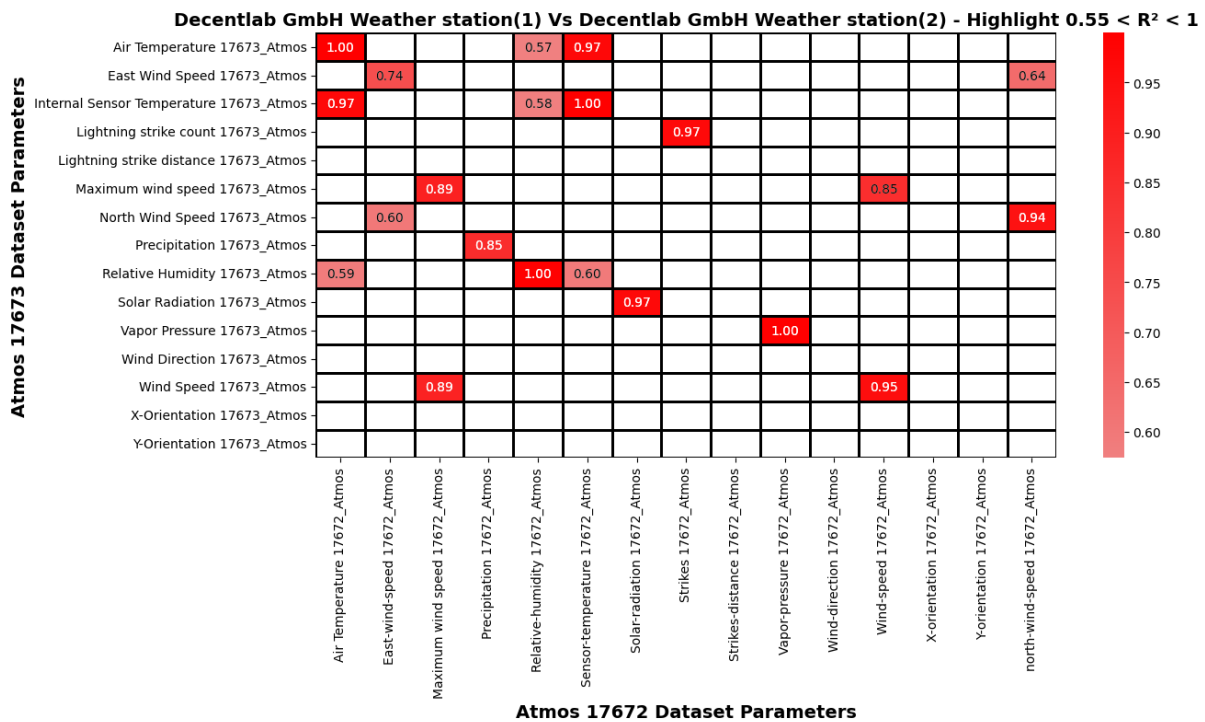


Figure 25. Simplified correlation heatmap of Decentlab weather station (1) Vs Decentlab weather station (2).



Note. Simplified Correlation heatmap depicting Pearson correlation coefficient (R) between 0.74 and 1.0 between the parameters measured by Decentlab weather station (1) Vs Decentlab weather station (2). Created by the author, [2023].

Figure 26. Simplified coefficient of determination ( $R^2$ ) heatmap of Decentlab weather station (1) Vs Decentlab weather station (2).



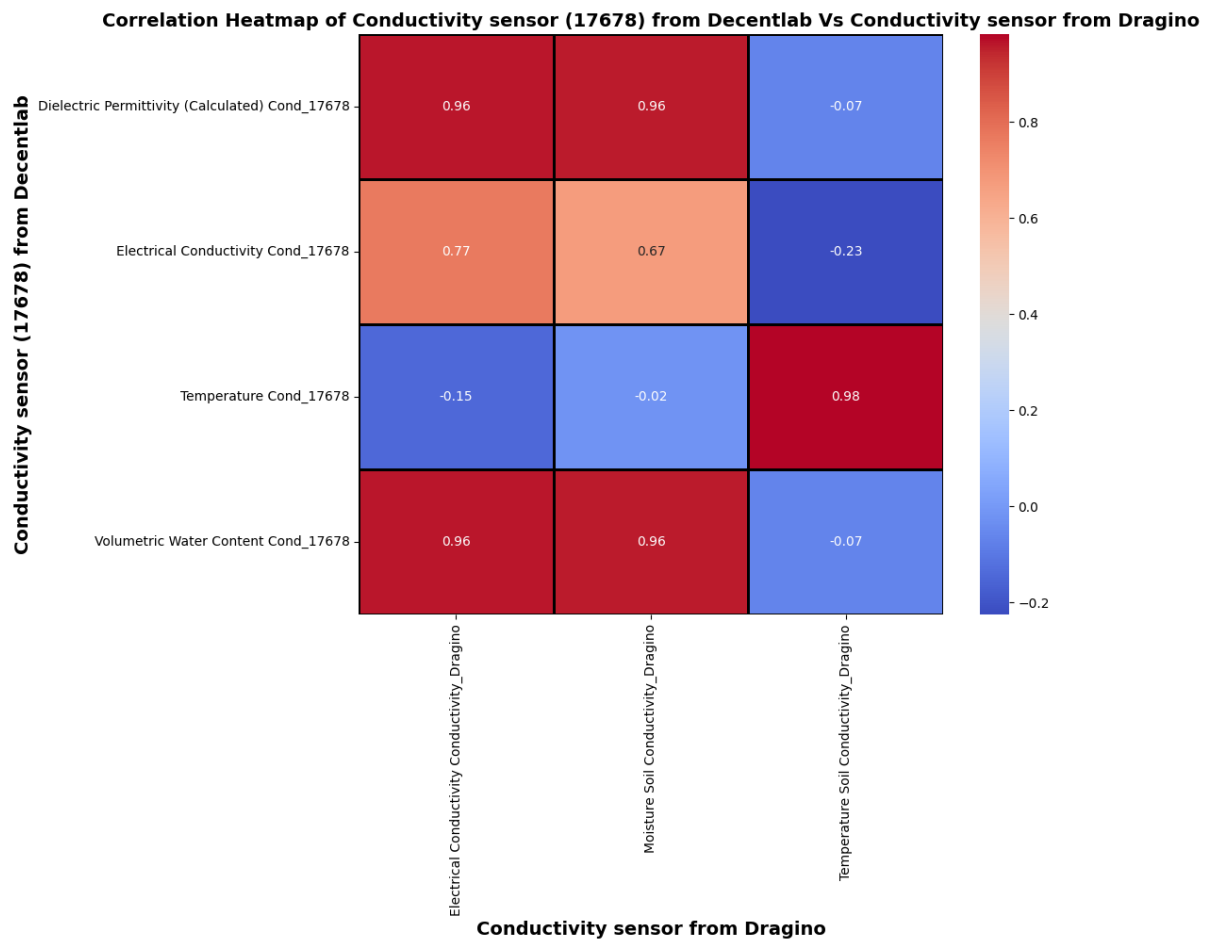
Note. Simplified correlation heatmap depicting coefficient of determination ( $R^2$ ) above 0.55 and 1 between the parameters measured by Decentlab weather station (1) Vs Decentlab weather station (2). Created by the author, [2023].

### Classification based on heatmaps:

From all three heat maps it can be interpreted that there exists a very strong correlation between all the parameters measured by both weather station supplied by Decentlab.

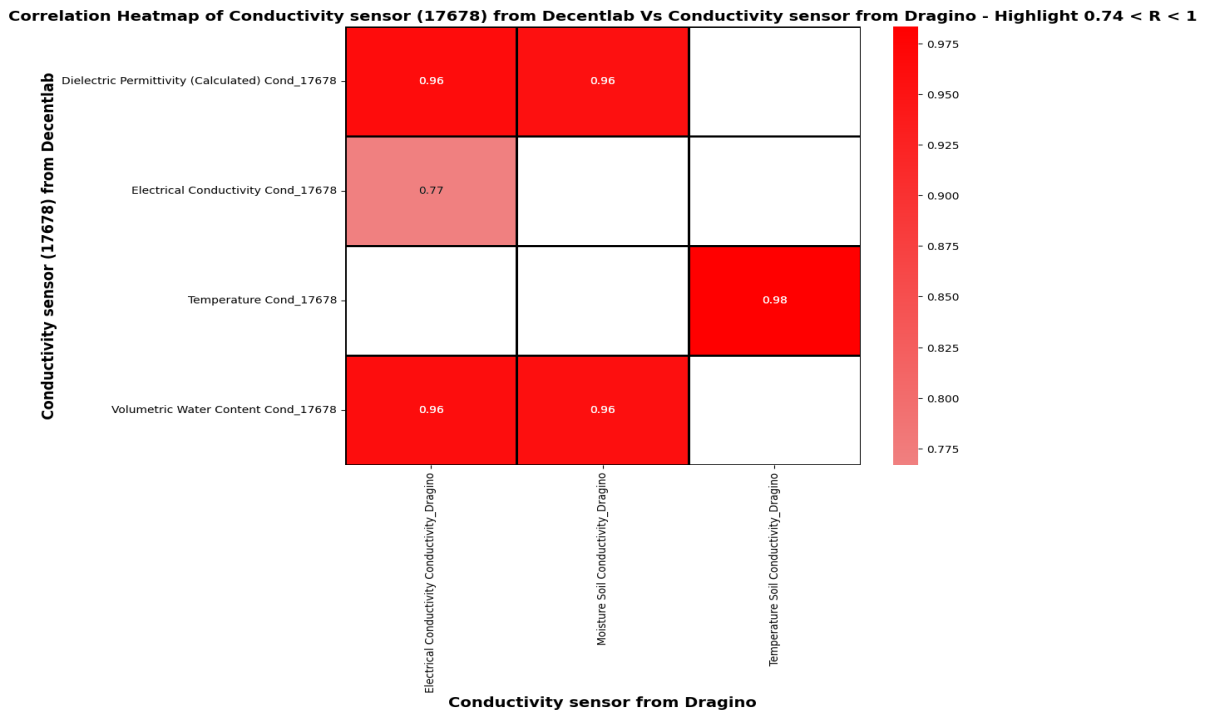
### 3.4.5. Dragino conductivity sensor Vs Decentlab Conductivity sensor

Figure 27. Overall correlation heatmap of Dragino conductivity sensor Vs Decentlab Conductivity sensor.



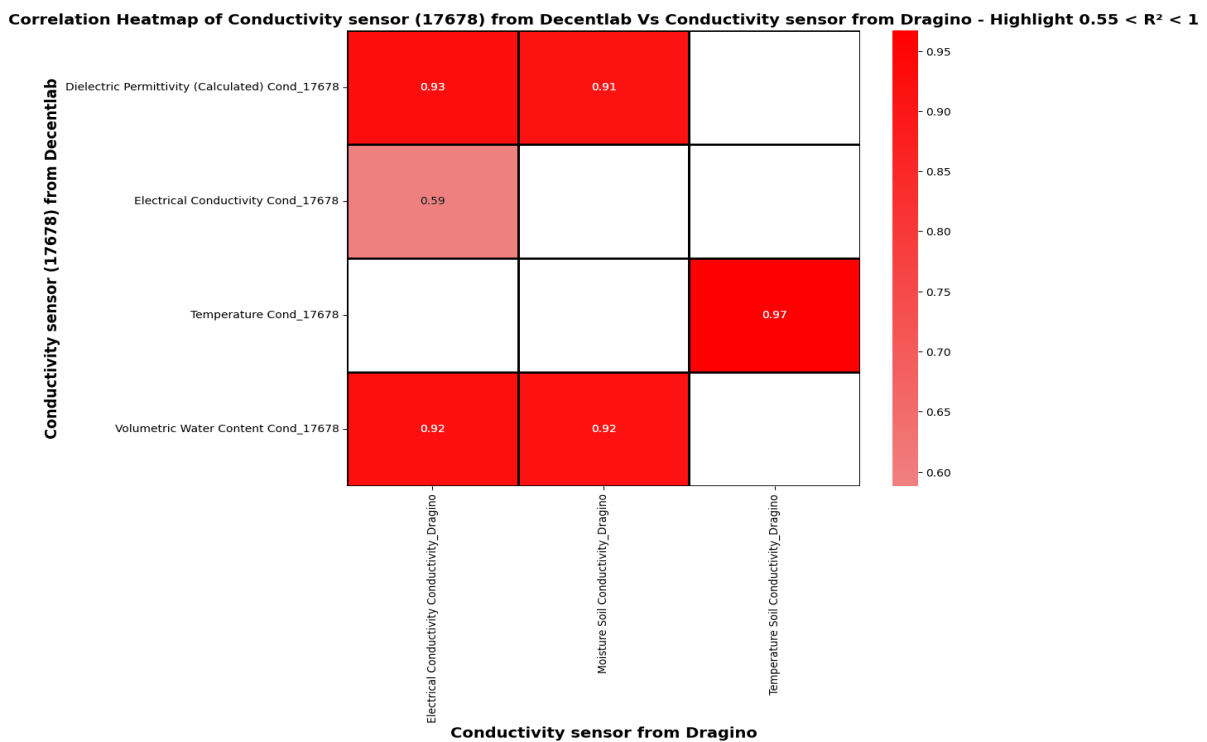
Note. Overall correlation heatmap depicting Pearson correlation coefficient (R) between all parameters measured by Dragino conductivity sensor Vs Decentlab Conductivity sensor. Created by the author, [2023].

**Figure 28.** Simplified correlation heatmap of Dragino conductivity sensor Vs Decentlab Conductivity sensor.



Note. Simplified Correlation heatmap depicting Pearson correlation coefficient (R) between 0.74 and 1.0 between the parameters measured by Dragino conductivity sensor Vs Decentlab Conductivity sensor. Created by the author, [2023].

**Figure 29.** Simplified coefficient of determination ( $R^2$ ) heatmap of Dragino conductivity sensor Vs Decentlab Conductivity sensor.



Note. Simplified correlation heatmap depicting coefficient of determination ( $R^2$ ) above 0.55 and 1 between the parameters measured by Dragino conductivity sensor Vs Decentlab Conductivity sensor. Created by the author, [2023].

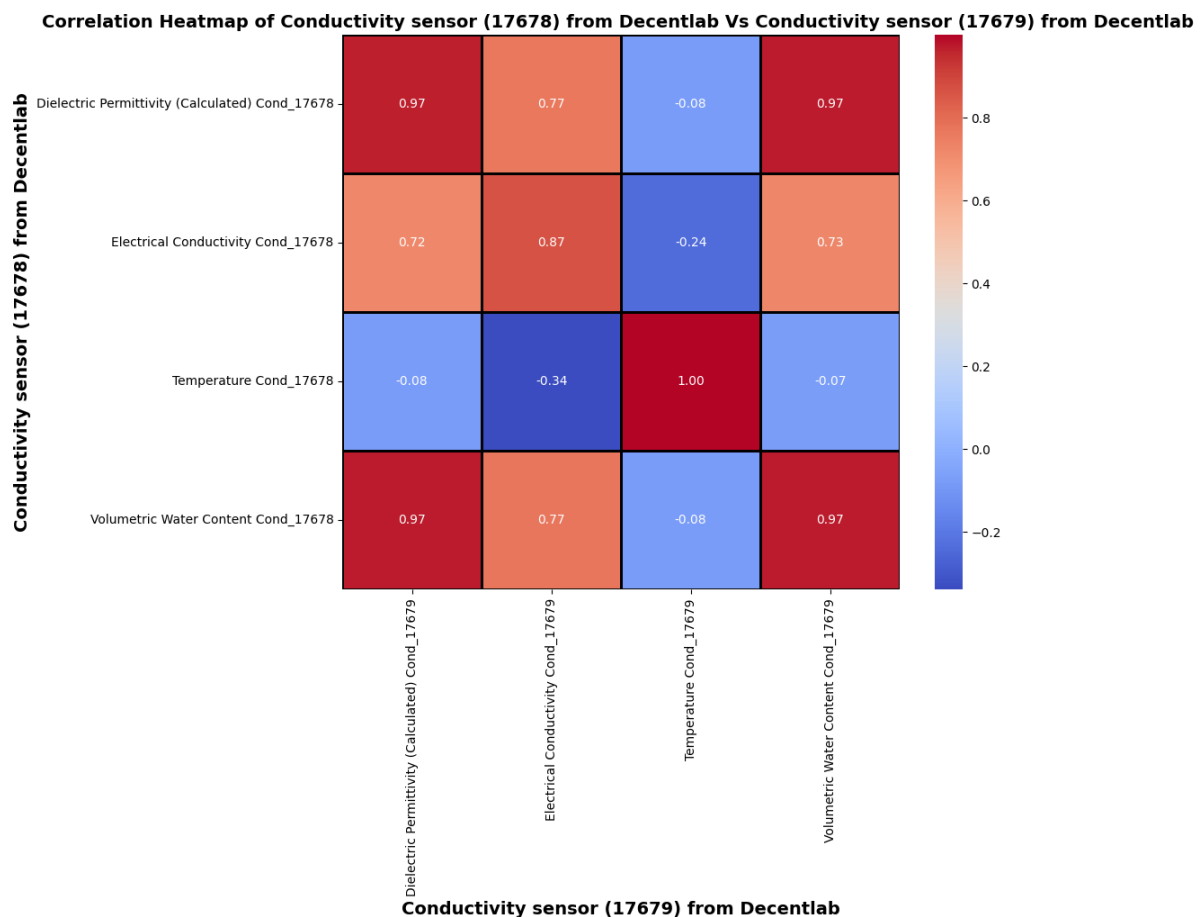
### Classification based on heatmaps:

From all three heat maps it can be interpreted that there exists a very strong correlation between temperature and moisture measured by affordable sensor variant with that of temperature and volumetric water content measured by expensive sensor variant.

There exists a weak to moderate correlation between electrical conductivity measured by affordable sensor variant with that electrical conductivity measured by expensive sensor variant.

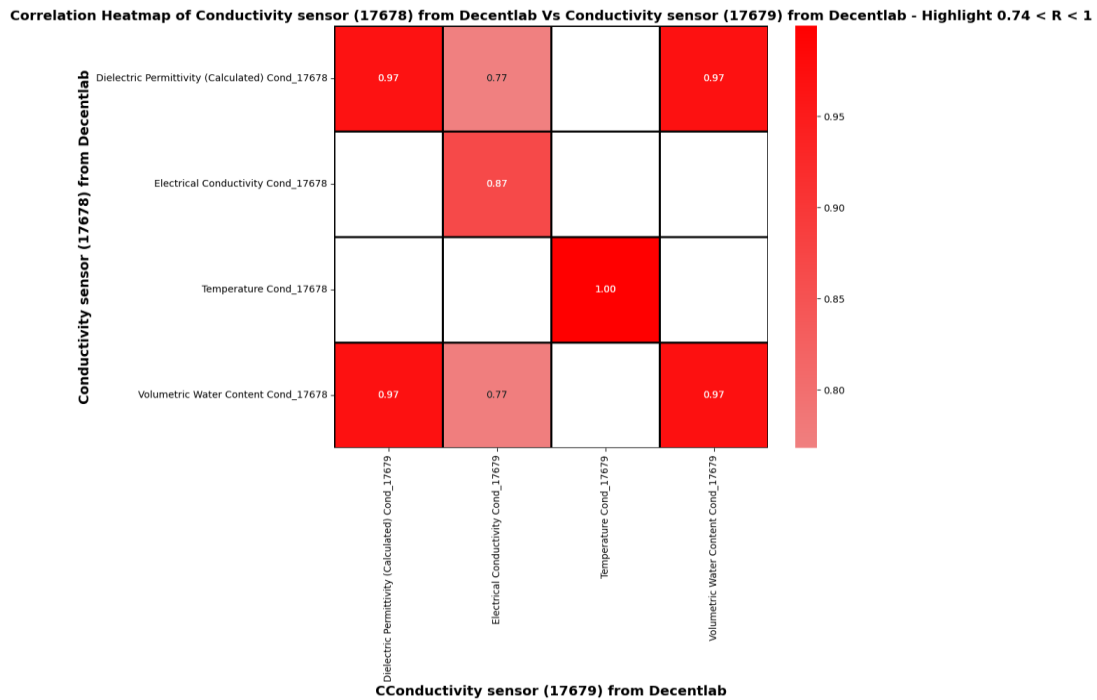
### 3.4.6. Conductivity sensor (17678) from Decentlab Vs Conductivity sensor (17679) from Decentlab

**Figure 30.** Overall correlation heatmap of Conductivity sensor (17678) from Decentlab Vs Conductivity sensor (17679) from Decentlab.



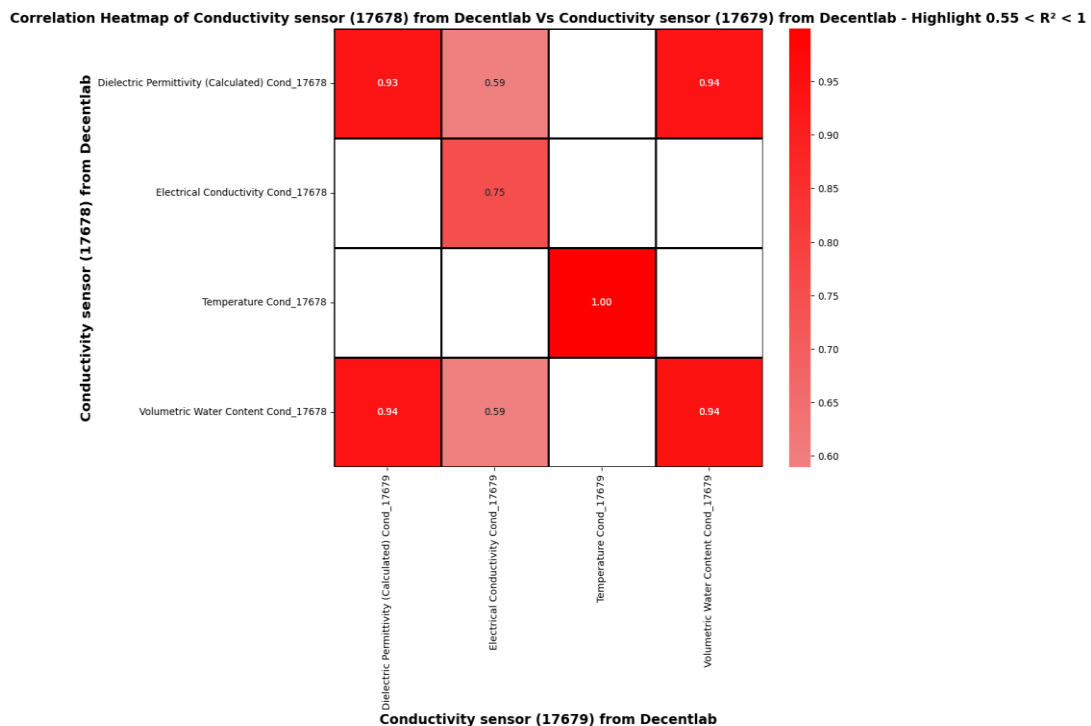
Note. Overall correlation heatmap depicting Pearson correlation coefficient (R) between all parameters measured by Conductivity sensor (17678) from Decentlab Vs Conductivity sensor (17679) from Decentlab. Created by the author, [2023].

**Figure 31.** Simplified correlation heatmap of Conductivity sensor (17678) from Decentlab Vs Conductivity sensor (17679) from Decentlab.



Note. Simplified Correlation heatmap depicting Pearson correlation coefficient (R) between 0.74 and 1.0 between the parameters measured by Conductivity sensor (17678) from Decentlab Vs Conductivity sensor (17679) from Decentlab. Created by the author, [2023].

**Figure 32.** Simplified coefficient of determination ( $R^2$ ) heatmap of Conductivity sensor (17678) from Decentlab Vs Conductivity sensor (17679) from Decentlab.



Note. Simplified correlation heatmap depicting coefficient of determination ( $R^2$ ) above 0.55 and 1 between the parameters measured by Conductivity sensor (17678) from Decentlab Vs Conductivity sensor (17679) from Decentlab. Created by the author, [2023].

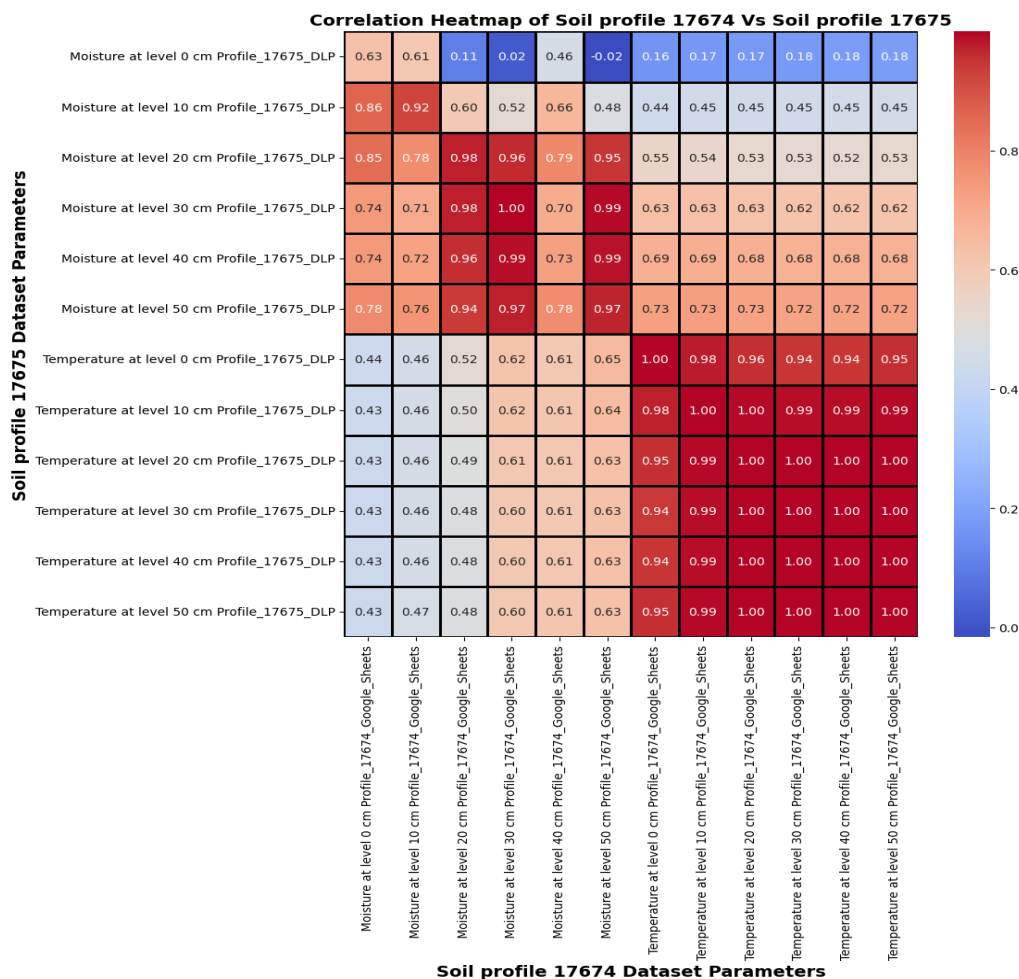
### Classification based on heatmaps:

From all three heat maps it can be interpreted that there exists a very strong correlation between temperature, moisture and dielectric permittivity measured by Conductivity sensor (17678) from Decentlab with that of temperature, moisture and dielectric permittivity measured by Conductivity sensor (17679) from Decentlab.

There exists a moderate to strong correlation between electrical conductivity measured by Conductivity sensor (17678) from Decentlab with that of electrical conductivity measured by Conductivity sensor (17679) from Decentlab.

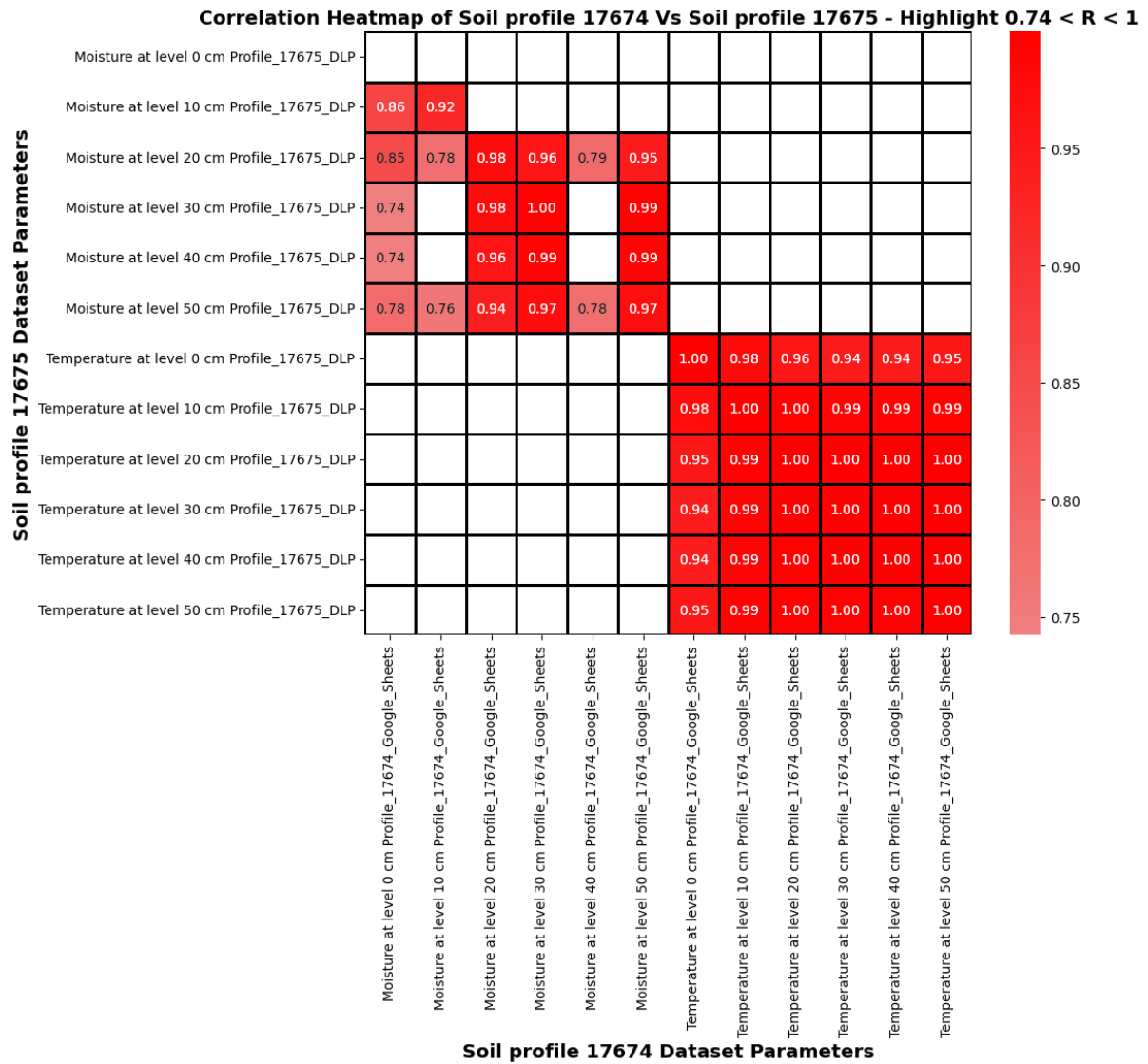
### 3.4.7. Soil profile sensor (17674) from Decentlab Vs Soil profile sensor (17675) from Decentlab

**Figure 33.** Overall correlation heatmap of Soil profile sensor (17674) from Decentlab Vs Soil profile sensor (17675) from Decentlab.



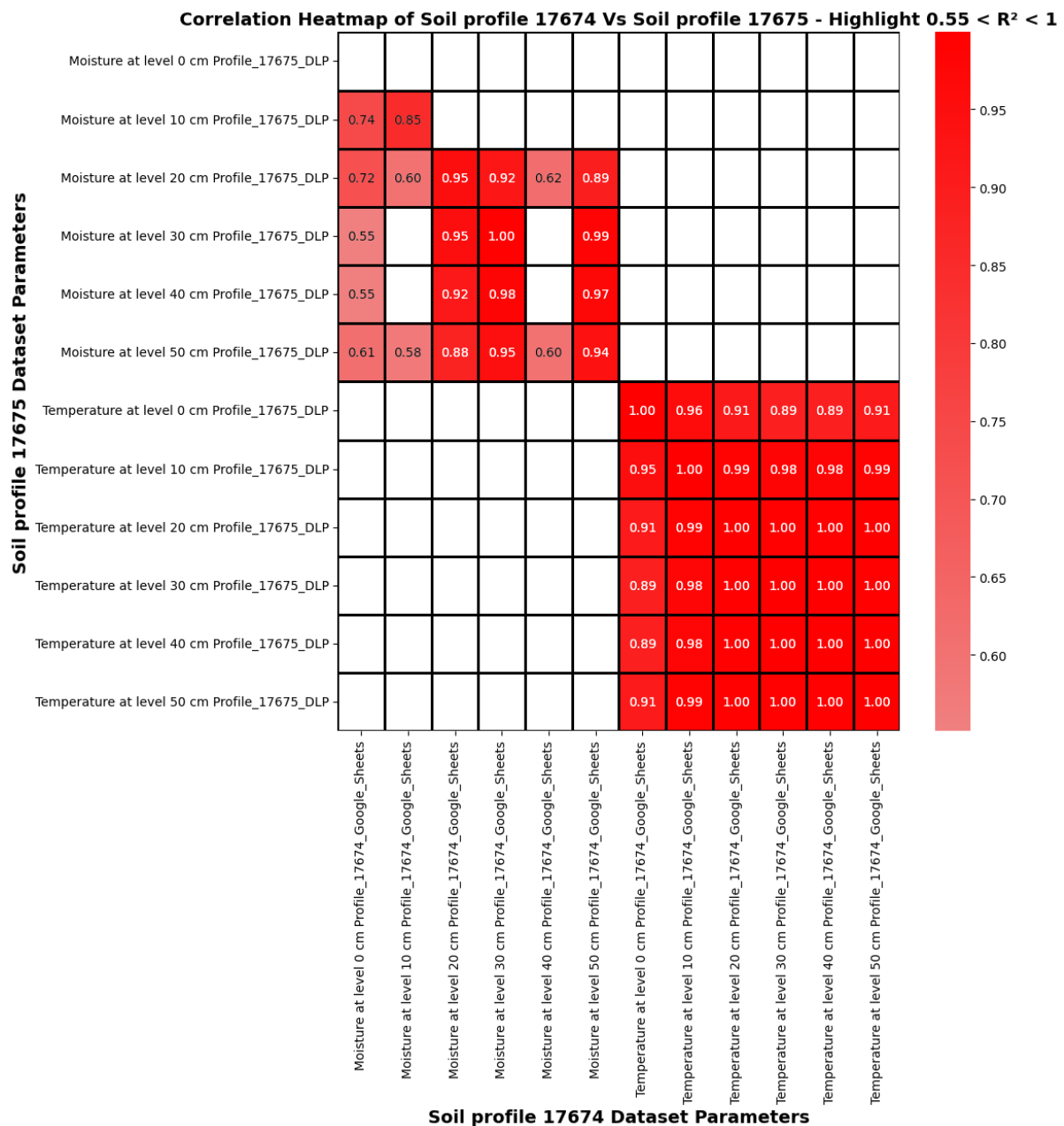
Note. Overall correlation heatmap depicting Pearson correlation coefficient (R) between all parameters measured by Soil profile sensor (17674) from Decentlab Vs Soil profile sensor (17675) from Decentlab. Created by the author, [2023].

**Figure 34.** Simplified correlation heatmap of Soil profile sensor (17674) from Decentlab Vs Soil profile sensor (17675) from Decentlab.



Note. Simplified Correlation heatmap depicting Pearson correlation coefficient (R) between 0.74 and 1.0 between the parameters measured by Soil profile sensor (17674) from Decentlab Vs Soil profile sensor (17675) from Decentlab. Created by the author, [2023].

**Figure 35.** Simplified coefficient of determination ( $R^2$ ) heatmap of Soil profile sensor (17674) from Decentlab Vs Soil profile sensor (17675) from Decentlab.



Note. Simplified correlation heatmap depicting coefficient of determination ( $R^2$ ) above 0.55 and 1 between the parameters measured by Soil profile sensor (17674) from Decentlab Vs Soil profile sensor (17675) from Decentlab. Created by the author, [2023].

### Classification based on heatmaps:

From all three heat maps it can be interpreted that there exists a very strong to perfect correlation between temperature at level 0, temperature at level 10, temperature at level 20, temperature at level 30, temperature at level 40, temperature at level 50, moisture at level 10, moisture at level 20, moisture at level 30 and moisture at level 50 measured by Decentlab soil profile sensor 17674 with that of temperature at level 0, temperature at level 10, temperature

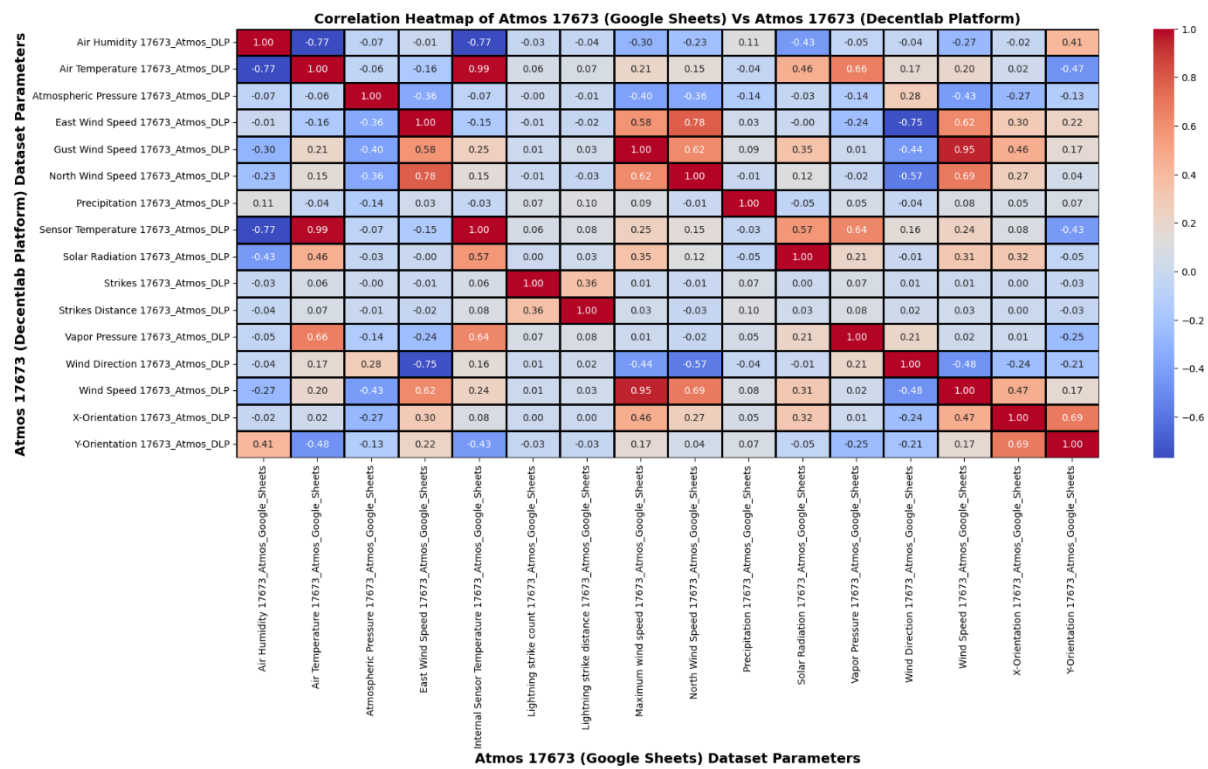


at level 20, temperature at level 30, temperature at level 40, temperature at level 50, moisture at level 10, moisture at level 20, moisture at level 30 and moisture at level 50 measured by Decentlab soil profile sensor 17675.

There exists negligible correlation between moisture at level 0 and moisture at level 40 measured by Decentlab soil profile sensor 17674 with that of moisture at level 0 and moisture at level 40 measured by Decentlab soil profile sensor 17675.

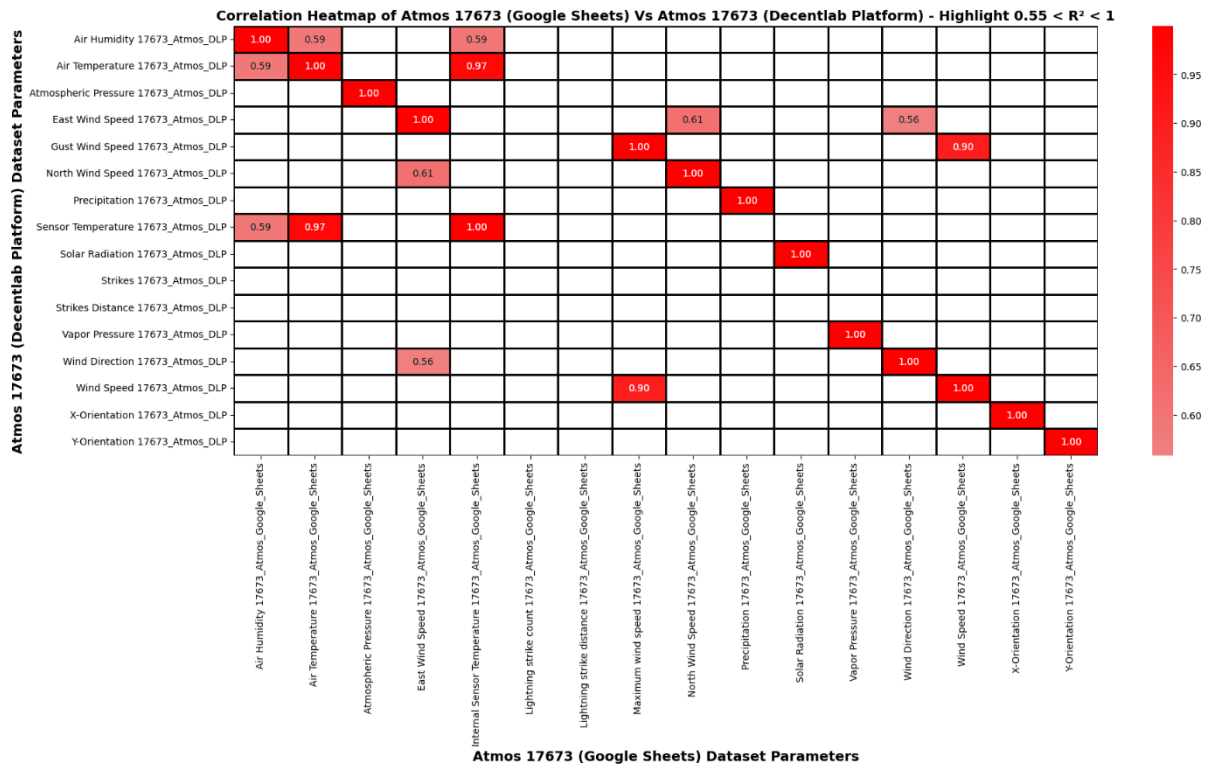
### 3.4.8. Decentlab weather station in Decentlab Platform vs Decentlab weather station in Google Sheets

Figure 36. Overall correlation heatmap of Decentlab weather station in Decentlab Platform vs Decentlab weather station in Google Sheets.



Note. Overall correlation heatmap depicting Pearson correlation coefficient (R) between all parameters measured by Decentlab weather station in Decentlab Platform vs Decentlab weather station in Google Sheets. Created by the author, [2023].

**Figure 37.** Simplified coefficient of determination ( $R^2$ ) heatmap of Decentlab weather station in Decentlab Platform vs Decentlab weather station in Google Sheets.



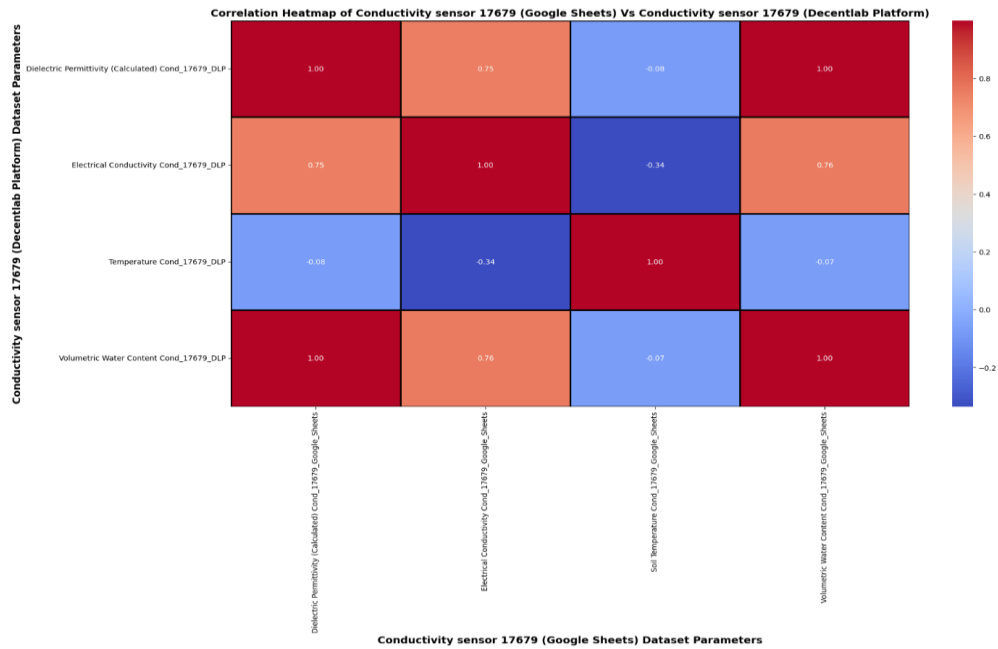
Note. Simplified correlation heatmap depicting coefficient of determination ( $R^2$ ) above 0.55 and 1 between the parameters measured by Decentlab weather station in Decentlab Platform vs Decentlab weather station in Google Sheets. Created by the author, [2023].

### Classification based on heatmaps:

From the two heat maps it can be interpreted that there is perfect correlation between the data measured through Decentlab platform and google sheets.

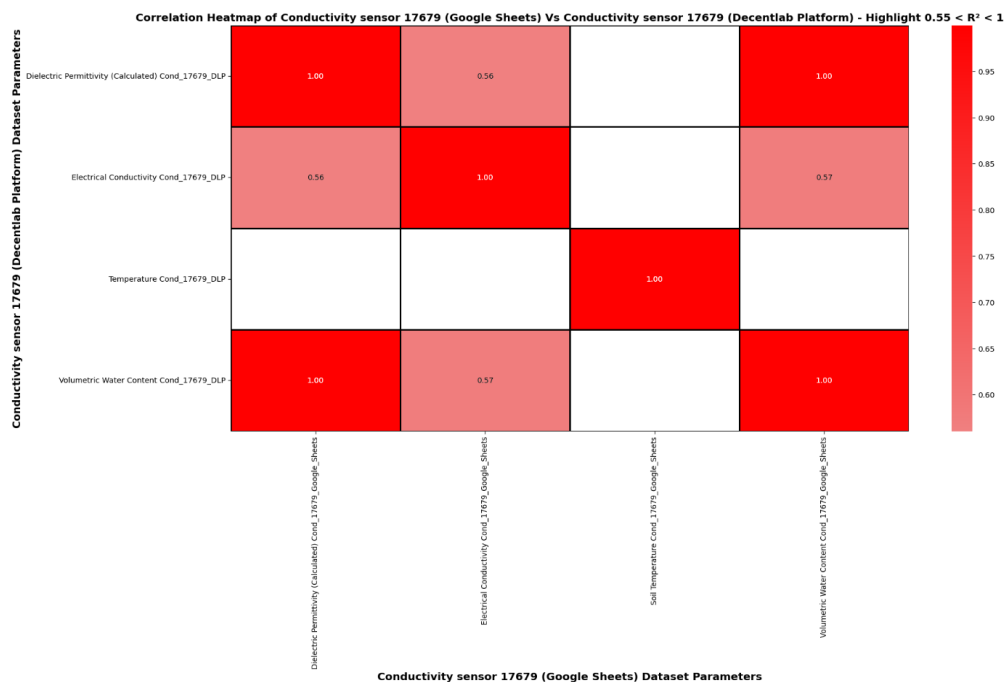
### 3.4.9. Decentlab Conductivity sensor in Decentlab Platform vs Decentlab Conductivity sensor in Google Sheets

**Figure 38.** Overall correlation heatmap of Decentlab Conductivity sensor in Decentlab Platform vs Decentlab Conductivity sensor in Google Sheets.



Note. Overall correlation heatmap depicting Pearson correlation coefficient (R) between all parameters measured by Decentlab Conductivity sensor in Decentlab Platform vs Decentlab Conductivity sensor in Google Sheets. Created by the author, [2023].

**Figure 39.** Simplified coefficient of determination ( $R^2$ ) heatmap of Decentlab Conductivity sensor in Decentlab Platform vs Decentlab Conductivity sensor in Google Sheets.



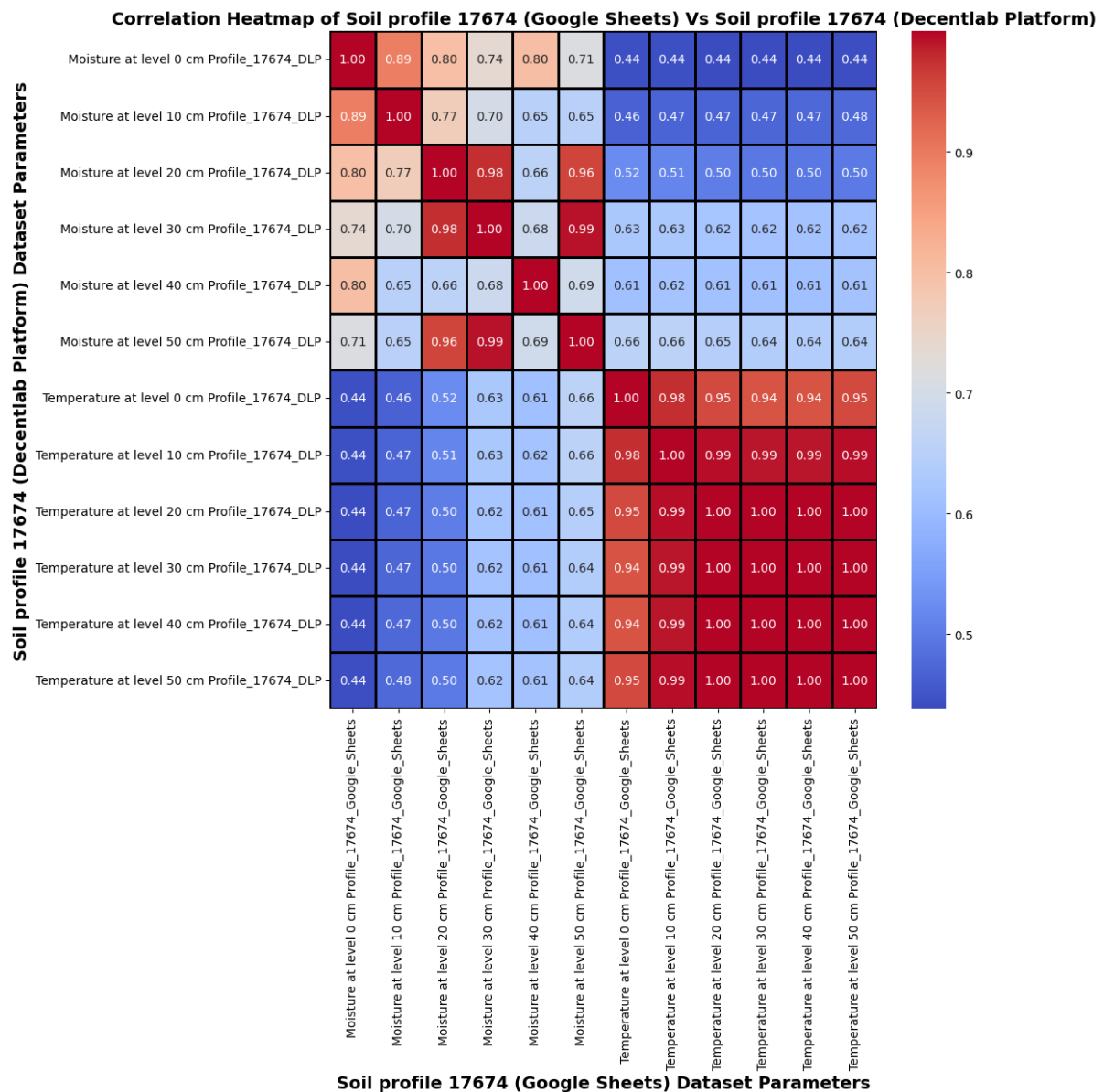
Note. Simplified correlation heatmap depicting coefficient of determination ( $R^2$ ) above 0.55 and 1 between the parameters measured by Decentlab Conductivity sensor in Decentlab Platform vs Decentlab Conductivity sensor in Google Sheets. Created by the author, [2023].

## Classification based on heatmaps:

From the two heat maps it can be interpreted that there is perfect correlation between the data measured through Decentlab platform and google sheets.

### 3.4.10. Decentlab soil profile sensor in Decentlab Platform vs Decentlab soil profile sensor in Google Sheets

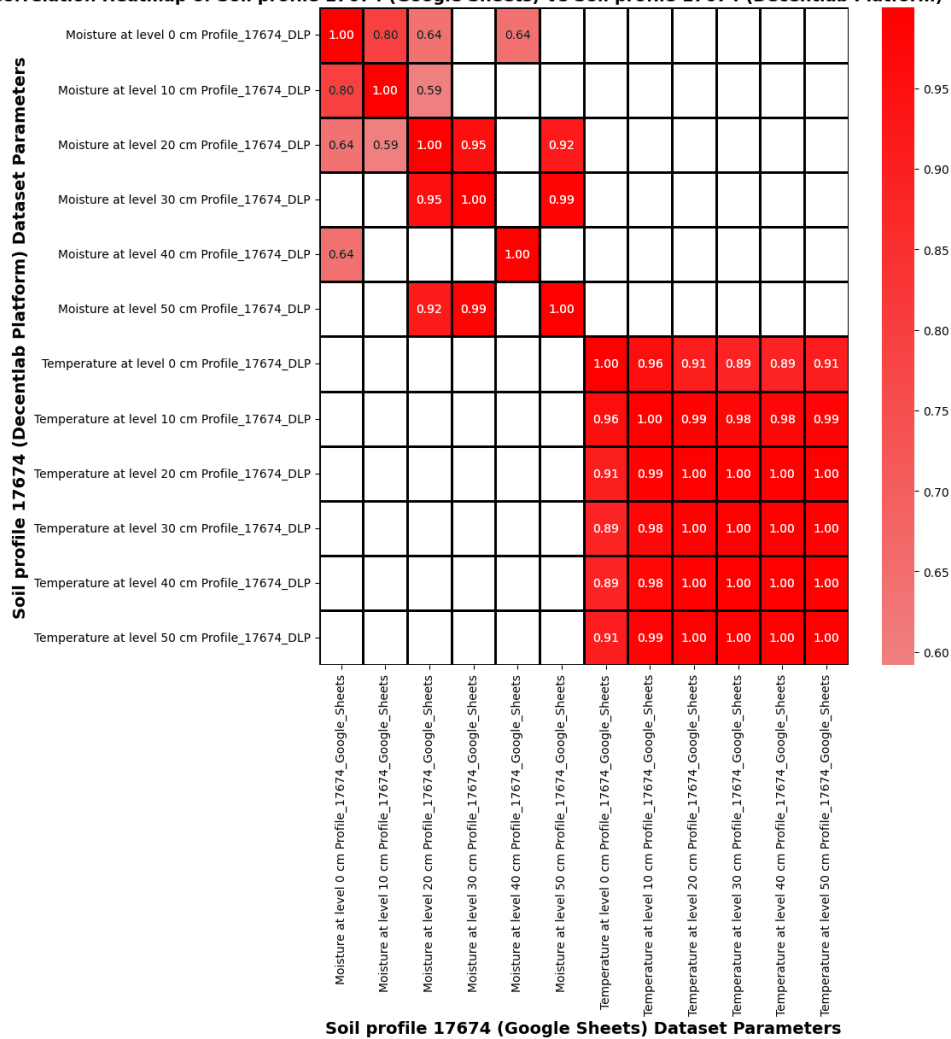
**Figure 40.** Overall correlation heatmap of Decentlab soil profile sensor in Decentlab Platform vs Decentlab soil profile sensor in Google Sheets.



Note. Overall correlation heatmap depicting Pearson correlation coefficient (R) between all parameters measured by Decentlab soil profile sensor in Decentlab Platform vs Decentlab soil profile sensor in Google Sheets. Created by the author, [2023].

**Figure 41.** Simplified coefficient of determination ( $R^2$ ) heatmap of Decentlab soil profile sensor in Decentlab Platform vs Decentlab soil profile sensor in Google Sheets.

**Correlation Heatmap of Soil profile 17674 (Google Sheets) Vs Soil profile 17674 (Decentlab Platform) - Highlight 0.55 <  $R^2$  < 1**



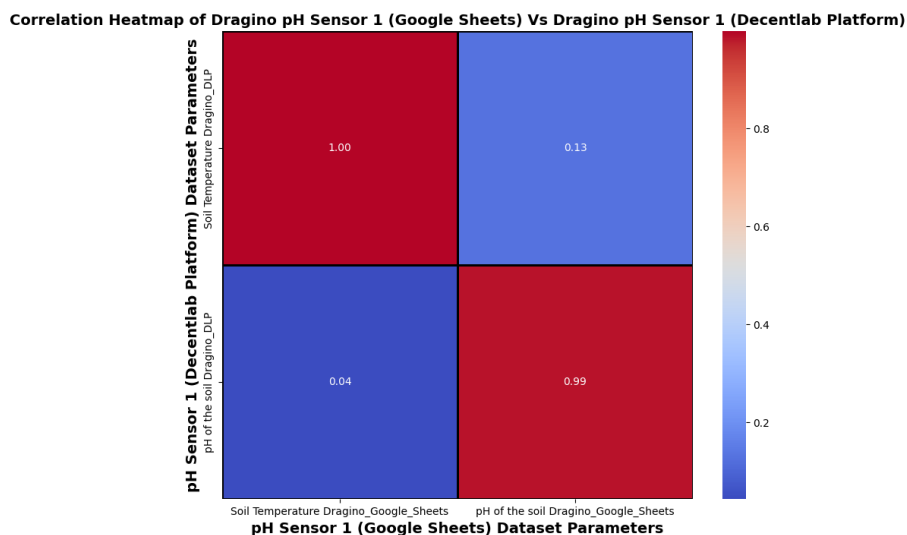
Note. Simplified correlation heatmap depicting coefficient of determination ( $R^2$ ) above 0.55 and 1 between the parameters measured by Decentlab soil profile sensor in Decentlab Platform vs Decentlab soil profile sensor in Google Sheets. Created by the author, [2023].

**Classification based on heatmaps:**

From the two heat maps it can be interpreted that there is perfect correlation between the data measured through Decentlab platform and google sheets.

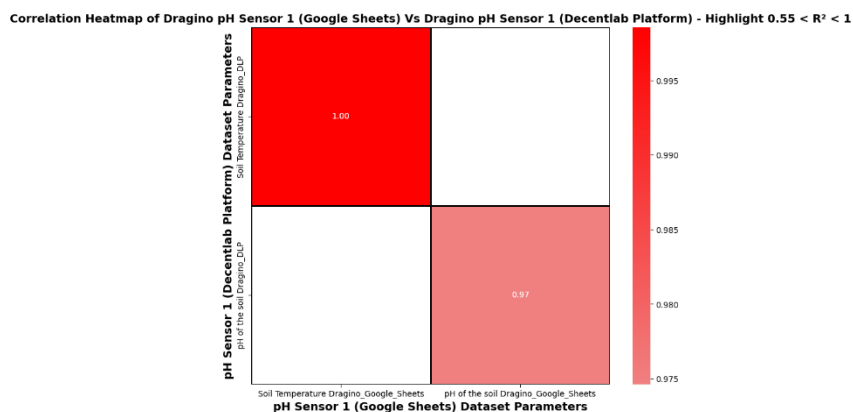
### 3.4.11. Dragino pH sensor in Decentlab Platform vs Dragino pH sensor in Google Sheets

**Figure 42.** Overall correlation heatmap of Dragino pH sensor in Decentlab Platform vs Dragino pH sensor in Google Sheets.



Note. Overall correlation heatmap depicting Pearson correlation coefficient (R) between all parameters measured by Dragino pH sensor in Decentlab Platform vs Dragino pH sensor in Google Sheets. Created by the author, [2023].

**Figure 43.** Simplified coefficient of determination ( $R^2$ ) heatmap of Dragino pH sensor in Decentlab Platform vs Dragino pH sensor in Google Sheets.



Note. Simplified correlation heatmap depicting coefficient of determination ( $R^2$ ) above 0.55 and 1 between the parameters measured by Dragino pH sensor in Decentlab Platform vs Dragino pH sensor in Google Sheets. Created by the author, [2023].

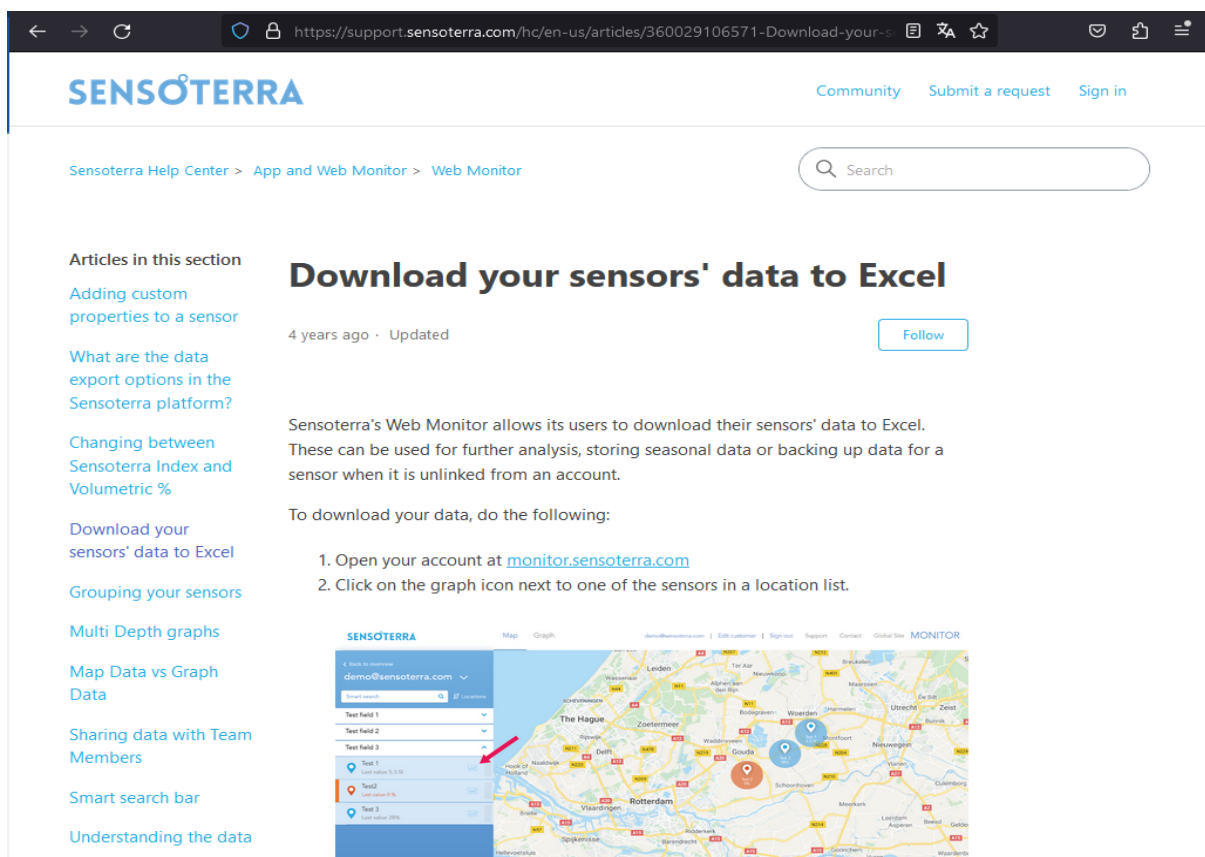
#### Classification based on heatmaps:

From the two heat maps it can be interpreted that there is very strong to perfect correlation between the data measured through Decentlab platform and google sheets.

### 3.4.12. Anomalies in gathering data from Sensoterra soil profile sensor.

Sensoterra soil profile sensor was selected and purchased as an affordable sensor variant for measuring the soil temperature and moisture at various levels in the soil. The physical installation was done successfully, and the software integration was done via the Sensoterra mobile application. Problems were faced with data extraction as there was no option for the same given in the mobile application. Upon searching the Sensoterra website for solution, a link was found from where data could be extracted. Upon clicking the link an unresponsive page popped up. Hence the data retrieval could not be achieved for Sensoterra.

Figure 44. Figure showing instruction to download data for Sensoterra sensor:



Note. Retrieved from <https://support.sensoterra.com/hc/en-us/articles/360029106571-Download-your-sensors-data-to-Excel>, accessed November 30, 2023.

Figure 45. Figure showing the non-responsive page from Sensoterra website.



Note. Retrieved from <https://support.sensoterra.com/hc/en-us/articles/360029106571-Download-your-sensors-data-to-Excel>, accessed November 30, 2023.

## 4. Conclusion, limits, recommendations, and future scope

### 4.1. Conclusion

A LoRaWAN test station was successfully set up at Hochschule Hof for the purpose of testing the affordable and expensive sensors variant in close to agriculture field like conditions. A data-driven method was developed to study the performance of both affordable and expensive LoRaWAN-based sensors in agriculture. This approach aims to evaluate the feasibility of using the more affordable sensor variant as an alternative to the expensive one in sensor-based precision agriculture. The following are the conclusions that can be gained from the data analysis of the data generated from affordable and expensive sensor variants,

1. The affordable variant of the weather station can be used to measure air temperature, air humidity, barometric pressure, UV Index and Light Intensity as effective as the expensive counterpart. Rain gauge and wind speed data measured by the affordable variant can be used to get a general idea of the environmental conditions, but the data is not precise enough to be used for scientific research. Affordable sensor variant cannot be used in place of expensive sensor variant gaining understanding regarding wind direction. It is also to be noted that there are certain parameters which is measured by expensive sensor variant only and not be affordable sensor variant.
2. As there is significant deviation in the weather data measured between the 2 affordable sensor variants (Sensecap weather station) when it comes to barometric pressure, wind direction and wind, additional studies are required for finding the actual performance.
3. Both expensive sensor variant shows excellent consistency between the weather data that is measured.
4. As there is significant deviation in the soil profile data measured by 2 expensive sensor variants when it comes to moisture at level 0 and moisture at level 40, additional studies are required for finding the actual performance.
5. For measuring soil temperature and soil moisture the affordable conductivity sensor variant can be used in place of expensive sensor conductivity variant. The affordable conductivity sensor variant can be used to gain a general idea on the electrical conductivity, but the data is not precise enough to be used for scientific research.
6. There is very high consistency between dielectric permittivity, temperature and volumetric water content of the data measured by the expensive conductivity sensor variant. It needs to be noted that the volumetric water content data produced by the expensive sensor variant is an exact value while that produced by affordable sensor variant is a



percentage value. The consistency drops when it comes to the measurement of electrical conductivity.

7. On checking the correlation between the data collected by Decentlab Platform and the data collected in google sheets between parameters measured by the same sensor, it can be concluded that the independent system that is set up at the university is functioning as expected, no data is being lost or corrupted, when the data is being transferred and the independent system can act as an effective alternative for the paid platform from Decentlab GmbH in terms of the functional part. The Decentlab Platform do provide graphical data visualisation that is currently not available in the independent system. Hence it can be concluded for the purpose of new sensor integration, data storage and functionality wise the independent system is more economical than the Decentlab platform and currently for the purpose of the data visualization Decentlab platform can be used. It is also to be noted that a visualization platform can be created to go in tandem with the independent system in the next phase of the project.
8. The graphical representation offered by the correlation heatmap is effective in providing deeper understanding of the correlations within the parameters. Hence it is a good choice to be used for sensor variant comparison.
9. Although there were high expectations for the Sensoterra multilevel soil profile sensor, it was found that the data extraction is a problem. It is hence recommended to go with another soil profile sensor for field implementation or to develop machine learning models that can predict the values from the surface level measurements which can occasionally be verified on site by the soil profile sensor from Decentlab GmbH.

The feasibility of using the affordable sensor variant instead of the expensive sensor variant was checked and the findings are given in the following page,

**Table 8.** Table showing the recommended sensor variant for measuring each parameter.

SI No	Type of sensor	Category	Expensive Variant	Affordable Variant	Recommended variant	
1	Weather Station	Name	Eleven Parameter Weather Station for LoRaWAN	8-in-1 LoRaWAN Weather Station		
		Model Number	DL-ATM41-001	S2120		
		Parameters Measured	Solar Radiation		Light Intensity, UV Index	Affordable Variant
			Precipitation		Rainfall Intensity	Expensive Variant (If precision is needed)
			Relative Humidity		Air Humidity	Affordable Variant
			Air Temperature		Air Temperature	Affordable Variant
			Horizontal Wind Speed		Wind Speed	Expensive Variant (If precision is needed)
			Wind Direction		Wind Direction	Expensive Variant
			Barometric Pressure		Barometric Pressure	Affordable Variant
			Vapor Pressure			Expensive Variant
			Wind Gust			Expensive Variant
			Tilt			Expensive Variant
			Lightning Strike Count			Expensive Variant
Lightning Average Distance			Expensive Variant			
Cost in Euro	3651.7	360				
2	Soil Conductivity Sensor	Name	Soil Moisture and Temperature Sensor for LoRaWAN	Soil Moisture, Temperature and Conductivity Sensor		
		Model Number	DL-TRS12-001	DRA LSE01		
		Parameters Measured	Volumetric Water Content (VWC)		Soil Moisture	Expensive Variant (If exact is needed or else affordable variant can be used)
			Temperature		Soil Temperature	Affordable Variant
			Bulk Electrical Conductivity		Soil Conductivity	Expensive Variant (If precision is needed)
Cost in Euro	1045	119				
3	Soil Profile Sensor	Name	Soil Moisture and Temperature Profile for LoRaWAN	Sensoterra Multi Depth Sensor for Soil Humidity		
		Model Number	DL-SMTP-001	Sensoterra Multi Depth Sensor		
		Specification	Moisture / Scaled frequency unit		Soil Moisture	Expensive Variant
			Temperature		Temperature	Expensive Variant
		Cost in Euro	1857	1070		
4	Soil pH Sensor	Name	Dragino Soil Temperature and pH Sensor		Affordable Variant (As the cost of integrating the sensor to the Decentlab Platform is very high)	
		Model Number	DRA LSPH01			
		Specification	pH Temperature			
		Cost in Euro	160 + 2346 integration cost = 2506	160		
5	Gateway	Name	Kerlink Wimet iStation 868 MHz	Dragino Outdoor LoRaWAN Gateway	Affordable Variant	
		Model Number		DLOS8-868-EC25-E		
		Specification	4G and Ethernet (PoE)	4G, WiFi and Ethernet (PoE)		
6	Network Server	Name	The Things Network	The Things Network	Affordable Variant	
		Cost in Euro	Included with the platform cost	Free (for upto 10 devices)		
7	Data Storage	Name	Decentlab Platform	Google Sheets	Affordable Variant	
		Cost in Euro	300	Free		
8	Visualisation	Name	Decentlab Platform	Nil	Expensive Variant	
		Cost in Euro	955	Nil		

Note. Created by the author, [2023].

## 4.2. Limits

- **Time.**

The data has been collected for a period of 2.5 months from August 1<sup>st</sup> to October 15<sup>th</sup>, 2023. In this time the weather is transitioning from summer to winter. For accurately knowing the performance of the affordable sensors with that of the expensive sensors, data needs to be collected all year around and under all seasons. This data is to be analysed to verify the results the findings of this thesis.

- **Reliability and accuracy of the measured data is not checked.**

In this thesis, the analysis does not guarantee the reliability and accuracy of the measured data. In this thesis, a customised methodology has been developed for understanding how well affordable sensor variant performs with that of expensive sensor variant. The reliability and accuracy of the measured data has not been checked here.

## 4.3. Recommendation

- **Recommendations for additional studies.**

Additional studies need to be carried out on the soil profile sensor supplied by Decentlab, conductivity sensor supplied by Decentlab, and the weather station supplied by Sensecap. This is because of slight inconsistency that is found in the measured data.

- **Recommendation for developing one platform for sensor performance evaluation, simulation, and interpretation.**

Currently a customised programme is developed for performing the data analysis of each sensor. It becomes impractical to develop customised programme for each sensor when many sensors are involved. Hence, it is recommended to develop a web-based platform that can seamlessly do the sensor integration, data analysis, data storage, data interpretation and simulation of various user defined conditions using the data measured. This platform can help in widescale economic deployment of LoRaWAN sensors for data collection.

- **Recommended to find new alternative for soil profile data measurements.**

As the data extraction problem was faced with the Sensoterra multilevel sensor, it is recommended to find another alternative sensor that is affordable and is capable for measuring the soil profile data.

## **4.4. Future scope of the study in authors perspective**

### **4.4.1. Development of internet connected applications for real-time measurement visualization.**

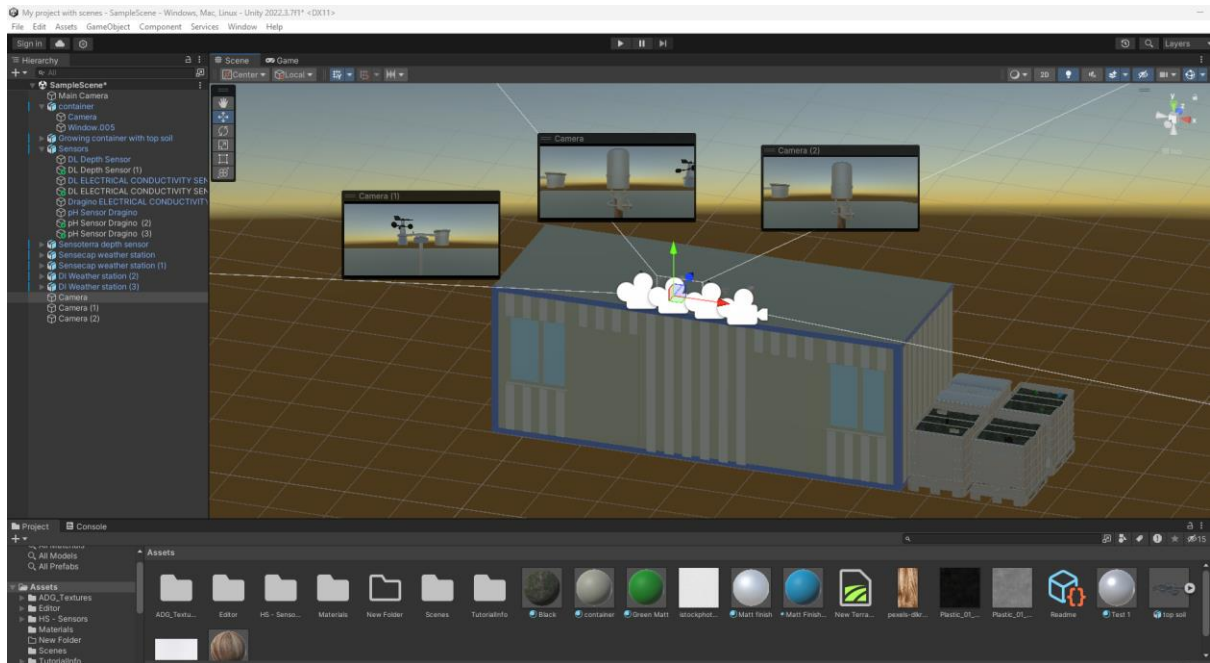
The current approach to data management from sensors involves continuous storage on Google Sheets. However, this method poses a significant challenge, especially for individuals with limited technical expertise, in interpreting the data effectively. There arises a necessity for a mechanism that can interpret this raw data into a more comprehensible and actionable format. One promising solution is the creation of an internet-connected application designed to seamlessly fetch data from Google Sheets, process it, and then present it in an easily understandable manner.

To enhance clarity and user interaction, the application should incorporate a feature that allows the creation of a virtual twin of the deployed field. This virtual twin would serve as an accurate visual representation, closely reflecting real-world conditions. The user interface should be navigable, enabling users to access near real-time updates of field conditions from any location conveniently.

In terms of functionality, it is imperative that the application offers a detailed visualization of each sensor, mirroring their actual physical placements. Users should have the option to select individual sensors, allowing them to access specific statistical data related to each sensor's performance and output. Additionally, to facilitate a comprehensive understanding, users should have access to historical data, represented graphically or pictorially, ensuring that the information is digestible and insightful regarding the prevailing site conditions.

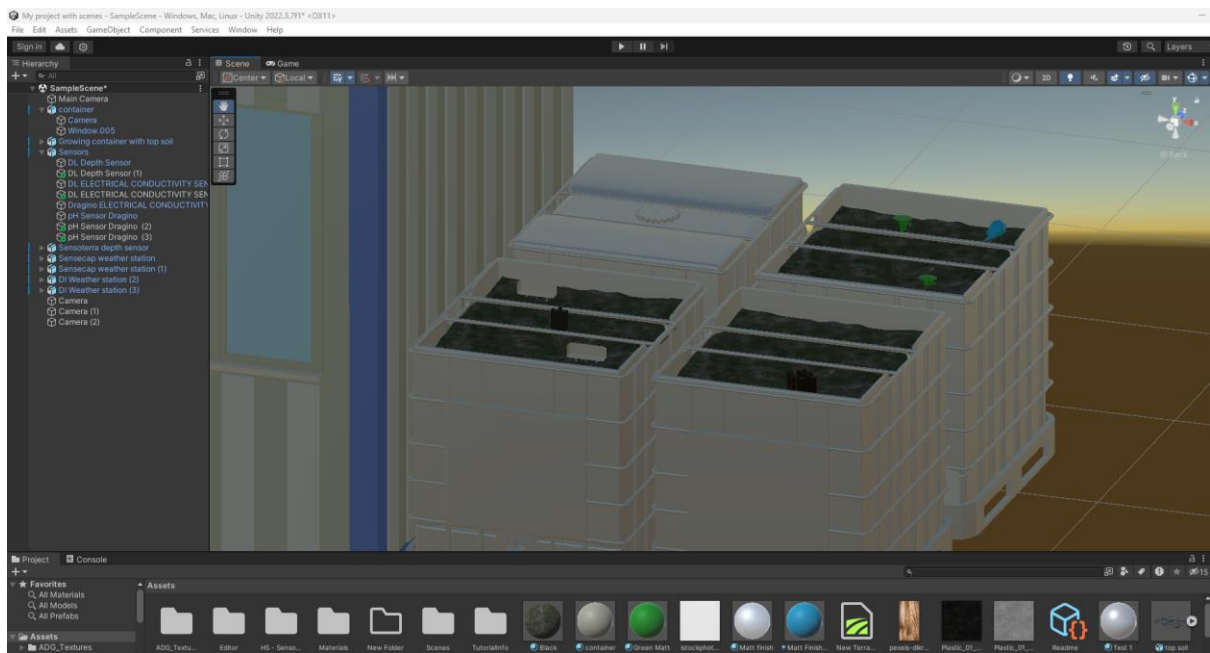
Initial efforts have been made towards the conceptualization and development phases of this application. Work has been commenced, laying the foundational elements essential for the application's functionality. However, due to prevailing time constraints, the project has not reached its full completion and realization. Thus, the comprehensive completion of this concept will not be encompassed within the scope of this master's thesis. The images below provide visual representations of the progress made on the web-based application.

**Figure 46.** Screenshot (1) of Preliminary work done in unity game engine.



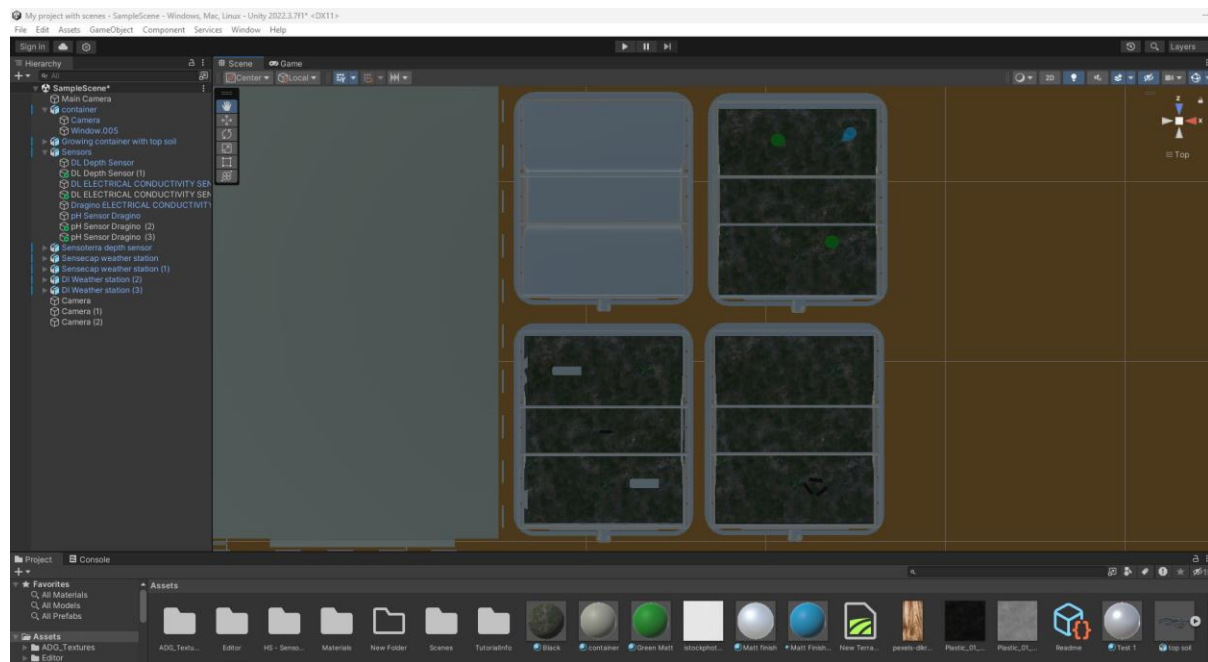
Note. Screenshot (1) of Preliminary work done for internet connected applications in Unity game engine by the author. Created by the author, [2023].

**Figure 47.** Screenshot (2) of Preliminary work done in unity game engine.



Note. Screenshot (2) of preliminary work done for internet connected applications in Unity game engine by the author. Created by the author, [2023].

**Figure 48.** Screenshot (3) of Preliminary work done in unity game engine.



Note. Screenshot (3) of preliminary work done for internet connected applications in Unity game engine by the author. Created by the author, [2023].

#### **4.4.2. Optimization of Sensor Utilization Through Correlation-Based Machine Learning Models**

The data analysis has facilitated the generation of a heatmap that displays various parameters with substantial correlations. From these heatmap, parameters displaying positive correlations ranging between 0.8 and 1.0, as well as negative correlations fluctuating between -0.8 and -1.0, can be identified. It is in the authors' opinion that these identified correlations demonstrate a promise in utilizing machine learning (ML) models for the accurate prediction of the respective parameters.

For the creation of effective ML models in the authors' opinion, it is recommended to initiate training using the historical data relevant to these parameters. Post-development, these models should undergo a meticulous validation process, wherein the predicted data is thoroughly compared and verified against the actual measured data. Such an approach aims to fine-tune the model's accuracy and reliability.

An essential benefit of this rigorous development and verification process lies in its capability to optimize the number of necessary sensors. This optimization proves to be particularly advantageous during actual field implementations, fostering operational efficiency. By employing ML models that are both precise and reliable, significant cost savings can be achieved, particularly in agricultural field implementations. By employing ML models that are

both precise and reliable, there is a potential to realize significant cost savings, making the approach highly economical and practical for real-life applications. The use of optimized models can streamline operations, reduce the need for excessive sensors, and minimize unnecessary expenses, thereby making the approach not only highly economical but also exceptionally practical for real-world agricultural applications.

#### **4.4.3. Integrating NDVI Cameras for Enhanced Monitoring of Growing Areas**

The Normalized Difference Vegetation Index (NDVI) is widely used to represent vegetation activity and terrestrial productivity (Liu Q. a.-G.-H., 2023). It is calculated as the ratio of the difference between the Near-Infrared band and the red band to their sum. The integration of NDVI cameras in growing areas can mark a significant progression in the realm of data collection and analysis. While existing research has demonstrated the capability of the NDVI to detect water stress in vegetation, there remains a necessity for more verification studies to substantiate these findings (Silva, 2016). The LoRaWAN test station provide an ideal platform for conducting these comprehensive verification studies.

**Figure 49.** *Agrocam NDVI Camera.*



Note. Retrieved from [www.agrocam.eu/](http://www.agrocam.eu/), accessed November 30, 2023.

In addition, similar camera technologies have been incorporated into drones like the DJI Mavic 3 Multispectral. Establishing a robust correlation between ground based LoRaWAN sensors and NDVI cameras can be instrumental in developing machine learning models. These models could further optimize the analysis of images captured by drones, enhancing the precision and effectiveness of agricultural monitoring and management.



#### 4.4.4. Integration of Drone Imaging and Sensor Data in Machine Learning Models for Precision Agriculture

Figure 50. DJI Mavic 3 Multispectral drone.



Note. Retrieved from [www.aonic.com/my/dji/mavic-3-multispectral/](http://www.aonic.com/my/dji/mavic-3-multispectral/), accessed November 30, 2023.

In the author's opinion, within the domain of precision agriculture and environmental monitoring, aerial imaging technologies, especially those provided by the DJI Mavic 3 Multispectral drone, hold the promise of becoming indispensable instruments in the field, assuming pivotal roles. Equipped with a highly integrated imaging system, the DJI Mavic 3 Multispectral drone features a 20MP red, green blue (RGB) camera and four 5MP multispectral cameras, capturing wavelengths across near-infrared, red edge, red, and green spectrums.

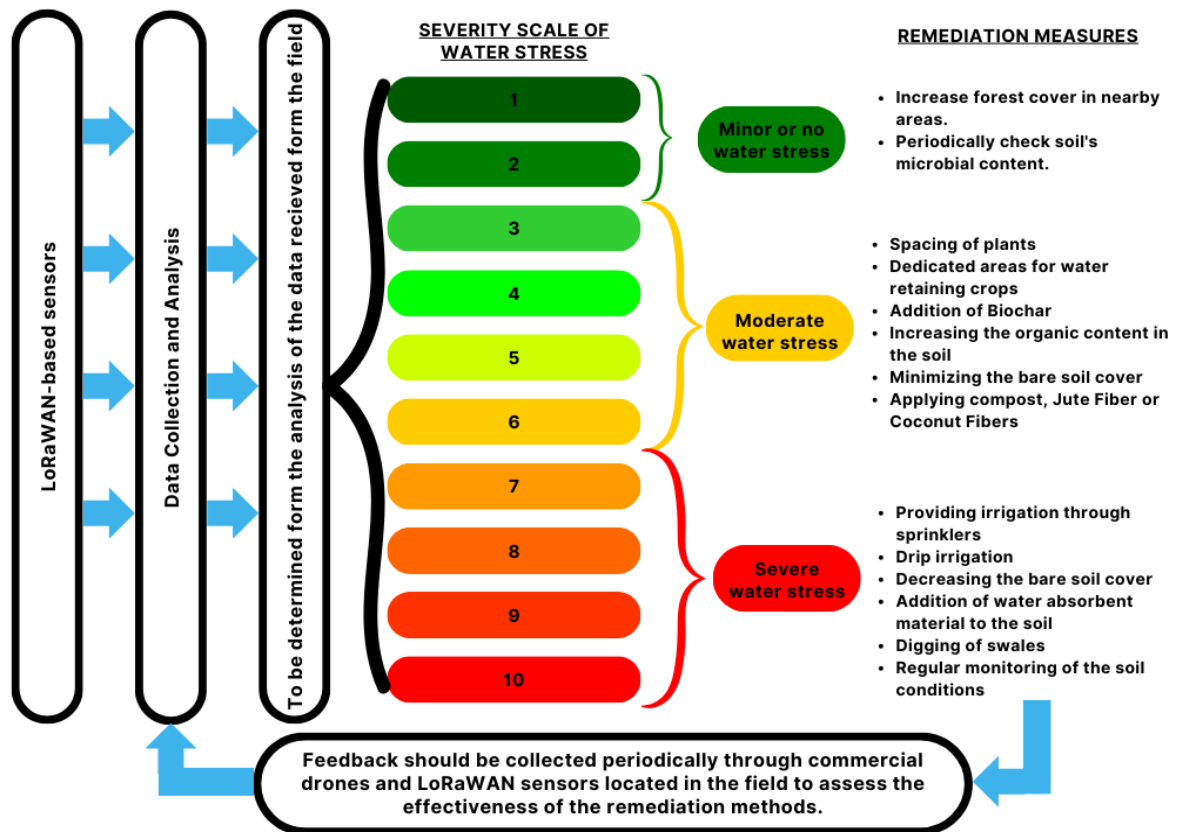
Integrating these multispectral images with the actual sensor readings can be used for the development of customised machine learning models. The goal of this integration is to amplify the accuracy and efficiency of condition assessment processes within agricultural domains. A successful integration has the potential to bring transformative advancement in agricultural analytics by significantly reducing, if not negating, the need for deployment of ground sensors.

It is in author's opinion that this optimization has to potential for substantial cost savings, enhancing the economic viability of agricultural operations, while maintaining, if not improving, the accuracy and reliability of field condition assessments.



#### 4.4.5. Concept of a severity scale developed by the author for assessing the extent of water stress.

Figure 51. Severity scale for assessing water stress.



Note. Severity scale for assessing the extend of water stress with remediation measures made by the author. Created by the author, [2023].

Although technical insights can be gained from analysing the collected data, it is the author's opinion that this needs to be transformed into actionable information. To this end, the author proposes a 'severity scale' that provides a methodology for converting raw sensor data into actionable information following analysis. For farmers who may lack technical proficiency, this user-friendly scale can help in interpreting the raw data by offering a clear understanding of the water stress levels in the entire field and practical steps for mitigating the same.

Continuous data collection is made possible through strategically placed LoRaWAN sensors within the fields, which transmit data to an online platform. Here, the data is stored and analysed using machine learning algorithms. Based on the analysis, agricultural regions within the field are classified on a water stress severity scale, visually represented in the image, ranging from 1 to 10 to indicate water stress levels. This number guides the application of remediation measures, color-coded for clarity, and tailored to the identified stress levels.

To ensure that these remediation strategies are effective, continuous feedback is essential. This feedback is garnered using the ground-based sensors and supplemented with image data collected by multispectral drones. Based on the gathered insights, further adjustments and fine-tuning of the remediation measures can be made.

#### **4.4.6. Remediation measures based on this severity scale to combat water stress.**

Improving the soil health to a point where the soil itself would be acting as a water storage medium (Alexandra Bot, 2005) is the main aim of implementing the remediation measures. On the severity scale recommended by the author, values 1 and 2 indicate regions of the field that are undergoing minor or negligible water stress. The mid-range values, from 3 to 6, correspond to areas that are experiencing moderate water stress. Finally, the higher values, from 7 to 10, signify areas that are grappling with severe water stress.

For those parts of the field that fall under the severe water stress category (values 7 to 10), urgent measures are needed to revitalize the conditions to support and sustain plant life. Some recommended strategies include providing irrigation through sprinklers (Anten, 2001), employing drip irrigation techniques (Chowdhury, 2016), reducing the expanse of exposed soil (Meyer, 2019), introducing water-absorbing materials into the soil (Asamatdinov, 2018), and excavating swales (Yuen, 2001). Additionally, in the authors' opinion, there should be a regular feedback monitoring system in place to check whether the remediation measures are effective in managing the water stress.

In regions marked by moderate water stress (values 3 to 6), the primary goal should be to make the field self-reliant concerning its water and nutrient needs. Implementing practices like proper spacing to prevent competition for water and nutrients (Zhou, 2010), dedicated areas in field for crops known for their water-retention properties (O'Neill, 2022), addition of biochar to the soil (Bruun, 2014), increasing its organic content (Huntington, 2003), minimizing exposed soil and applying compost or natural fibres like jute or coconut can significantly mitigate moderate water stress (Joothi, 2014) (Syakir, 2021).

For regions of the field that are currently experiencing minor or no water stress (values 1 and 2), the main objective should be the preservation of these optimal conditions. One effective method is to increase the forest cover in the vicinity of the field, which can act as a natural buffer, maintaining the microclimate and preventing rapid fluctuations in soil moisture levels (Ilstedt, 2016). Regularly analysing the soil's microbial content can also provide insights into

its health and indicate if any preventive measures are needed to maintain the current favourable conditions.

#### **4.4.7. Field Implementation and virtual twin of Dr. Hader's agricultural field**

The agricultural field of Dr. Hader has been identified for the initial field implementation. A predominant challenge identified in this field is the uneven distribution of water stress. This water stress arises from a combination of climatic factors and the field's inherent topography. Consequently, the field displays varied regions, with some areas experiencing significant water stress and others remaining unaffected.

Given this imbalance, a universal solution for solving the problem of water stress would not be appropriate for the entire field area. Instead, a more customised approach is required where the field is segmented based on varying degrees of water stress. The "Severity Scale of Water Stress," as outlined in the previous sections, can be used to divide the field into various segments based on water stress levels. Based on this classification, tailored remediation measures can be recommended to enhance the field's self-reliance, thereby reducing its dependency on external water and fertilizer inputs.

To assess the effectiveness of the implemented measures, an iterative feedback mechanism is integral. This mechanism incorporates aerial imagery via multispectral drones and real-time data collection from LoRaWAN sensors embedded within the field. The continuous monitoring provided by these tools offers invaluable insights, through which the application of the remediation methods can be monitored and further optimised.

## Appendix

Sample code used for generating the correlation heatmaps of soil conductivity sensor (17678) from Decentlab Vs soil Conductivity sensor from Dragino.

```
import numpy as np
import pandas as pd
import seaborn as sns
import matplotlib.pyplot as plt
from matplotlib.colors import LinearSegmentedColormap
from datetime import datetime

Cond_17678_DLP_Raw = pd.read_csv("Path of the file")

Cond_17678_DLP_Raw = Cond_17678_DLP_Raw.drop('Timezone Offset', axis=1)
Cond_17678_DLP_Raw = Cond_17678_DLP_Raw.drop('16778.battery', axis=1)

prefix_to_remove = '16778.metergroup-teros12-'
new_columns = {col: col.replace(prefix_to_remove, '') for col in
Cond_17678_DLP_Raw.columns}
Cond_17678_DLP_Raw.columns = [col.replace(prefix_to_remove, '') for col in
Cond_17678_DLP_Raw.columns]

rename_dict = {
    'Timestamp': 'A_Timestamp',
    'dp': 'Dielectric Permittivity (Calculated) Cond_17678',
    'ec': 'Electrical Conductivity Cond_17678',
    'temperature': 'Temperature Cond_17678',
    'vwc': 'Volumetric Water Content Cond_17678'
}
Cond_17678_DLP_Raw.rename(columns=rename_dict, inplace=True)

sorted_columns_Cond_17678_DLP_Raw = sorted(Cond_17678_DLP_Raw.columns)
Cond_17678_DLP_Raw = Cond_17678_DLP_Raw[sorted_columns_Cond_17678_DLP_Raw]

try:
    Cond_17678_DLP_Raw = Cond_17678_DLP_Raw.astype(float)
    print("Conversion successful. Here's your DataFrame:")
    print(Cond_17678_DLP_Raw)
except ValueError as e:
    print(f"Conversion error: {e}")

Cond_17678_DLP_Raw['A_Timestamp'] =
pd.to_datetime(Cond_17678_DLP_Raw['A_Timestamp'])
Cond_17678_DLP_Raw['A_Timestamp'] =
Cond_17678_DLP_Raw['A_Timestamp'].dt.strftime('%Y-%m-%d %H:%M')
for column in Cond_17678_DLP_Raw.columns:
    if column != 'A_Timestamp':
        Cond_17678_DLP_Raw[column] = pd.to_numeric(Cond_17678_DLP_Raw[col-
umn], errors='coerce')

datetime_format = "%d-%m-%Y %H:%M:%S"
start_datetime_str = '01-08-2023 00:00:00'
end_datetime_str = '16-10-2023 00:00:00'
start_datetime = datetime.strptime(start_datetime_str, datetime_format)
end_datetime = datetime.strptime(end_datetime_str, datetime_format)
```

```

date_range = pd.date_range(start=start_datetime, end=end_datetime,
freq='1min')

new_dataset_Cond_17678_DLP_Raw = pd.DataFrame(date_range, columns=['A_Timestamp'])

new_dataset_Cond_17678_DLP_Raw['A_Timestamp'] = new_dataset_Cond_17678_DLP_Raw['A_Timestamp'].dt.strftime('%Y-%m-%d %H:%M')

new_dataset_Cond_17678_DLP_Raw['A_Timestamp'] = new_dataset_Cond_17678_DLP_Raw['A_Timestamp'].astype(str)

Cond_17678_DLP_Raw['A_Timestamp'] = Cond_17678_DLP_Raw['A_Timestamp'].astype(str)
merged_dataset_Cond_17678_DLP_Raw = new_dataset_Cond_17678_DLP_Raw.merge(Cond_17678_DLP_Raw, left_on='A_Timestamp', right_on='A_Timestamp', how='left')

columns_to_interpolate = ['Dielectric Permittivity (Calculated) Cond_17678', 'Electrical Conductivity Cond_17678', 'Temperature Cond_17678', 'Volumetric Water Content Cond_17678']

merged_dataset_Cond_17678_DLP_Raw[columns_to_interpolate] = merged_dataset_Cond_17678_DLP_Raw[columns_to_interpolate].interpolate()

Conductivity_Dragino_Google_Sheets = pd.read_csv("Path of the file")

Conductivity_Dragino_Google_Sheets = Conductivity_Dragino_Google_Sheets.drop('bat', axis=1)
Conductivity_Dragino_Google_Sheets = Conductivity_Dragino_Google_Sheets.drop('Temp', axis=1)

rename_dict = {
    'datetime': 'A_Timestamp',
    'Conduct': 'Electrical Conductivity Conductivity_Dragino',
    'Temp Soil': 'Temperature Soil Conductivity_Dragino',
    'Moisture Soil': 'Moisture Soil Conductivity_Dragino'
}

Conductivity_Dragino_Google_Sheets.rename(columns=rename_dict, inplace=True)

sorted_columns_Conductivity_Dragino_Google_Sheets = sorted(Conductivity_Dragino_Google_Sheets.columns)
Conductivity_Dragino_Google_Sheets_sorted = Conductivity_Dragino_Google_Sheets[sorted_columns_Conductivity_Dragino_Google_Sheets]

try:
    Conductivity_Dragino_Google_Sheets_sorted = Conductivity_Dragino_Google_Sheets_sorted.astype(float)
    print("Conversion successful. Here's your DataFrame:")
    print(Conductivity_Dragino_Google_Sheets_sorted)
except ValueError as e:
    print(f"Conversion error: {e}")

```

```

Conductivity_Dragino_Google_Sheets_sorted['A_Timestamp'] =
pd.to_datetime(Conductivity_Dragino_Google_Sheets_sorted['A_Timestamp'],
dayfirst=True)
Conductivity_Dragino_Google_Sheets_sorted['A_Timestamp'] = Conductiv-
ity_Dragino_Google_Sheets_sorted['A_Timestamp'].dt.strftime('%Y-%m-%d
%H:%M')

for column in Conductivity_Dragino_Google_Sheets_sorted.columns:
    if column != 'A_Timestamp':
        Conductivity_Dragino_Google_Sheets_sorted[column] = pd.to_nu-
meric(Conductivity_Dragino_Google_Sheets_sorted[column], errors='coerce')

datetime_format = "%d-%m-%Y %H:%M"

start_datetime_str = '01-08-2023 00:00'
end_datetime_str = '16-10-2023 00:00'

start_datetime = datetime.strptime(start_datetime_str, datetime_format)
end_datetime = datetime.strptime(end_datetime_str, datetime_format)

date_range = pd.date_range(start=start_datetime, end=end_datetime,
freq='1min')

new_dataset_Conductivity_Dragino_Google_Sheets_sorted = pd.Data-
Frame(date_range, columns=['A_Timestamp'])
new_dataset_Conductivity_Dragino_Google_Sheets_sorted['A_Timestamp'] =
pd.to_datetime(new_dataset_Conductiv-
ity_Dragino_Google_Sheets_sorted['A_Timestamp'], dayfirst=True)
new_dataset_Conductivity_Dragino_Google_Sheets_sorted['A_Timestamp'] =
new_dataset_Conductiv-
ity_Dragino_Google_Sheets_sorted['A_Timestamp'].dt.strftime('%Y-%m-%d
%H:%M')
new_dataset_Conductivity_Dragino_Google_Sheets_sorted['A_Timestamp'] =
new_dataset_Conductiv-
ity_Dragino_Google_Sheets_sorted['A_Timestamp'].astype(str)

Conductivity_Dragino_Google_Sheets_sorted['A_Timestamp'] = Conductiv-
ity_Dragino_Google_Sheets_sorted['A_Timestamp'].astype(str)
Conductivity_Dragino_Google_Sheets_sorted = Conductiv-
ity_Dragino_Google_Sheets_sorted.reindex(sorted(Conductiv-
ity_Dragino_Google_Sheets_sorted.columns), axis=1)

merged_dataset_Conductivity_Dragino_Google_Sheets = new_dataset_Conductiv-
ity_Dragino_Google_Sheets_sorted.merge(Conductiv-
ity_Dragino_Google_Sheets_sorted, left_on='A_Timestamp',
right_on='A_Timestamp', how='left')

columns_to_interpolate = ['Electrical Conductivity Conductivity_Dragino',
'Temperature Soil Conductivity_Dragino', 'Moisture Soil Conductivity_Dragi-
no']

merged_dataset_Conductivity_Dragino_Google_Sheets[columns_to_interpolate] =
merged_dataset_Conductivity_Dragino_Google_Sheets[columns_to_interpo-
late].interpolate()

merged_dataset_Cond_17678_DLP_Raw
merged_dataset_Conductivity_Dragino_Google_Sheets

```

```

merged_df = pd.merge(merged_dataset_Cond_17678_DLP_Raw , merged_da-
taset_Conductivity_Dragino_Google_Sheets, on='A_Timestamp')

merged_df.sort_values(by='A_Timestamp', inplace=True)

correlation_matrix = merged_df.drop(columns=['A_Timestamp']).corr()

atmos_cols = [col for col in merged_df.columns if col.endswith('_Dragino')]
sensecap_cols = [col for col in merged_df.columns if
col.endswith('Cond_17678')]

reordered_corr_matrix = correlation_matrix.loc[sensecap_cols, atmos_cols]

plt.figure(figsize=(10,8))
sns.heatmap(reordered_corr_matrix, annot=True, fmt=".2f", cmap='coolwarm',
linewidths=2, linecolor='black')
plt.xlabel('Conductivity sensor from Dragino', fontsize=14, font-
weight='bold')
plt.ylabel('Conductivity sensor (17678) from Decentlab', fontsize=14, font-
weight='bold')

plt.title('Correlation Heatmap of Conductivity sensor (17678) from De-
centlab Vs Conductivity sensor from Dragino', fontsize=14, font-
weight='bold')
plt.show()

cmap = LinearSegmentedColormap.from_list('red_gradient', ['lightcoral',
'red'], N=256)

mask = (reordered_corr_matrix >= 0.74) & (reordered_corr_matrix < 1)

plt.figure(figsize=(10,8))
sns.heatmap(reordered_corr_matrix, annot=True, fmt=".2f", cmap=cmap, lin-
ewidths=2, linecolor='black', cbar=True, mask=~mask)

for i, row in enumerate(reordered_corr_matrix.values):
    for j, val in enumerate(row):
        if mask.iloc[i, j]:
            plt.gca().text(j+0.5, i+0.5, f"{val:.2f}",
                ha='center', va='center',
                fontsize='medium',
                color='white' if val > 0.85 else 'black')

plt.xlabel('Conductivity sensor from Dragino', fontsize=14, font-
weight='bold')
plt.ylabel('Conductivity sensor (17678) from Decentlab', fontsize=14, font-
weight='bold')

plt.title('Correlation Heatmap of Conductivity sensor (17678) from De-
centlab Vs Conductivity sensor from Dragino - Highlight 0.74 < R < 1',
fontsize=14, fontweight='bold')
plt.show()

r_squared_matrix = reordered_corr_matrix ** 2

```

```

cmap = LinearSegmentedColormap.from_list('red_gradient', ['lightcoral',
'red'], N=256)

mask = (r_squared_matrix >= 0.55) & (r_squared_matrix < 1)
plt.figure(figsize=(10,8))
sns.heatmap(r_squared_matrix, annot=True, fmt=".2f", cmap=cmap, lin-
ewidths=2, linecolor='black', cbar=True, mask=~mask)

for i, row in enumerate(r_squared_matrix.values):
    for j, val in enumerate(row):
        if mask.iloc[i, j]:
            plt.gca().text(j+0.5, i+0.5, f"{val:.2f}",
                            ha='center', va='center',
                            fontsize='medium',
                            color='white' if val > 0.85 else 'black')

plt.xlabel('Conductivity sensor from Dragino', fontsize=14, font-
weight='bold')
plt.ylabel('Conductivity sensor (17678) from Decentlab', fontsize=14, font-
weight='bold')
plt.title('Correlation Heatmap of Conductivity sensor (17678) from De-
centlab Vs Conductivity sensor from Dragino - Highlight  $0.55 < R^2 < 1$ ',
          fontsize=14, fontweight='bold')
plt.show()

```



## Affidavit

I certify that this thesis does not incorporate without acknowledgement any material previously submitted for a degree or diploma in any university; and that to the best of my knowledge and belief it does not contain any material previously published or written by another person where due reference is not made in the text.

Hof

Date: 14.12.2023

Signature



---

Thanipparambu Narayanan Kutty Harikrishnan

## References

- Ahuja, S. (2021). *Chapter 1 - Overview: modern water purity and quality, Handbook of Water Purity and Quality (Second Edition)*. Amsterdam: Academic Press.
- Alexandra Bot, J. B. (2005). *The Importance of Soil Organic Matter: Key to Drought-resistant Soil and Sustained Food Production*. Rome: FOOD AND AGRICULTURE ORGANIZATION OF THE UNITED NATIONS.
- Anten, M. (2001). Development of sprinkler irrigation in mountain environments : experiences from Northern Peru. *SNV Netherlands Development Organization*.
- Apostolaki, S. a. (2019). *Freshwater: The Importance of Freshwater for Providing Ecosystem Services*.
- Asamatdinov, A. (2018). New Water-Keeping Soil Additives. *Modern Chemistry & Applications*.
- Benesty, J. a. (2009). Pearson Correlation Coefficient. In J. a. Benesty, *Noise Reduction in Speech Processing* (pp. 1--4). Berlin, Heidelberg: Springer Berlin Heidelberg.
- Bernacchi, C. J. (2015). Terrestrial Ecosystems in a Changing Environment: A Dominant Role for Water. *Annual Review of Plant Biology*, 599-622.
- Bhattacharya, P. R. (2023). Internet of Things and smart sensors in agriculture: Scopes and challenges. *Journal of Agriculture and Food Research*.
- Bruun, E. a.-N. (2014). Biochar amendment to coarse sandy subsoil improves root growth and increases water retention. *Soil Use and Management*.
- Chang, C.-W. a. (2001). Near-Infrared Reflectance Spectroscopy–Principal Components Regression Analyses of Soil Properties. *Soil Science Society of America Journal*, 480-490.
- Chicco, D. a. (2021). The coefficient of determination R-squared is more informative than SMAPE, MAE, MAPE, MSE and RMSE in regression analysis evaluation. *PeerJ Computer Science*, e623.
- Chowdhury, P. a. (2016). Implication of Feasible Techniques for Irrigation in Hill Agriculture.
- Cosgrove, W. J. (2015). Water management: Current and future challenges and research directions. *Water Resources Research*, 4823-4839.
- Fereres, E. a. (2006). Deficit irrigation for reducing agricultural water use. *Journal of Experimental Botany*, 147-159.
- Fukase, E. a. (2017). *Economic Growth, Convergence, and World Food Demand and Supply*. World Bank Group.
- Goh, Y. a. (2023). Long Range Wide Area Network (LoRaWAN) for Oil Palm Soil Monitoring. In *IoT and Agriculture* (pp. 97-124).
- Hsiao, T. (2003). Systematic improvement of agricultural water-use efficiency., (pp. 14-15).

- Hsiao, T. a. (2007). A systematic and quantitative approach to improve water use efficiency in agriculture. *Irrigation Science*, 209-231.
- Huntington, T. (2003). Available Water Capacity and Soil Organic Matter.
- Ilstedt, U. a. (2016). Intermediate tree cover can maximize groundwater recharge in the seasonally dry tropics. *Scientific Reports*.
- Joothi, P. a. (2014). Studies on the moisture retention capacity of coir pith, as a function of time. *International Journal of ChemTech Research*, 5049-5052.
- Karagulian, F. a. (2019). Review of the Performance of Low-Cost Sensors for Air Quality Monitoring. *Atmosphere*.
- Kumar, A. a. (2018). The Impact of Wireless Sensor Network in the Field of Precision Agriculture: A Review. *Wireless Personal Communications*.
- Laishram, J. a. (2012). Soil quality and soil health: A review. *International Journal of Ecology and Environmental Sciences*.
- Lal, R. (2015). Restoring Soil Quality to Mitigate Soil Degradation. *Sustainability*, 5875--5895.
- Liu, H.-Y. a. (2019). Performance Assessment of a Low-Cost PM2.5 Sensor for a near Four-Month Period in Oslo, Norway. *Atmosphere*.
- Liu, Q. a.-G.-H. (2023). The response and sensitivity of global vegetation to water stress: A comparison of different satellite-based NDVI products. 103341.
- Lowenberg-DeBoer, J. a. (2019). Setting the Record Straight on Precision Agriculture Adoption. *Agronomy Journal*, 1552-1569.
- M. Tahat, M. a. (2020). Soil Health and Sustainable Agriculture. *Sustainability*.
- Masi, Y. V. (2020). Adoption of precision farming tools: A context-related analysis. *Land Use Policy*.
- McKenzie, A. M. (2021). Chapter 1 - Global groundwater: from scarcity to security through sustainability and solutions. In *Global Groundwater* (pp. 3-20). Elsevier.
- McNabb, D. (2019). Agriculture and Inefficient Water Use.
- Meyer, N. a.-E. (2019). Cover crops reduce water drainage in temperate climates: A meta-analysis. *Agronomy for Sustainable Development*.
- O'Neill, A. a. (2022). Fresh Air for the Mire-Breathing Hypothesis: Sphagnum Moss and Peat Structure Regulate the Response of CO<sub>2</sub> Exchange to Altered Hydrology in a Northern Peatland Ecosystem. *Water*.
- Quante, M. a. (2006). Water in the Earth's atmosphere. *Journal De Physique Iv - J PHYS IV*, 37-61.
- Ramson, J. a.-S. (2021). A Self-Powered, Real-Time, LoRaWAN IoT-based Soil Health Monitoring System. *IEEE Internet of Things Journal*.

- Rodríguez, I. C. (2020). Systematic literature review of implementations of precision agriculture. *Computers and Electronics in Agriculture*.
- Rosegrant, M. a. (2009). Water for Agriculture: Maintaining Food Security Under Growing Scarcity. *Annual Review of Environment and Resources*.
- Rosegrant, M. W. (2009). Water for Agriculture: Maintaining Food Security under Growing Scarcity. *Annual Review of Environment and Resources*, 205-222.
- Sadowski, S. a. (2020). Wireless Technologies for Agricultural Monitoring using Internet of Things Devices with Energy Harvesting Capabilities.
- Sanjeevi, P. a. (2020). Precision agriculture and farming using Internet of Things based on wireless sensor network. *Transactions on Emerging Telecommunications Technologies*.
- Schober, P. a. (2018). Correlation Coefficients: Appropriate Use and Interpretation. *Anesthesia & Analgesia*.
- Shannon, D. a. (2018). *An Introduction to Precision Agriculture*.
- Sharma, B. a. (2015). Water use efficiency in agriculture: measurement, current situation and trends. In B. a. Sharma, *Water use efficiency in agriculture: measurement, current situation and trends*.
- Shettima Lawan, M. a. (2021). *Development of a community system for water reclamation from grey water in Gujba: a conceptual method*. International Journal of Environment and Waste Management.
- Shiklomanov, I. (1993). World Fresh Water Resources. In P. Gleick, *Water in Crisis: A Guide to the World's Fresh Water Resources*. Oxford University Press.
- Silva, G. a. (2016). NDVI Response to Water Stress in Different Phenological Stages in Culture Bean. *Journal of Agronomy*, 1-10.
- Singh, D. K.-N. (2022). LoRa based intelligent soil and weather condition monitoring with internet of things for precision agriculture in smart cities. *IET Communications*, 604-618.
- Singh, R. K. (2020). Leveraging LoRaWAN Technology for Precision Agriculture in Greenhouses. *Sensors*.
- Spachos, S. S. (2020). Wireless technologies for smart agricultural monitoring using internet of things devices with energy harvesting capabilities. *Computers and Electronics in Agriculture*, 105338.
- Sriphanthaboot, W. a. (2021). Smart Multi-Level Soil Moisture Sensing System. In *2021 Second International Symposium on Instrumentation, Control, Artificial Intelligence, and Robotics (ICA-SYMP)* (pp. 1-4).
- Syakir, M. a. (2021). Application of Cellulosic Fiber in Soil Erosion Mitigation: Prospect and Challenges. *BioResources*.

- Yuen, E. a. (2001). Water harvesting techniques for small communities in arid areas. *Water science and technology : a journal of the International Association on Water Pollution Research*, 189-94.
- Zhou, X. a. (2010). Plant and row spacing effects on soil water and yield of rainfed summer soybean in the northern China. *Plant, Soil and Environment*.